NATIONAL LIBRARY
OTTAWA

CANADA

BIBLIOTHÈQUE NATIONALE
OTTAWA

NAME OF AUTHOR...*Habib-ul-Rahman Mian*...

TITLE OF THESIS...*Histological and Cytochemical Studies*
...*on some Genetic Male-sterile*
...*Lines of Barley (Hordeum vulgare L.)*

UNIVERSITY...*U of A*...

DEGREE FOR WHICH THESIS WAS PRESENTED...*Ph.D.*...

YEAR THIS DEGREE GRANTED...*1973*...

Permission is hereby granted to THE NATIONAL LIBRARY

OF CANADA to microfilm this thesis and to lend or sell copies

of the film.

The author reserves other publication rights, and

neither the thesis nor extensive extracts from it may be

printed or otherwise reproduced without the author's

written permission.

(Signed)...*Habib-ul-Rahman*...

PERMANENT ADDRESS:

...*315-B*...
...*People Colony, LYALLPUR*
...*WEST PAKISTAN*

DATED...*27.3*...1973

NL-91 (10-68)

THE UNIVERSITY OF ALBERTA

HISTOLOGICAL AND CYTOCHEMICAL STUDIES ON SOME GENETIC

MALE-STERILE LINES OF BARLEY (*HORDEUM VULGARE* L.)

by

(C) HABIB-UL-RAHMAN MIAN

A THESIS

SUBMITTED TO THE FACULTY OF GRADUATE STUDIES AND RESEARCH

IN PARTIAL FULFILMENT OF THE REQUIREMENTS FOR THE DEGREE
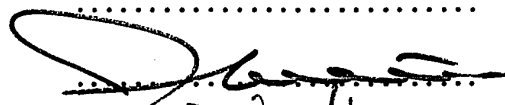
OF DOCTOR OF PHILOSOPHY
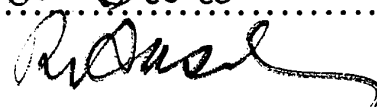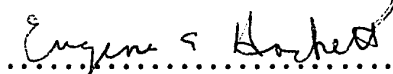

DEPARTMENT OF GENETICS

EDMONTON, ALBERTA

SPRING, 1973

THE UNIVERSITY OF ALBERTA

FACULTY OF GRADUATE STUDIES AND RESEARCH

The undersigned certify that they have read,
and recommend to the Faculty of Graduate Studies and Research
for acceptance, a thesis entitled Histological and Cytochemical
Studies on some Genetic Male-sterile Lines of Barley (*Hordeum
vulgare* L.) submitted by Habib-ul-Rahman Mian in partial
fulfilment of the requirements for the degree of Doctor of
Philosophy.

....
Supervisor

....
External Examiner

Date...... *15/3/73* ....

وَقُل رَّبِّ زِدْنِي عِلْمًا ۝

And say, Oh my God increase me in knowledge.

ABSTRACT

Cellular and tissue morphogenesis and quantitative changes of
nuclear nucleoproteins were analysed to determine the nature and time
of action of five non-allelic *ms* (male-sterility) genes in male steriles
of *Hordeum vulgare* L. The action of all five is almost entirely restricted
to the sporogenous and tapetal tissues of the anther. Histologically
the development of these two tissues is similar to that of the normal
anthers up to the completion of meiosis which is completely normal.
Subsequently their behaviour becomes distinctly deviant.

In *ms 5, 9, 14,* and *18* the microspores begin to deteriorate soon
after meiosis and are almost completely deformed at a period corresponding
to that just before the microspore division in normal anthers. In *ms 10*
deleterious effects on the microspores first appear midway between the
end of meiosis and the beginning of microspore karyokinesis.

The tapetum remains nondegenerative and persistent in *ms 5, 10,* and
14 but suddenly collapses after the free microspore stage in *ms 9.* In *ms 18*
it shows an unusually early effect during the meiotic period consisting of
a failure in the last nuclear division (karyokinesis) of tapetum which
results in an early collapse of this tissue.

Nuclear DNA and histone in sterile sporogenous and tapetal tissues
as measured by microspectrophotometry increases at the normal rate during
the premeiotic S phase. However, in the sporogenous tissues, the subse-
quent DNA and histone synthesis that normally culminates in microspore
mitosis is distinctly lacking. Thus in all male-steriles, except those of
ms 10, the microspore nuclei show an actual loss in these two macromolecules
and in *ms 10* there is an initial rise only for a short period, followed by

a dramatic drop.

The tapetal tissue shows variable behaviour which seems to be specific for each male-sterile line with respect to the DNA-histone changes in sporogenous and tapetal tissues throughout anther development.

The behaviour of sporogenous and tapetal tissues thus lends support to the hypothesis that there is transport of substances, critical to development, between the sporogenous tissue and tapetum. The effects on DNA-histone turnover, first in the sporogenous tissue and then in the tapetum, suggest that the action of *ms 5* and *9* is initiated within the microspores when they are still invested in the callose wall. On the other hand a reverse sequence indicates that the action is initiated in tapetal tissue in *ms 10* and *14*. The effect in *ms 18* is due to a direct consequence of defective tapetal functioning.

All male-steriles after the completion of meiosis, specifically at the free microspore stages, depict a drastic reduction in the nucleolar volume and hence in rRNA synthesis of microspores. This is accompanied by a high frequency of binucleolate microspore nuclei.

ACKNOWLEDGEMENTS

TABLE OF CONTENTS

LIST OF TABLES

LIST OF FIGURES

INTRODUCTION

The utilization of male-sterility in plants has great potential for the economic exploitation of heterosis through mass hybridization. This potential has in fact been actually realized in such crops as corn, sorghum, onion, and tomato. Virtually all species of crop plants have been shown to produce some male-sterile variants; and three different inheritance systems governing the male-sterile (*ms*) character have been identified (Jain 1959). Genetic male-sterility is entirely under the control of rare, recessive, nuclear genes, whereas cytoplasmic male-sterility is under the control of cytoplasmic genes and follows a maternal inheritance pattern. The third type requires the interaction of both nuclear and cytoplasmic genes, *ms ms* nuclear genotypes in male-sterile cytoplasm being required for its expression.

In addition to their economic use, male-sterile genes are of considerable value in genetic studies for they can be used to provide an excellent model system for investigating the functions of cell organelles and other cell components in development. A large number of genetic male-sterile mutants have been described in barley (*ms* 1 to *ms* 19 by Hockett *et al.* 1968*b*) and have been investigated in enough detail to indicate the nature of morphological and histological defects which are involved in the male-sterile anther development. Recent studies by Roath and Hockett (1971) on *ms* 6, *ms* 7, and *ms* 8 indicate that both meiosis and the formation of tetrads are normal. Differences in morphogenic details of the tapetal and sporogenous tissues first begin to appear at the onset of the free microspore stage and culminate in non-functional pollen grains.

1

The present investigations seek to analyze the precise time and mode of action of some of the male-sterility (*ms*) genes in barley. An attempt has been made to study the effect of these genes at the histological level, involving properties and behaviour of component tissues, and at the cytochemical level, involving quantitative changes in the macromolecules (*i.e.* DNA, RNA, and histone) during anther morphogenesis in both male-sterile and male-fertile plants.

LITERATURE REVIEW

In those crop plants where a diligent search has been made for male-sterile variants some form of male-sterility has as a rule been found. In some cases it has been shown to be under either nuclear or cytoplasmic control, in others influenced by a combination of both. Gene controlled male-sterile barley (*Hordeum vulgare*) strains were first described by Suneson (1940), and since then several more strains have been added to the list (Hockett *et al.* 1968*b*). The possibility of using genetic male-sterile barley for the production of hybrid varieties (Weibe 1960; Ramage 1965) has encouraged plant breeders to become familiar with its expression and genetic basis.

According to Gabelman (1956) male-sterility may manifest itself in different forms. It may include situations of 1) pollen sterility, due to pollen abortion; 2) staminal sterility, where the stamens are severely malformed or rudimentary; and 3) functional sterility which results from failure of anthers to dehisce, though the pollen may be normal. Usually, however, the term male-sterility is referred to as the sterility due to pollen abortion.

A worldwide collection of male-sterile barley lines is being maintained by Hockett and co-workers at Bozeman, Montana, U.S.A. Nineteen of these male-sterile stocks have been assigned the permanent designations *ms* 1 through *ms* 19. Hockett *et al.* (1968*a*) have tested sixteen of these lines for allelism and have discussed their origin, selfing behavior and anther morphology. From diallel crosses they found that all 16 of these male-sterile mutants were monogenically determined by

3

different nonallelic genes. All but one of these mutants are known to have originated as spontaneous mutants. Mutant line *ms* 3 (the single exception) was derived from F$_2$'s of acetone-treated seed in the cultivar Gateway C.I. 10072 (Kasha and Walker 1960).

These breeding studies indicated that on *a priori* reasoning, male (pollen) sterility, at least in barley, is a manifestation of a multigenic control process. The cytological or biochemical delineation of the regulating mechanism is so far not known. A beginning has nevertheless been made to clarify the histochemical processes involved in male sterility of barley through histological and histochemical studies of several mutants (Whited 1967; Roath and Hockett 1971; Nalepa 1971).

Roath and Hockett (1971) investigated the anther and pollen development of three barley male-sterile lines, namely *ms* 6, *ms* 7, and *ms* 8. They compared histological variabilities in the tapetal and sporogenous tissues of the anthers at four sequential stages of development, i.e. meiotic, quartet, free microspore and anther dehiscence. According to them, there were no visible differences with respect to the tapetal and sporogenous tissues of the anthers of *ms* 6 and its fertile counterpart throughout the above stages except for an indication of some separation of tapetal cells at the beginning of premeiosis. In *ms* 7 the microspores become periplasmodial at the free microspore stage and then disintegrate through the subsequent stages. The tapetal cells start swelling from telophase II, vacuolize at the free microspore stage and disintegrate at anther dehiscence. In anthers of the fertile counterpart the tapetum persists as a thin layer of cells throughout the above stages. Mutant line *ms* 8 exhibits a somewhat intermediate behaviour. Tapetal cells

appear either normal, or swollen and degenerating, at the free micro-
spore stage. Pollen grains appear normal up to the free microspore
stage but slowly deform and become shriveled at anther dehiscence.

Histological studies unequivocally indicate that in both fertile
and sterile strains of barley the development of all tissues of the
anther takes place in the same manner up to the tetrad stage (Roath and
Hockett 1971). This has also been shown by Rick (1948) in tomatoes
(*Lycopersicon esculentum*); Zenkteler (1962) in carrots (*Daucus carota*);
Brooks *et al.* (1966) in sorghum (*Sorghum vulgare*); Filion and Christie
(1966) in orchard grass (*Dactylis glomerata*); Harney *et al.* (1967) in
male-sterile plants of *Pelargonium hortorum*. The differences in anther
tissue according to these workers start appearing after the tetrad stage.
Furthermore, the inferences drawn from histological studies on plants of
different genera indicate strikingly analogous courses of events in the
development of anthers of male-sterile varieties. Most obvious abnormal-
ities have been shown to occur without exception in either the tapetal
tissue or sporogenous tissue or both.

The pollen grains of male-sterile strains of various plants
are considerably smaller than normal and they have relatively less, and
highly vacuolated, cytoplasm (Rick 1948; Zenktler 1962; Herich 1965;
Roath 1969). The tapetal tissues on the other hand are characterized by
persistent, vacuolated and hypertrophic cells rather than the degener-
ating ones seen in normal counterparts at the free microspore stage
(Zenkteler 1962; Brooks 1966; Harney 1967; Roath 1969). Similar results
have also been shown by Alam (1967) in his studies on Sudan grass (*Sorghum
arundinaceum*) and by Joppa (1966) in common wheat (*Triticum aestivum*).

The tapetal tissue has been ascribed considerable significance for the crucial function of anthers by Py (1932). He suggests that the period from the meiotic interkinesis to the young tetrad is probably that of maximum metabolic activity in the cytoplasm of the tapetum. In her explanation of the structure of the angiosperm anther, Esau (1953) described the tapetum as nurse tissue which nourishes the pollen mother cells (PMC) or young microspores. During meiosis in paeony (*Paeonia tenuifolia*) anthers, the content of protein and RNA in the cytoplasm of tapetal cells increases, reaching a maximum by the time tetrads separate (Sauter and Marquardt 1967). The PMC's, on the other hand, show a drop in their cytoplasmic protein and DNA content at the time of microspore formation, but after mitotic division of the pollen nucleus these substances reaccumulate in association with the breakdown of tapetum.

The active incorporation of ^{14}c-glycine in tapetal cells of *Lilium longiflorum* takes place when the PMC are between late prophase and tetrad stages (Taylor 1959). Autoradiographs of paeony anthers supplied with ^{3}H-leucine and ^{3}H-cytidine, precursors of protein and RNA respectively, show maximum grain counts in the cytoplasm of the tapetum during the meiotic divisions (Sauter 1969). These authors have suggested that during the meiotic stages proteins and RNA or their precursors are probably supplied to the PMC by the tapetal tissue. Cooper (1952) from his studies on *Lilium regale* and *L. henryi* has shown that at the onset of meiosis chromatin-like globules move from the tapetal nuclei to the inner faces of the cells, pass through the tapetal cell walls and migrate between the microsporocytes which absorb them pinocytotically. In hemp (*Cannabis sativa*) and *Silene pendula*, Heslop-Harrison (1962, 1963, 1971)

has shown that at early prophase of meiosis a pollen wall material, sporopollenin, is synthesized by the tapetum, which moves into the anther loculus and is principally deposited on the exine of developing pollen grains.

The advent of quantitative cytochemistry, particularly with the Feulgen-nucleal reaction (Lessler 1953; Patau and Swift 1953; Kasten 1958; Srinivasachar and Patau 1959; Hardonk and van Duijn 1964) showed that any genome has a constant, C value of DNA. This amount is precisely doubled in the course of genome replication. Consequently all interphase nuclei of an organism that are not in S-period have DNA amounts which are multiples of this basic C value. The exceptions to this rule have been due to tissues or cells having aneuploid nuclei (Miksche 1967; Grant 1969; Collins *et al.* 1970; Cox *et al.* 1970), asynchronous replication within a genome (Pasteels and Lison 1950; Rudkin 1969; Chooi 1971; Collins *et al.* 1970), meiotic irregularities (La Cour 1956; Faurez-Firlefyn 1950; Swift 1950; Kurnik and Herskowitz 1952) and the physiological state of the nuclei (Ely and Ross 1951; Lacomte and de Smul 1952; Moore 1952).

Ris and Mirsky (1949) first demonstrated the validity of the Feulgen technique for the *in vivo* quantitation of nuclear DNA. Their conclusion was based on measurements of individual Feulgen-stained nuclei in calf and rat liver cells by microphotometry and microchemical analysis of isolated nuclei. The photometric data gave C, 2C, and 4C amounts of DNA in various cells. This was expected on the assumption that the amount of DNA per genome was constant and that cells differ only according to the degree of euploidy.

The first study on plant nuclei was made by Schrader and Leuchtenberger (1949) who determined DNA amounts in interphase nuclei of *Tradescantia paludosa* by Feulgen cytophotometry. Relative amounts of DNA in root, leaf, tapetal tissue, and microspores were found to be 5.5, 9.0, 12.0, and 6.0 respectively. Since the root, leaf and tapetum all showed the diploid chromosome number, the authors postulated that "the amount of DNA carried in a given chromosome may vary in different tissues." As they suggest, one possibility could be variable strandedness of individual chromosomes.

Swift (1950) measured Feulgen-stained nuclei from leaf, staminal hairs, petal, and tapetum of the same *Tradescantia* species (*T. paludosa*). Data from leaf tissue showed only one DNA class with a relative value of 8.5. The tissues from petal and tapetum had two DNA classes, averaging 8.6 and 16.9 for petal, 8.5 and 16.4 for tapetum. Staminal hairs showed three classes with average values of 8.5, 16.9, and 33.6 and the haploid microspore value found was 4.4. Similar studies were made by Pasteels and Lison (1951) on *T. virginiana*. The DNA amount in the tapetal nuclei measured by these workers averaged three times the haploid value.

The tapetal tissue reveals an interesting and unique pattern of DNA synthesis. There appears to be a close relationship between cellular events during developmental stages of the anther and the DNA values in tapetum. Moss and Heslop-Harrison (1967) have demonstrated, in maize, that shortly before the onset of meiosis tapetal nuclei are 2C. Between pachytene and metaphase I the tapetal nuclei divide without cytokinesis and consequently these cells become multinucleate. This nuclear division is not preceded by DNA synthesis so that a population of 1C nuclei is

present. By the time microspores dissociate from tetrads, the tapetal

nuclei continue DNA synthesis and at this stage the nuclei range from 1C

to 4C. The authors have suggested the possibility that the tapetum

supplies soluble DNA precursors to the sporogenous tissue which are not

measurable by the Feulgen technique. Furthermore, they have postulated

that the DNA synthesis prior to pollen mitosis and the division of

generative nuclei is at the expense of tapetal nuclear DNA.

The methods for cytochemical study of RNA in cell nuclei are

deplorably unsatisfactory. Though several attempts have been made, so

far no staining methods are available that show absolute specificity for

RNA. The prime impediments to *in situ* RNA quantitation have been its

biochemical diversity and the fact that a significant part of it is often

not available for staining with basic dyes. In eukaryotic cells three

different RNA types (i.e. sRNA, rRNA, and mRNA) have already been recog-

nised and evidence for other RNA species such as those of chloroplast

(Stutz and Noll 1967) and mitochondrial origin (Fukuhara 1970) has

recently been put forth. Each of these RNA species vary widely in their

structure solubility and biochemical properties. Evidently, because of

these complexities, cytochemical techniques do not usually give a correct

picture of the *in situ* quantitative variation of RNA.

Nevertheless, Swift (1966) has pointed out that the bulk of RNA

in the nucleolus is protein-bound and with suitable fixatives may be

localized. Several procedures have been described which utilize basic

dyes for the specific staining of nucleolar RNA. The most frequently

used dyes have been pyronin (Brachet 1940), azure B (Flax and Himes 1952),

toluidine blue (Love 1962) and cresyl violet (Ritter, Di Stefano and

Farah 1961). The studies of Brachet (1940) have shown that the cyto-
plasm and nucleoli of tissues stained in Unna-Pappenheims' methyl-green-
pyronin mixture after incubation in RNase show no colour but are stained
deep pink in undigested tissues. This mixture of basic dyes, moreover,
gave differential staining of DNA- and RNA-containing structures when
both were present in the tissue. The green staining of nuclei was
demonstrated to be due to DNA and the deep pink colour of cytoplasm and
nucleoli was found to be due to RNA.

On the basis of their studies on purified DNA and RNA, and on
tissue sections, Kurnick (1950), Kurnick and Mirsky (1950), and Kurnick
(1955) concluded that highly polymerised DNA is selectively stained
with methyl green. Both RNA and lower polymers of DNA were preferen-
tially stained with pyronin. Azure B and toluidine blue have not been
promising for staining nucleoli since they show shifts in colour with
dye concentrations and condensation of nucleic acids (Swift 1966). The
basic dye cresyl violet has been recommended by Ritter *et al.* (1961)
for determinations of relative RNA amounts *in situ*. From cytophotometric
studies using one-wavelength method on rat liver and starfish oocytes,
the authors concluded that after digestion with DNase the dye specifi-
cally binds with the cellular RNA. The dye has been assumed to carry a
stoichiometric relationship with nucleic acids since extended staining
periods and increased dye concentrations do not alter the spectrophoto-
metric absorption curve, but this proportionality did not seem to hold
when the density of absorbing molecules in the light path was fairly high.
Tissue sections stained with cresyl violet showed a peak absorption at
a wave length of 585 nm.

From a comparative viewpoint Swift (1966) has indicated that pyronin has been very useful as a specific nucleolar stain in conjunction with methyl green when DNA is enzymatically removed from the tissue.

Nucleolar RNA was measured in *Vicia faba* root-tip cells by Woodard *et al.* (1961) from 4 micron paraffin sections extracted with DNase and stained in azure B. They observed a diphasic synthesis of nuclear RNA. The nucleoli appearing after cell division increase rapidly in size and RNA content up to interphase and more slowly thereafter. A second rapid synthetic phase sets in from the ensuing prophase and RNA contents increase to approximately three times the telophase value. During early prophase the nucleolus is rapidly absorbed and chromosomes and cytoplasm show a net increase of RNA.

Changes in cytoplasmic RNA concentration in the tapetum and sporogenous tissue of maize anthers have been investigated by Moss and Heslop-Harrison (1967) using pyronin Y microspectrophotometry. The data suggest that RNA values in sporogenous tissue falls during early pollen mother cell stages. The concentration increases at leptotene and reaches a maximum between this stage and pachytene and then gradually drops to about half the value at the young microspore stage. The concentration in tapetum is low initially becuase of rapid tissue growth during the early PMC stages. Tapetal RNA synthesis then speeds up until the microspores are released from tetrads. From these observations the authors claim that the RNA syntheses of tapetal and sporogenous tissues are independent of each other.

The ubiquity of basic proteins (hostones and protamines) in the nuclei of eukaryotic organisms is now well recognised. Since 1950

(Stedman and Stedman 1950), speculations concerning such proteins asso-
ciated with DNA have attributed to them several functions, such as a role
in the regulation of gene expression in differentiated cells (Stedman and
Stedman 1950; Comings 1967; Akinrimisi *et al.* 1965; Berlowitz 1965;
Ru-chih *et al.* 1965; Dahmus and Bonner 1970), mediation of nuclear
controlled cytoplasmic processes, perhaps as chromosomal products which
participate in gene-cytoplasm communication (Caspersson 1950), and a
structural function in the chromatin (Wilkins *et al.* 1959; Cole 1962).
Characteristic inhibition of DNA function has been ascribed to the
histones (Stedman and Stedman 1951; Huang and Bonner 1962; Alfrey and
Mirsky 1963; Barr and Butler 1963; Dulbecco 1964) but they may not be the
ultimate regulatory components of the genetic system of complex organisms
(Butler 1965; Clevar 1968).

A major obstacle to the *in vivo* study of histones has been the
lack of sensitive and reliable techniques. The technique developed by
Alfert and Geschwind (1953) for cytochemical localization of histone
was, however, an important breakthrough. Their procedure was to stain
nuclei in tissue sections with the acid stain fast green FCF at an
alkaline pH after the removal of DNA by digestion in hot trichloroacetic
acid (TCA).

Tests of this technique on purified histones and cellular systems
not only gave repeatable results but also showed that the dye was
selectively bound by basic groups specific to nucleohistones (Ansley
1958; Berlowitz *et al.* 1970; Noeske 1971). The stoichiometric relation
between histones and dye bound is such that microspectrophotometric
quantitation can be made (Noeske 1971). Thus this technique has

been used extensively for fast green-cytophotometry of histones in nuclei of tissue sections (Ansley 1954; Blotch *et al.* 1955; Alfert 1956; Rasch *et al.* 1959; Berlowitz 1965; Antropova *et al.* 1970; Bogdanov *et al.* 1971).

The temporal relations between nuclear DNA and histone synthesis in an organism varies with cell type and stage of the cell cycle. Alfert and Geschwind (1953) indicated a possible constancy of histone amounts relative to DNA amounts per nucleus in somatic mammalian cells. In contrast, Stedman and Stedman (1950) gave evidence of variability of histones within various cell types of an organism. These results were reported from their investigations on different tissues of ox (*Bos taurus*), fowl (*Gallus domesticus*), cod (*Gadus sp.*), (*Salmo spp.*), and man (*Homo sapiens*). In 1951 the same authors found an obvious case of cell specificity in fowl. Histones isolated from spleens, thymus glands, and erythrocytes differed significantly from each other in composition. The arginine content of erythrocyte histones, for instance, was smaller than that of the lymphocyte histones. The difference, although not very large, was certainly outside the limits of experimental error.

Histone levels showed quantitative correlation with DNA content in different cell types in *Tradescantia paludosa* (Rasch and Woodard 1959). In leaf, petal, and anther wall a 1:2:4 series of DNA-Feulgen values and fast green-histone values were found. Histone values from meristems, integuments of young ovaries and growing root tips were 4C at prophase and half as much at telophase, and showed a spread of

interclass values between the 2C and 4C amounts in interphase nuclei. The mean nuclear amounts in individual pollen mother cells have been shown to be 9.21; in dyads 4.23; in microgametes 1.77, and in eggs 2.11. The authors have also pointed out that the degree of these variations was correlated with marked changes in nuclear volume, but was independent of DNA content, whereas the DNA/histone ratio remained constant in nuclei or differentiated tissue.

In a later work Woodard *et al.* (1961) studied nucleoprotein changes in *Vicia faba* root meristems. They followed an ingenious approach in investigating these changes by both microphotometry and autoradiography. The microphotometric data represents the net amount and autoradiographic data show the trends of synthesis. They have inferred that although RNA and total protein content vary considerably during the cell cycle (a slow, almost linear increase in nuclei and nucleoli during most of interphase, followed by rapid increase at the end of interphase and a sharp reduction in prophase) the DNA and histone exhibited a relative stability (the telophase amounts of the latter two substances were half those of the parent cell). From post telophase to prophase there was a simultaneous doubling of DNA and histone and DNA synthesis was diphasic with a peak at interphase and a minor peak just preceding prophase.

Microphotometric measurements of DNA and histones were also made by Meek (1964) from different tissues of mice. Using Feulgen staining for DNA and fast green for histone, he observed that the DNA/histone ratio remained constant in interstitial cells, spermatogonia undergoing mitosis and spermatocytes at interphase.

According to the findings of Alfert (1955), Bloch and Godman
(1955) and Gall (1959), there was a parallel increase of both Feulgen-
DNA and fast green-histone amounts during the interphase period culmi-
nating in mitosis in somatic cells. This led them to infer that,
quantitatively, DNA and histone maintain a relative constancy and are
synthesized simultaneously. Other workers in later reports, however,
claim that histone synthesis may be independent of DNA synthesis or
may occur at different times in the cell cycle. Lindner *et al.* (1963)
was able to demonstrate that Ehrlich ascites tumor cells treated with 5-
fluorouracil did not show DNA synthesis; nevertheless histone amounts
continued to increase, with an associated increase in nuclear volume.
Independent synthesis of DNA and histone have also been observed by
Flamm and Birnstiel (1964) in stem cells of tobacco (*Nicotiana tabacum*
Var. Xanthi). These authors found that during inhibition of DNA
synthesis with 5-fluorodeoxyuridine the synthesis of RNA, histones,
and other nuclear proteins remained unchanged, and concluded that mitosis
in these cells was not an obligatory feature of histone synthesis.
These results were based upon experiments with cell-free extracts of
isolated nuclei so that initiation and termination of DNA synthesis
probably does not coincide in different nuclei.

From *in vitro* studies Bogdanov and Antropova (1971) provided
evidence that in spermatocytes of newts (*Triturus vulgaris*) DNA and
histone synthesis do not exactly coincide. By means of two-wavelength
cytophotometry of DNA (Feulgen stain) and histone (alkaline fast green)
they showed that the doubling of histone content of the nuclei began
in premeiotic interphase and continued up to the end of leptotene,

while DNA values reached 4C in such nuclei before the onset of lepto-
tene. The histone content at this stage was only 3C, and did not
increase to 4C until zygotene. This shows that the process of histone
doubling is somewhat delayed as compared with the DNA replication.
Similar results have also been reported by Antropova and Bogdanov
(1970) from the cytophotometric study of nuclear DNA and histone
amounts in meiotic tissue of Hemipteran *(Pyrrhocoris apterus)* testes.

The statement made by Bonner and Ts'o (1964) in discussing the
role of histones *in vitro* systems fits very well the results reviewed
above. They have concluded that, "The ratio of histone to DNA varies
from cell type to cell type in the same organism, and varies from
period to period during the life cycle," and that, "net histone syn-
thesis and histone turnover can take place in the absence of DNA
synthesis."

MATERIALS AND METHODS

Source and maintenance of male-sterile barley lines

The seed of all genetic male-sterile barley mutants used in these studies was obtained from Dr. E. A. Hockett, Agriculture Research Station, Montana State University, Bozeman, Montana, U.S.A. For preliminary testing of male-sterile behavior, plants were grown in greenhouse flats as well as in the field. The greenhouse crop was supplemented with fluorescent light for two to six hours depending upon the available sunlight. The aims of the testing procedure were to select a group of four to six male-sterile mutants, representing the widest possible range of phenotypic differences (and hence emphasizing the etiological differences). The selection was made on the basis of heading time, pollen type, source, linkage group, and completeness of male-sterility character.

Of the 21 numbered genetic male-sterile lines (Hockett *et al.* 1968*b*) so tested, five (*ms* 5, *ms* 9, *ms* 10, *ms* 14, and *ms* 18) were selected for further study. The source and characteristics (as observed under growth chamber conditions) of these five mutant lines are given in Table 1.

Male-sterility in each selected line segregates as a monogenic trait and plants with homozygous recessive genotypes (*ms ms*) are sterile. Seed stocks are increased by sib-pollinating male-steriles or by self-pollinating heterozygous plants indexed through progeny testing.

For histological and cytophotometric studies the plants were grown in controlled-environment growth chambers (Biological Sciences Building, University of Alberta) with a continuous eight hour light period followed by a 16 hour dark period. Diurnal temperatures were 55° and 40° C, and

17

TABLE I. CHARACTERISTICS OF SELECTED MALE-STERILE LINES

Male sterile symbol	Genotype	Varietal source	Linkage group	R E M A R K S
ms 5	ms 5 ms 5	Carlsberg II C.I.10114	III	Two-rowed; anthesis occurs when head has completely emerged out of the boot; completely self-sterile; anthers about 1/2 the length of fertile sib; pollen grains shrunken, rarely round, with no protoplast. Pollen show no staining in acetocarmine. A spontaneous mutant.
ms 9	ms 9 ms 9	Vantage C.I.7324	not known	Six-rowed; early; completely self-sterile; anthers about 3/4 the normal length; pollen grains deformed; a few appear round with scanty cytoplasm, which shows weak staining in acetocarmine. A spontaneous mutant.
ms 10	ms 10 ms 10	Compana C.I.5438	I	Two-rowed; early; spike may not emerge from the boot at the time of anthesis; stamen poorly developed; anthers short and compressed; completely self-sterile; pollen grains sickle shaped, with no or little cytoplasm; some pollen grains show staining in acetocarmine. A spontaneous mutant. Compana.
ms 14	ms 14 ms 14	Unitan C.I.10421	I	Six-rowed; completely self-sterile; spike emerged out of the boot at anthesis; anthers very small, about 1/3 the normal ones; pollen grains completely distorted and without cytoplasmic contents. A spontaneous mutant.
ms 18	ms 18 ms 18	Compana C.I.5438	not known	Two-rowed; early; spike half-emerged from the boot at anthesis; completely self-sterile; anthers collapsed but almost as long as those of the fertile sib. Pollen grains may be round or shriveled, some weakly stainable in acetocarmine. A spontaneous mutant.

relative humidity 70 per cent. These conditions favoured tillering.
When seedlings were two weeks old, they were moved to a 13 hour day,
70° and 40° diurnal temperatures, and 60 per cent relative humidity.
Plants were watered daily and fertilized with 20-20-20 NPK three times
during the growing period: at seeding time, at three weeks after seeding,
and at close to heading.

Collection of material for histology and cytophotometry

For histological and cytochemical observations anther development
was divided into six different stages to provide a base line for plotting
the data. To facilitate the determination of the developmental stage of
sampled anthers, efforts were made to establish correlations between
developmental stages and the growth trends of flag leaf, side tillers,
and internodes. Replicated observations established a reasonably precise
relationship between anther development and internode length. Growth
rate of flag leaves and side tillers, however, showed considerable vari-
ation within each mutant line. These characters, therefore, proved unfit
as appropriate anther-stage markers, and the length between the second
and fourth nodes was, therefore, used as the sole criterion to pinpoint
the developmental stage of the anther. These stages, and their relation-
ship with culm growth are shown in Figure 1. The six developmental
stages of the anther are illustrated in Figures 3 and 4.

In the male-sterile lines studied, all tillers showed complete
male-sterility. Since the secondary tillers occasionally showed addi-
tional floral abnormalities (e.g. abnormal pistils, fused anthers,
cleistogamous florets and others described elsewhere), and internode

Fig. 1. Relationship of culm growth with the development of anther. Ordinate: distance (in inches) between the second and fourth node from the base. Abscissa: different developmental stage of the anther. (P) Primordial; (P$_1$) Premeiotic; (M) Meiotic; (PM) Postmeiotic; (FM) Free microspore; (MN) Mononucleate.

(●–·—·–●) *ms 5*;   (●– —–●) *ms 9*;   (●–··—··–●) *ms 10*;

(●------●) *ms 14*;   (●———●) *ms 18*.

INTERNODE LENGTH (inches)

DEVELOPMENTAL STAGES OF ANTHER
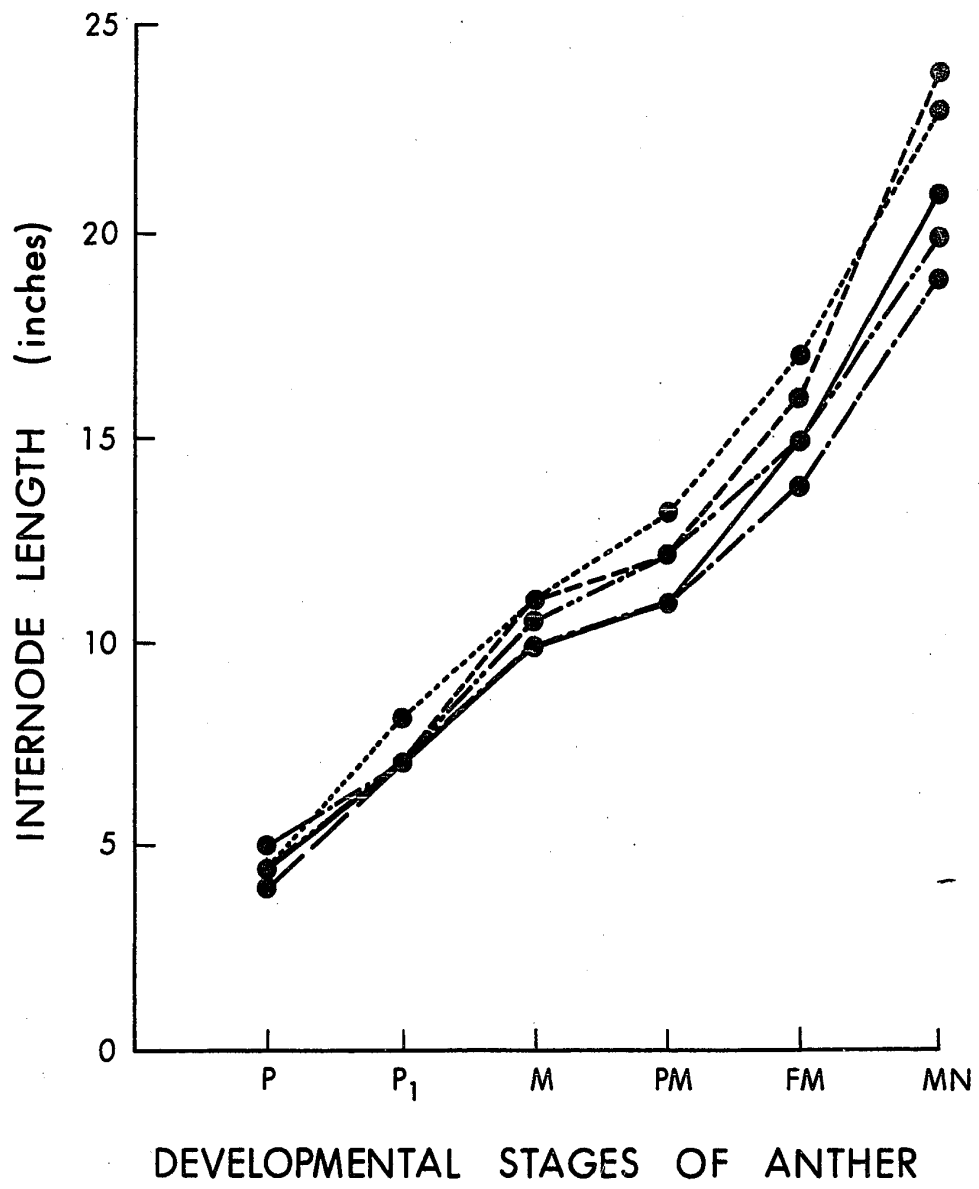
length as a marker for anther development was not correctly applicable to them, samples were therefore procured only from the primary tillers. Samples at any one developmental stage were drawn simultaneously both from male-sterile and male-fertile plants of each line under study. These were then processed identically for direct comparison of mutant behaviour with normal.

The following sampling procedure was adopted throughout the experiments:

(i)   Three to five primary tillers were selected from both male-sterile and male-fertile plants and clearly marked for further identification. A record was kept of each sample drawn.

(ii)   A lengthwise incision of the sheath in the region of the inflorescence was made with a sharp sterile razor blade. The inflorescence was then exposed by gently bending the culm, and 2 to 3 spikelets were excised. The sheaths were then resealed by slipping-on a piece of soda straw. (This same incision could be opened again at a later date to obtain more samples of another developmental stage.)

This procedure, despite its tedious nature, was necessary to provide satisfactory samples of different developmental stages from each spike. At least three sequential and overlapping stages could be obtained per inflorescence.

Fixing of tissue

The fixative formula described below was used to fix tissues both for histological and cytochemical investigations.

Ethanol	50 ml.
Glacial acetic acid	5 ml.
Glutaraldehyde 50%	10 ml.
Distilled water	35 ml.

This formula was selected after fixing trial batches of material in several other fixative fluids such as Farmer's acetic-alcohol, Carnoys' fluid, Bouins' fluid, and the CRAF series of fixatives. The fixative used appears to give a more satisfactory and artifact-free fixation of both nucleus and cytoplasm than any of the other fixatives.

Spikelets or anthers removed from the inflorescence were quickly immersed in cold (3°C) fixative and then placed in a refrigerator at 0°C for eight hours. After fixation the tissue was washed in running water in order to remove excess fixative reagents. The material was then dehydrated through the tert-butanol ascending series, infiltrated and embedded in 'tissue mat' (Fisher Scientific Co.). The blocks were identified and, if necessary, were stored in airtight glass vials at 10°C. Several anthers representing the same developmental stage were included in a single embedding block. These were then co-oriented close together as shown in Figure 2. This arrangement proved ideal in facilitating the comparative study, since transverse, tangential, and longitudinal sections were obtained adjacent to each other on the same slide.

Microtome sectioning

Tissue-mat blocks containing the tissue were sectioned with a Leitz rotary microtome. The blocks were chilled before mounting in the
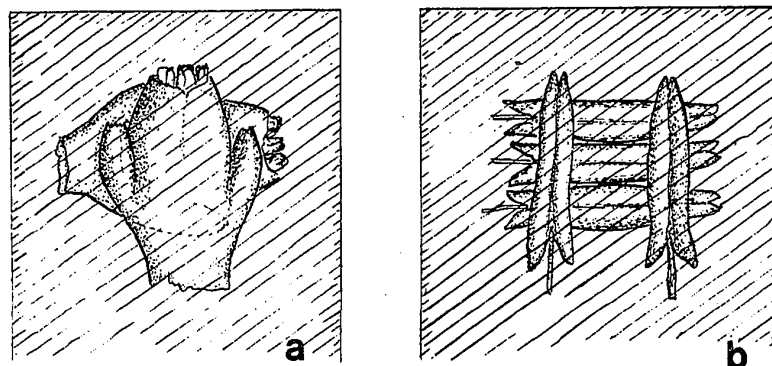
Figure 2. Arrangement of spikelets and anthers in the embedding block.

(a) Spikelets with very small anthers. (b) Large anthers.

microtome to control the uniformity of section thickness. Each block

was cut to give section-thickness classes of 5, 7, 10 and 15 microns.

Five slides with a minimum of five sections each were prepared from each

thickness class. Ribbon pieces were floated over 0.3 ml. distilled water

on slides smeared with Mayer's albumin fixative and stretched at 50°C for

50 seconds. This step was rigidly controlled to prevent possible losses

of any cell ingredients in hot water (Jonsson *et al.* 1958). Slides were

dried and processed through various staining procedures for histological

study and microspectrophotometric measurements of DNA, histone, and RNA.

The finished slides were mounted in 'Euparal' (Flatters and Garnett Ltd.,

refractive index 1.485). 'Corning' process clean 1 mm. thick slides and

No. 1 22X40 mm. coverslips were used throughout the work.

Staining procedures

For histology and microspectrophotometric measurements of nuclear

DNA and histones the staining techniques adopted were as follows:

Histology

For histological observations sections of seven or ten microns thickness were used. Good differential staining of antheridial tissue was obtained by Feder's (1968) modification of Weigert's hematoxylin technique. Slides were deparaffinized, hydrated, and stained in the above dye for 6 min. After staining they were washed in running tap water for 2 min., dehydrated in an ascending ethanol series and mounted in *Euparal.*

DNA Estimations

The Feulgen reaction as modified by McLeish and Sunderland (1961) was used to stain nuclei for microspectrophotometric measurements of DNA. To eliminate possible variations due to DNA breakdown during HCl hydrolysis of tissue, a sub-maximal hydrolysis time of 9.5 min. (maximum of the curve is 11 min.) in 1 N HCl at 60°C was selected. Slides were kept in distilled water maintained at 60°C for 1 min. before transferring to the HCl-bath so as to keep a steady 60°C temperature while the tissue was exposed to the HCl in the hydrolysis bath.

The staining procedure was as follows:

1. Deparaffinize in xylene and hydrate.

2. Rinse in distilled water at 60°C for 1 min.

3. Hydrolyze in 1 N HCl at 60°C for 9.5 min.

4. Stain in leucobasic fuchsin for 45 min. at room temperature (25-27°C).

5. Rinse in distilled water and wash through three 5-min. changes of 5 ml. of 10% $K_2S_2O_5$ in 5 ml. 1 N HCl and 100 ml. distilled water.

6.   Wash in running water for 20 minutes.

7.   Dehydrate through ethanol series and amount in·*Euparal*.

The stained nuclei showed maximum absorption of light at

λ 565 nm. and measurements were made at λ 565 nm. and λ 480 nm. using

the two-wavelength method.

Histone Estimation

The nuclear histones were stained for microspectrophotometric

measurements according to the technique described in Alfert and

Geschwind (1953) with slight modifications as follows:

Slides were rinsed for 1 min. in distilled water at 90°C before

transferring to hot trichloroacetic acid (TCA) for complete removal of

DNA.   This step was introduced to avoid temperature losses in the TCA

bath.   Following hydrolisis, slides were washed in three changes of 70°

ethanol as in the original technique, immersed in distilled water adjusted

to a pH of 8.4 for 2 min. and transferred to freshly prepared 0.1% aqueous

fast green FCF (Edward Gurr Ltd. England) for histone staining.   A test

run in a series of staining solutions ranging from pH 7.6 to 9 with

intervals of 0.2 showed maximum and most stable fast green staining of

histones in barley anthers at pH 8.4, hence the stain was adjusted to

this pH with 0.5 N NaOH.   After 30 minutes' staining, sections were

rinsed in distilled water to remove excess stain, differentiated in

N-butanol for 5 min. and mounted in *Euparal*.   Microspectrophotometric

measurements were made by two-wavelength method at λ 630 nm. and λ 622 nm.

Nucleolar RNA

For the study of nucleoli in male-fertile and male-sterile barley

anthers, slides were prepared with 5 micron thick sections and using

pyronin Y as the nucleolar stain. Before staining, deparaffinized and
hydrated sections were extracted with DNase (Worthington DNase I) to
free the nucleoli of chromatin reticulum. Sections thicker than 5 micron
and those not treated with DNase showed very weak or no staining. A
0.06 mg/ml solution of DNase in 3×10^{-3} M $MgSo_4$ in distilled water adjusted
to pH 6.5 with 0.5 N NaOH was prepared, and slides were kept in it for 24
hr at 37°C. The slides were then washed in two 5 min changes of
distilled water and stained in methyl green-pyronin (Edward Gurr Ltd.
England). The stain was prepared by dissolving 0.6 g of dye in 7.5 ml
95% ethanol and 292.5 ml Gomori's acetate buffer pH 4 (Gomori, 1955).
The slides were stained for 30 min, rinsed in two changes of distilled
water, differentiated in N-butanol and mounted in *Euparal*.

Microspectrophotometry

Microspectrophotometric measurements were made with a Zeiss MPM
Microscope Photometer which accommodates an in-line 'Veril 3200' gradu-
ated interference monochromator and a photometer head with an RCA type
1P 28 photomultiplier. A band width of 0.1 mm of selected wavelength was
focussed on a specimen plane of the microscope and then measured through
an apochromatic 40X oil immersion objective (n.a. 1.0) using immersion
oil of 1.515 refractive index.

The relative amounts of absorbing materials were calculated by
the formula suggested by Pollister *et al.* (1969), using two-wavelength
method. All estimations for DNA, histones and nucleolar RNA were made
from interphase nuclei of the tapetal and sporogenous tissues at different
stages of anther development. Triplicate readings were taken from sets
of 20 nuclei for each developmental stage, and these three readings were

averaged for calculating the final values. Standard errors are given to show the magnitude of variation within the 20 measurements and the t-test is applied to show the significance of differences between the tissues of sterile and of fertile phenotypes at any particular stage of anther development.

With a view to establishing perspective, the ontogeny of different

tissue systems of normal barley anthers is outlined below. This will

form a base line for comparisons of the behaviour of anthers of male-sterile

lines described later. The course of events (which proceed synchronously

in the four lobes of anther) typifies the anthers of the main tillers as

observed under the light microscope. To facilitate study, the develop-

mental sequence in the anther has been divided into six stages, namely:

primordial (P); premeiotic (P_1); meiotic (M); postmeiotic (PM); free

microspore (FM) and mononucleate (MN).

Histology of Fertile Anthers

Primordial Stage

The anther is a four-lobed structure in cross section, the wall of

each lobe having different tissues arranged in concentric layers. At the

centre of these layers, which may be three at this stage, there is a core

of one to two spherical or polyhedral cells: the archesporium (Fig. 3.1).

All three wall layers show mitotic activity. The cells of the epidermis

or outer boundary, and the hypodermal cells immediately beneath, all

divide tangentially. The innermost, parietal layer, lying adjacent to

the central core, however, divides both tangentially and radially, giving

rise to a fourth layer of cells between the hypodermis and parietal layer.

The four wall layers are now distinguishable as epidermis, endothecium,

middle layer and tapetum, each represented by a single row of cells

running around the central core (Fig. 3.2). From this time on, mitotic

activity may be observed in all of the four tissue layers and consists

entirely of tangential divisions. Meanwhile archesporial cells undergo several mitotic divisions, finally forming a mass of 5 - 7 cells which directly differentiate into the primary sporogenous tissue.

Premeiotic Stage

Before the onset of meiosis the mitotic activity is completely abolished in both the sporogenous and tapetal tissues. The nuclei in the cells of these tissues become differentiated and larger than those of the surrounding tissues. The chromatin within the nuclei of microsporocytes appears as dense spherical bodies located accentrically in an optically clear nuclear sap (Figs. 3·3, 4·2).

Meiotic Stage

The clear sap area abserved at the premeiotic stage with further dilation of the nuclear membrane, increases during meiotic prophase to a maximum at diakinesis. The cytoplasm of meiocytes develops several lamellar structures which run radially between the plasmalemma and the nuclear membrane like the spokes of a wheel. These structures appear during the early prophase and persist until late diakinesis (Fig. 4·4). At the beginning of zygotene the nucleolus becomes more conspicuous and later moves to one side of a large cluster of chromosomal threads (Fig. 27). The attachment of the nucleolus to its nucleolus-organizer (NO) chromosome is easily observed at diakinesis. The majority of cells have one large nucleolus attached to two bivalents. Rarely, however, cells with two nucleoli are also observed, in which case they are attached to separate chromosomes. Immediately after the disappearance of nucleoli, nuclear membrane, and the cytoplasmic lamellar structures, metaphase I sets in. Precisely during the period when meiocytes are at prophase I the nuclei

of tapetal cells undergo synchronous karyokineses (division of nucleus without cell plate formation), so that during or before the period when meiocytes are at metaphase I all the tapetal cells are binucleate (Fig. 4·5). The anthers of secondary tillers occasionally show abnormalities in this respect (e.g. asynchronous division of tapetal nuclei).

In any event, the tapetal spindle is always oriented along the longer axis of the anther and the daughter nuclei remain in this alignment for the rest of their life (Fig. 4·5). The enlargement of tapetal cells continues up to a stage when microsporocytes are at diakinesis or metaphase I.

Cell enlargement in tapetal and sporogenous tissues observed throughout these stages seemingly is at the expense of endothecium and the middle layer. During the course of their enlargement the cells of the latter two tissues shrink considerably, so that their nuclei become ellipsoidal. This effect is more pronounced, however, in the middle layer than in the endothecium (Figs. 3·3, 3·4).

Postmeiotic Stage

Upon completion of meiosis the four meiotic products remain enclosed within a callose wall, wherein they become delimited by the formation of premexine, a cellulosic wall which provides a framework for the deposition of actual exine substance, the sporopollenin. The tetrads have large centrally located nuclei with loosely arranged chromatin. Cells of the middle layer and endothecium show further shrinkage and a loss of structural details during this stage (Fig. 3·5).

The end of meiosis also marks the beginning of tapetal degeneration. The most obvious changes associated with the decline of tapetal cells are:

the loss of granular structure of cytoplasm, and gradual collapse of cells associated with the abatement of cytoplasm. It becomes difficult to distinguish nucleus from cytoplasm and eventually a complete deformation of the original cellular shape is noted (Figs. 3·6 - 3·8). In some instances a loss of contact between tapetal cells was seen during the early meiotic stages; these cells, however, subsequently followed the usual tapetal degeneration pattern.
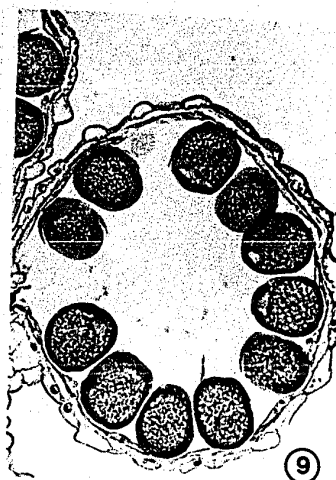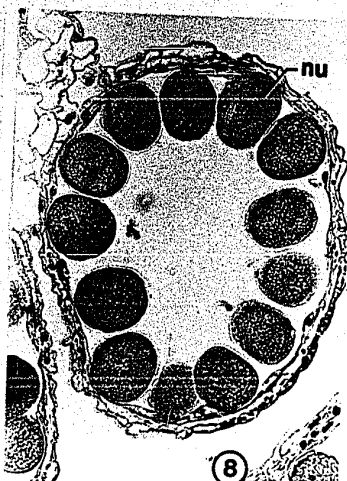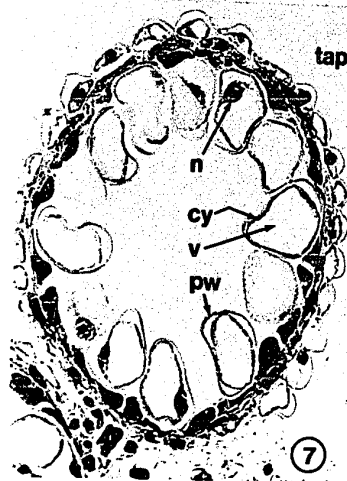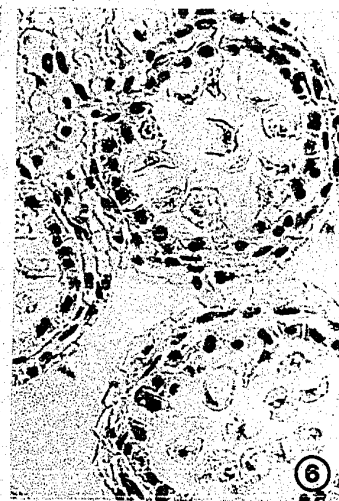
Free Microspore Stage

The release of young microspores from the callose capsule marks the beginning of the FM stage. The cells at this time resemble the meiocytes at diakinesis in that the cytoplasm contain lamellar structures, but are much smaller in diameter (Fig. 4·9). This stage is short and transitory and microspores soon enter into a phase of rapid growth.

Mononucleate Stage

The young microspores rapidly increase in circumference and develop many vacuoles, which merge into a large central vacuole occupying almost the entire cell, leaving only a thin cytoplasmic layer along the wall (Fi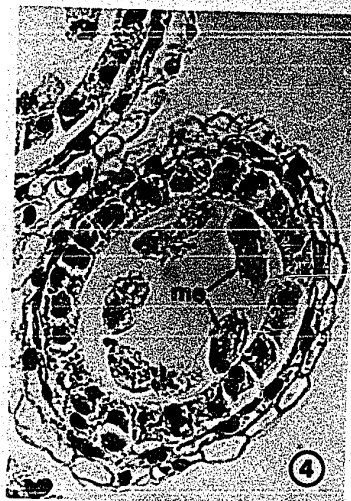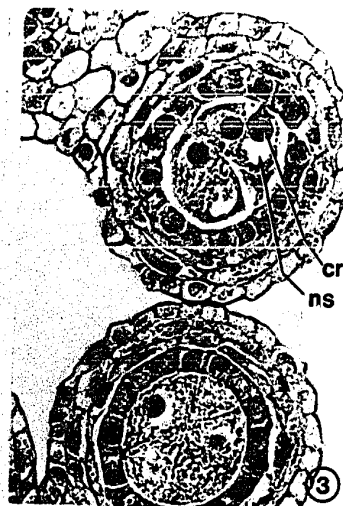g. 3·7). Microspore mitosis occurs while the maturing pollen grain is still in this vacuolated state. Pollen grains develop very thick exine and eventually accumulate a considerable amount of starch. These three events in sequence: (i) microspore mitosis giving rise to a tube and two sperm nuclei, (ii) development of pollen wall, and (iii) accumulation of starch, mark the completion of pollen differentiation (Figs. 3·7 - 3·9 and 4·10 - 4·12).

Fig. 3. Cross-sections of anthers from male-fertile plants (several
lobes shown) showing type-samples of the typical developmental stages
used in the histological and cytochemical analysis. 1, early stage
showing formation of the middle layer (m) between epidermis (e) and
parietal layer (Pl); central core occupied by archesporial cells. X2800.
2, primordial stage showing four layered sporangial wall; epidermis (e),
endothecium (en), middle layer (m), and tapetum (tap); the archesporium
has differentiated into primary sporogenous tissue (sp). X2600. 3,
premeiotic stage; sporogenous tissue nuclei are large with condensed
spherical chromatin, located eccentrically in clear nuclear sap (ns).
X2590. 4, meiotic stage; the meiocytes (me) at telophase I; tapetal
cells are now binucleate. X1870. 5, postmeiotic stage. X1800. 6, free
microspore stage. X1700. 7, mononucleate stage; growing pollen grains
have a large central vacuole (v); tapetum (tap) in advanced stage of
degeneration. X890. 8, 9, mature sporangium with fully developed pollen
grains; nuclei scarcely visible; the tube nuclei at this stage contain
large nucleoli (nu). X800.
Stages 1, 8, and 9 shown here to complete the anther developmental
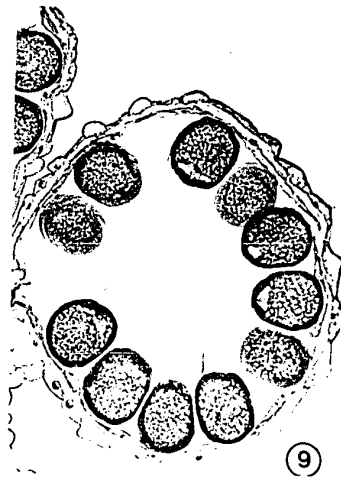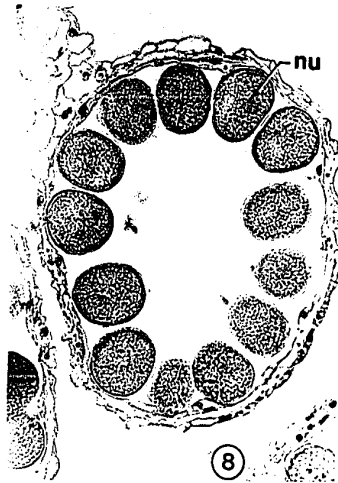sequence, were not included in the actual analysis.

Figure 2 — labels: e, en, m, tap, sp; pl, as, e, m

Figure 3 — labels: cr, ns

Figure 4 — label: me

Figure 5

Figure 6

Figure 7 — labels: tap, n, cy, v, pw

Figure 8 — label: nu

Figure 9
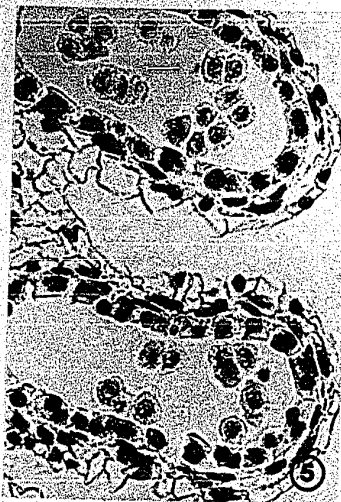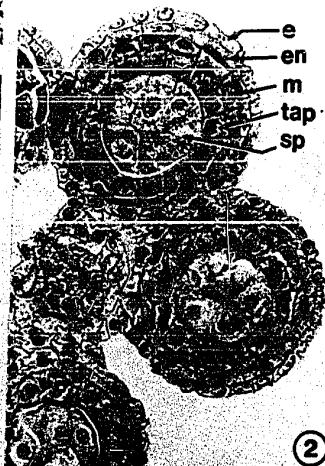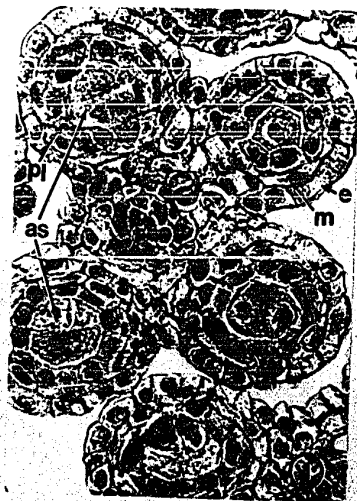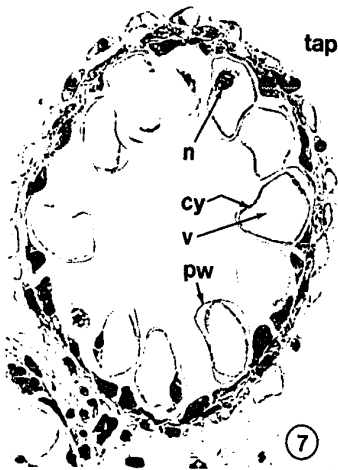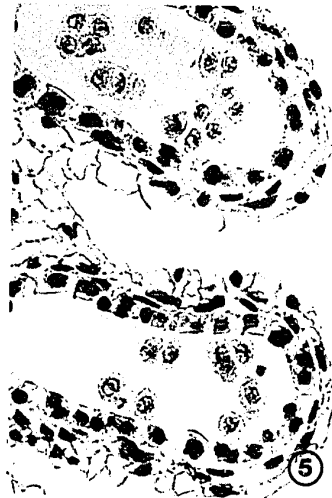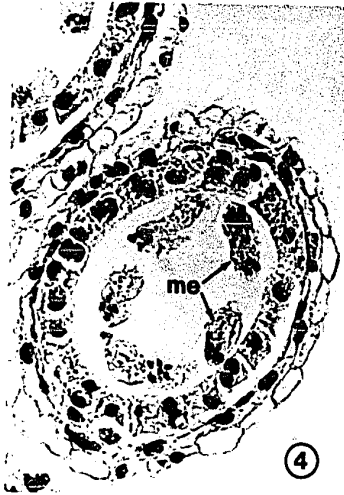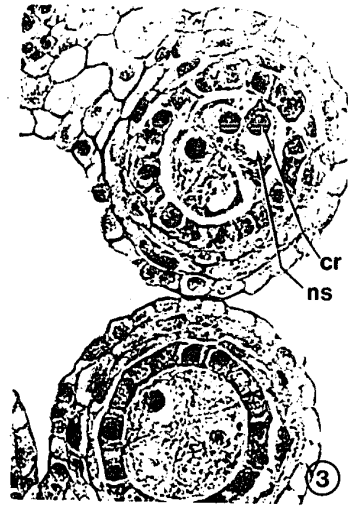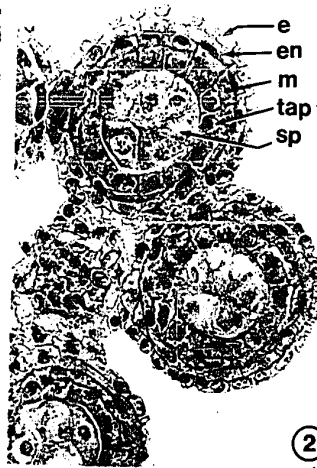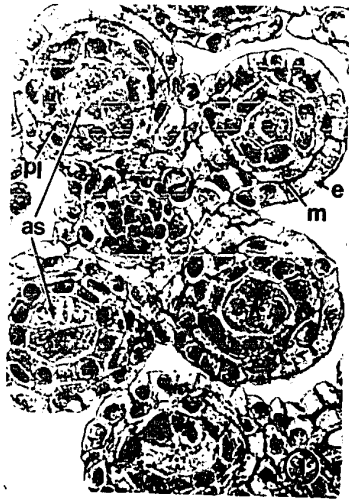
Fig. 4. Longitudinal sections of anthers from male-fertile plants showing type samples of stages as in Fig. 3. 1, primordial stage, showing archesporium (as) with large nuclei (n), nucleoli (nu) and tissues of the sporangial wall. X2800. 2, premeiotic stage with sporogenous tissue (sp) with condensed spherical chromatin (cr) in clear nuclear sap (ns); tapetum well developed with mononucleate cells. X1200. 3, meiocytes at pachytene with large nucleoli (nu); tapetal nuclei at karyokinetic prophase. X1700. 4, diakinesis; note cytoplasmic lamellar structures around meiocyte nuclei; tapetal cells binucleate. X900. 5, tangential section of tapetum at late meiotic stage showing binucleate cells with nuclei oriented along the long axis of the anther. X900. 6, metaphase I. X900. 7, telophase I. X830. 8, postmeiotic stage. X900. 9, free microspore stage. X750. 10, growth and vacuolation of free microspores; tapetum degenerating. X800. 11, mononucleate stage; tapetal cells (tap) have almost degenerated. X800. 12, fully differentiated pollen grains, each with tube nucleus (nv) and generative nuclei (ng). X800.
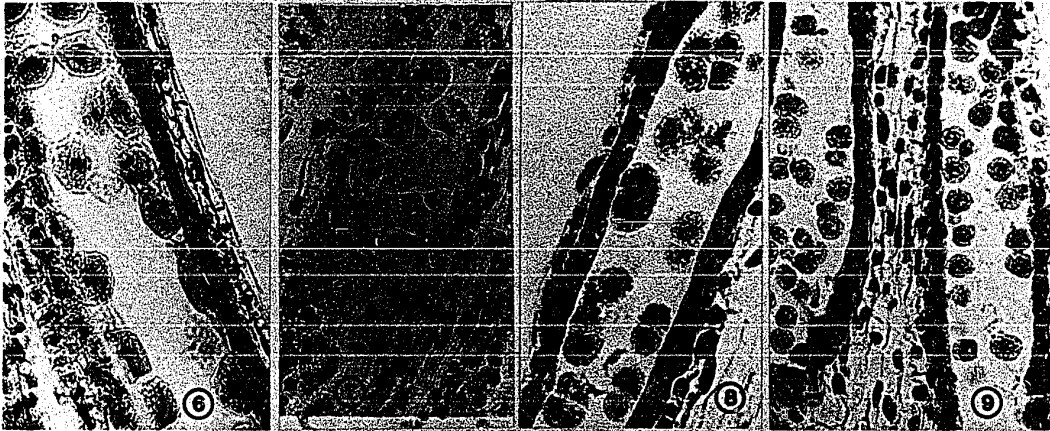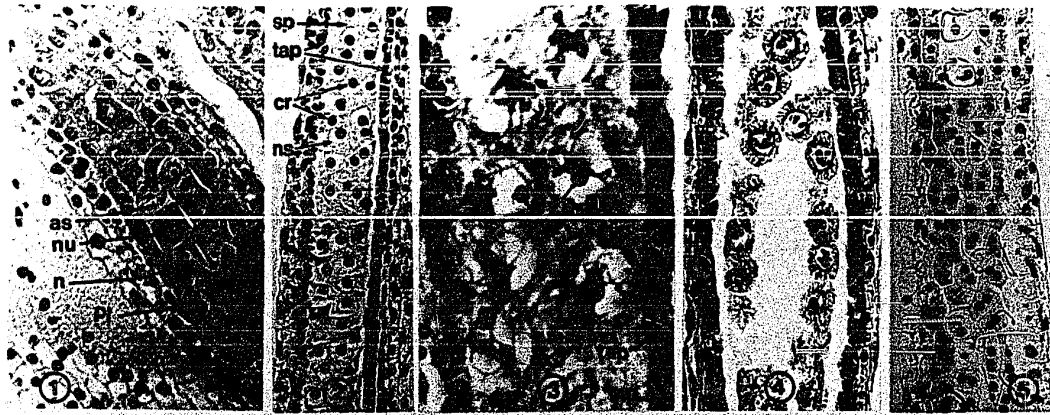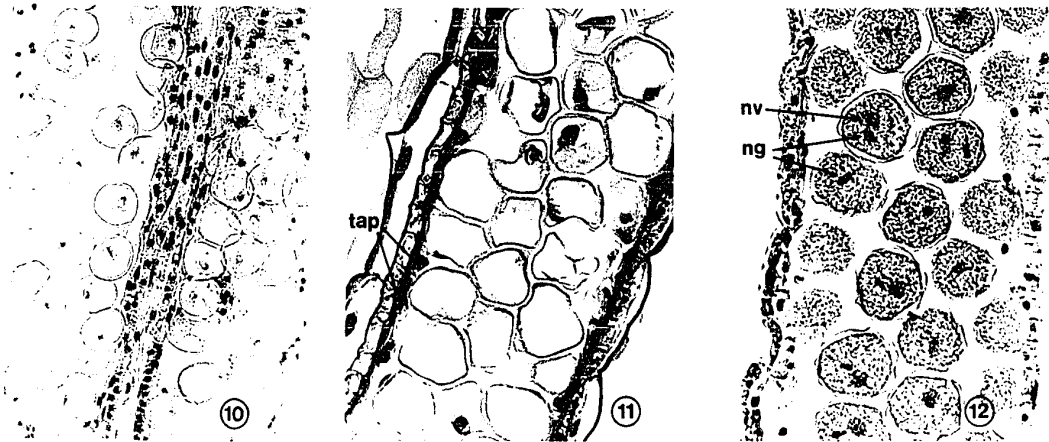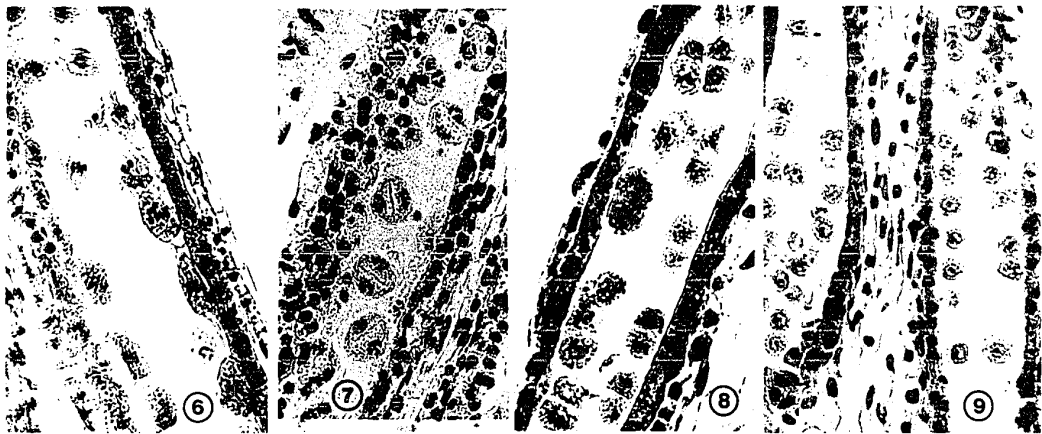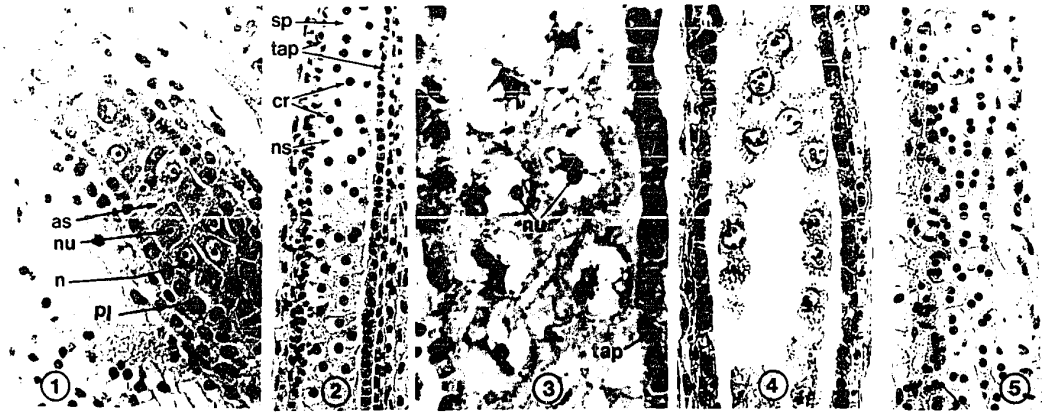
Histology of Sterile Anthers

ms 5

In both timing and morphology the different aspects of anther
development through the succession of primordial (P), premeiotic (P_1)
and meiotic (M) stages seem identical to the normal (viz. fertile anthers
of this line). The developmental pattern, however, begins to deviate
during the postmeiotic (PM) stage. The release of meiotic products from
the callose wall is relatively delayed and the microspores start vacuo-
lation while still within the tetrad capsule. At the same time an inward
curving of microspore walls in the cross-septa of tetrads is observed,
giving these cells a half-moon shape (Fig. 5·3). After release from the
callose envelope the young microspores do not grow in diameter or wall-
thickness, although morphologically their nuclei appear normal.

During the mononucleate (MN) stage microspores accumulate deeply
staining cytoplasm and grow in diameter (Fig. 5·5). During this period,
however, nuclear and cytoplasmic degeneration become evident. Nuclei of
these cells, although maintaining normal size and appearance for some
time, never undergo mitotic division. Cytoplasmic degradation takes two
forms: the first involves a change in consistency and the second a change
in quantity. Thus at the time the pollen cytoplasm would normally be full
of starch they are completely depleted, and what remains is the sporangial
lumen containing only the shrivelled ghosts of pollen (Fig. 5·6).

The tapetal tissue does not degenerate as it normally would from
the late meiotic stages (e.g. late telophase); instead the cells start to
swell, show loss in cytoplasm, and have comparatively thin and weak walls.
The nuclei in these cells, however, remain apparently similar to those of

Fig. 5. Cross-sections of *ms 5* anthers. 1, premeiotic stage. X2400.
2, meiotic stage; meiocytes at early diakinesis. X1800. 3, post-
meiotic stage, note incurving of tetrad septa walls. X1730. 4, free
microspore stage, the few microspores present are flaccid (at this
stage the whole anther becomes very weak and no good sections could
be obtained). X1500. 5, mononucleate stage; microspores completely
deformed; tapetum hypertrophied but binucleate. X1400. 6, transverse
and longitudinal sections of anthers corresponding to mature stage;
microspores devoid of cytoplasm and nuclear material; tapetal cells
completely disintegrated. X1400.
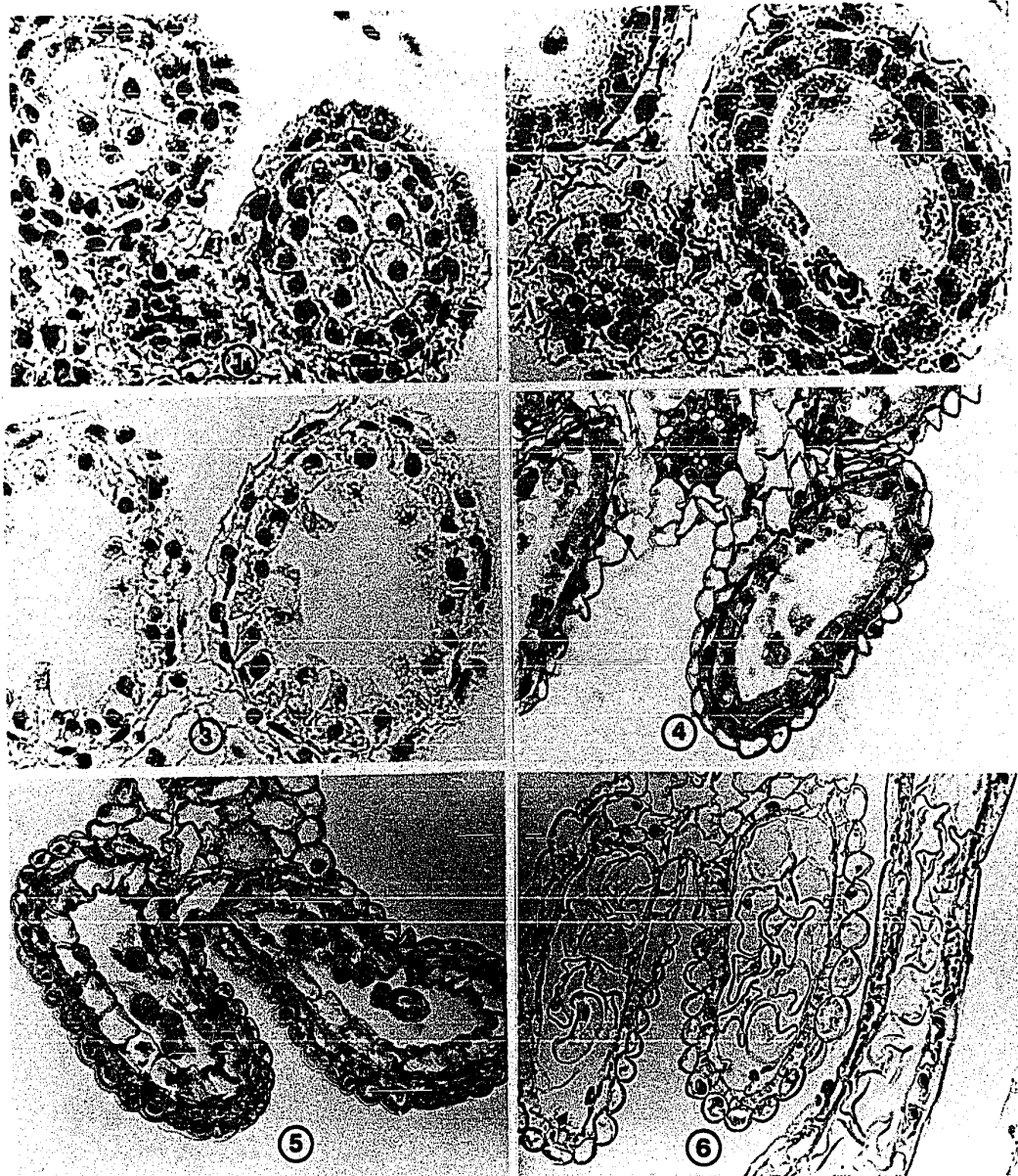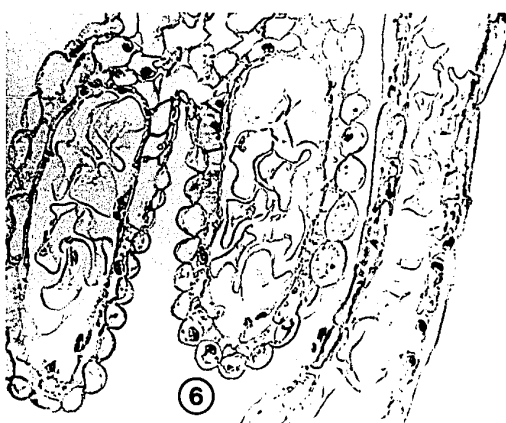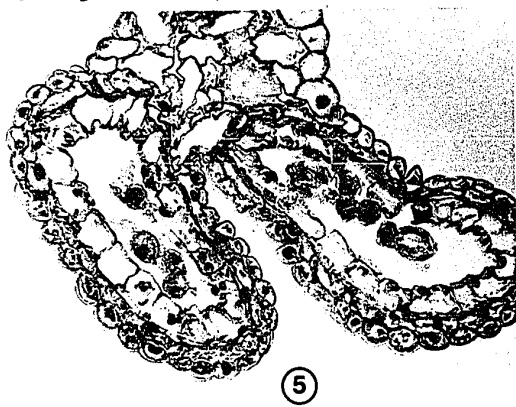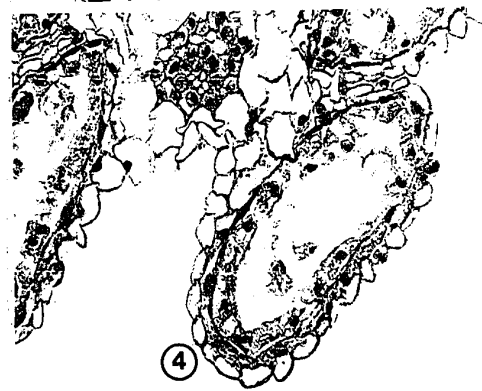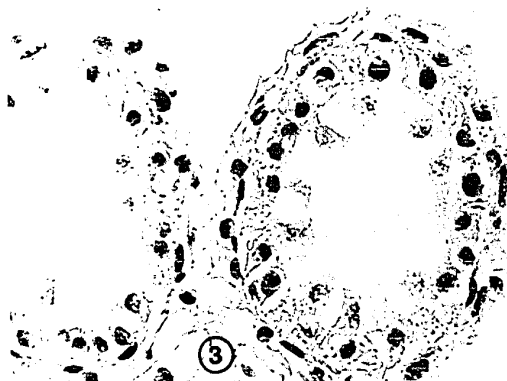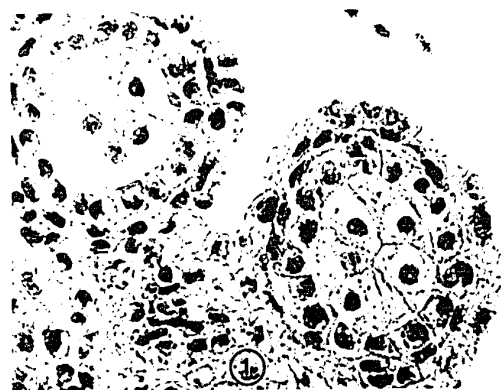
normal anthers (Figs. 5·3, 5·4). During the MN stage the tapetum en-
larges greatly and forms a thick cushion of a single layer of enlarged
highly-vacuolate cells along the inner lining of the sporangial lumen
(Fig. 5·5). This tissue is eventually obliterated, leaving only a thin
layer of wall material (Fig. 5·6).

These observations lead to the inference that deviation from
normal first appears at the FM stage, whereas tapetal abnormality becomes
ostensible earlier, during the late meiotic stages. The endothecium and
middle layer display changes identical to those of normal anthers.

ms 9

The anther development at P, P$_1$ and M is closely similar to the
normal (Figs. 6·1, 6·2). The first indication of deviation appears at
the PM stage (Fig. 6·3), when the nuclei and cytoplasm of microspores and
tapetal cells stain relatively darker than those of normal.

After dissociation of tetrads, the microspores tend to enlarge,
but their growth seems to be arrested soon after the free microspore stage.
The richness and granular structure of the cytoplasm declines during the
FM stage, so that in the ensuing MN stage the cytoplasm is significantly
decreased in amount and displaced toward the middle of the cell. In
addition they appear thin-walled but with visibly normal nuclei (Fig. 6·4),
which later degenerate, losing their spherical shape and staining capacity
(Fig. 6·4). Subsequently the microspores collapse and become clumped
(see Figs. 6·5, 6·6).

The tapetal cells first increase in radial thickness and then from
FM they suffer a relatively rapid degeneration. This degeneration, how-
ever, is different from that of the normal anther in that an excessive

Fig. 6. Cross sections of sterile anthers of *ms 9* at different stages
of development. 1, 2, premeiotic and meiotic stages; the microspores
in 2 are at pachytene; shrinkage in sporogenous and tapetal tissue is
an artifact. X850. 3, postmeiotic stage, microsporocytes and tapetal
cells heavily stained, tapetum radially enlarted. X1250. 4, mononu-
cleate stage; tapetal degeneration different from normal (see Fig. 3·7
for comparison). X480. 5, 6, post-mononucleate stage; note structure
of anther lumen, sporogenous and tapetum have completely lost their
cellular organization. X480.
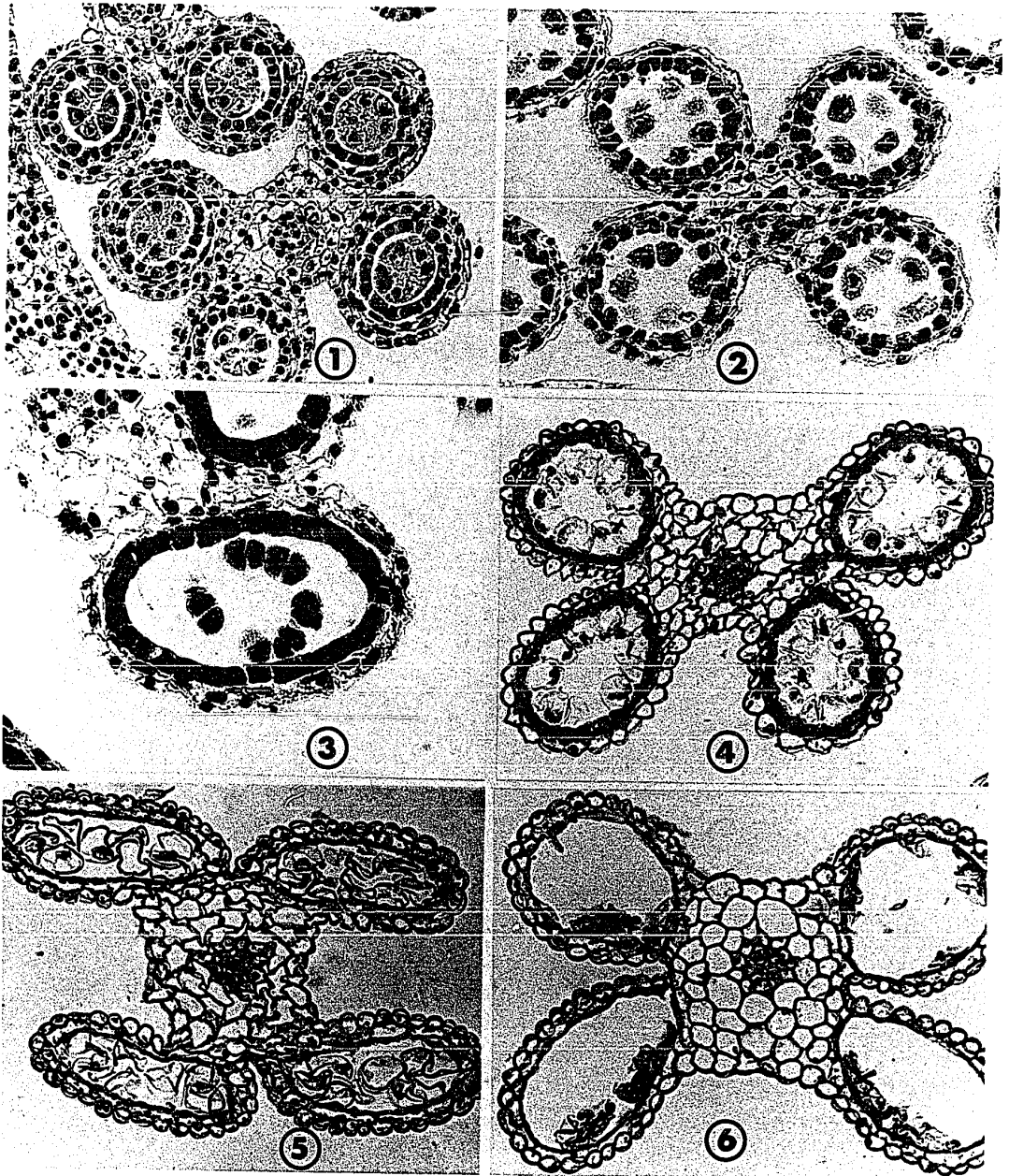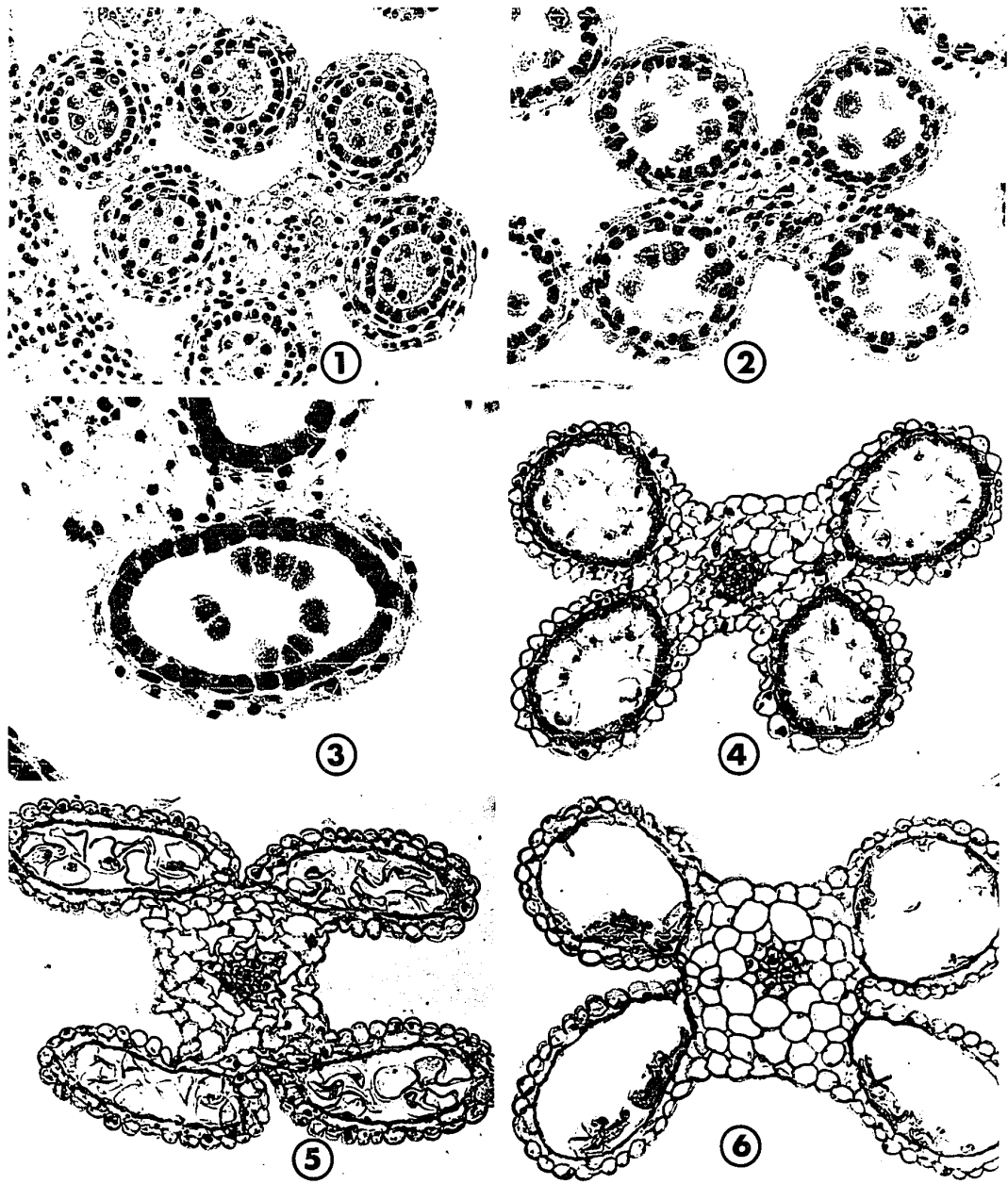
loss of the cytoplasm and cell turgidity is apparent at the FM stage
(Fig. 6·4) and from then on further structural degradation reduces it to
a thick band in which no cellular details are visible (Figs. 6·5, 6·6).

It may be inferred that further growth of microspores is impeded
soon after their emergence from tetrads and an obvious cessation in
their growth is coincidental with the relatively faster breakdown of
tapetum during the FM-MN period.

ms 10

The developmental pattern and general morphology are normal up to
the PM stage, except for a delayed or extended mitotic activity in the
tapetum (Fig. 7·1). In about 15% of *ms 10* anthers (from a sample of 85
anthers studied) the tapetal nuclei exhibited mitotic activity up to as
late as leptotene, whereas in the normal course this activity terminates
before the initiation of meiosis. Despite this delay in mitotic activity
and karyokinesis the tapetal cells are able to complete the process and
are invariably binucleate by meiotic prophase II.

After release from tetrads the microspores grow to about the normal
dimensions up to early MN, but microspore mitosis does not occur and the
nuclei subsequently lose their spherical shape and stainability. Later
at FM the pollen cytoplasm develops a tendency to withdraw from the wall
in a clump (Fig. 7·4) rather than to line it, as in normals. The pollen
wall later folds inward, giving a deformed, often sickle-shaped appear-
ance to the pollen grains (Fig. 7·5). Their dimensions vary significantly
from anther to anther, but remain almost the same within the four lobes
of an anther.

In tapetal cells postmeiotic degeneration is identical to that of

Fig. 7. Cross-sections of sterile anthers of *ms 10* at various developmental stages: 1, premeiotic stage; some tapetal cells still showing mitotic activity. X2600. 2, meiotic stage. X1900. 3, postmeiotic stage. X1870. 4, mononucleate stage; microspores show deficiency in cytoplasm; tapetum shows signs of degeneration. X900. 5, late mononucleate stage, showing darkly stained, rich tapetal cytoplasm; grossly deformed mononucleate pollen. X1200. 6, still later mononucleate stage; note heavy vacuolation or loss of tapetal cytoplasm. X1200.
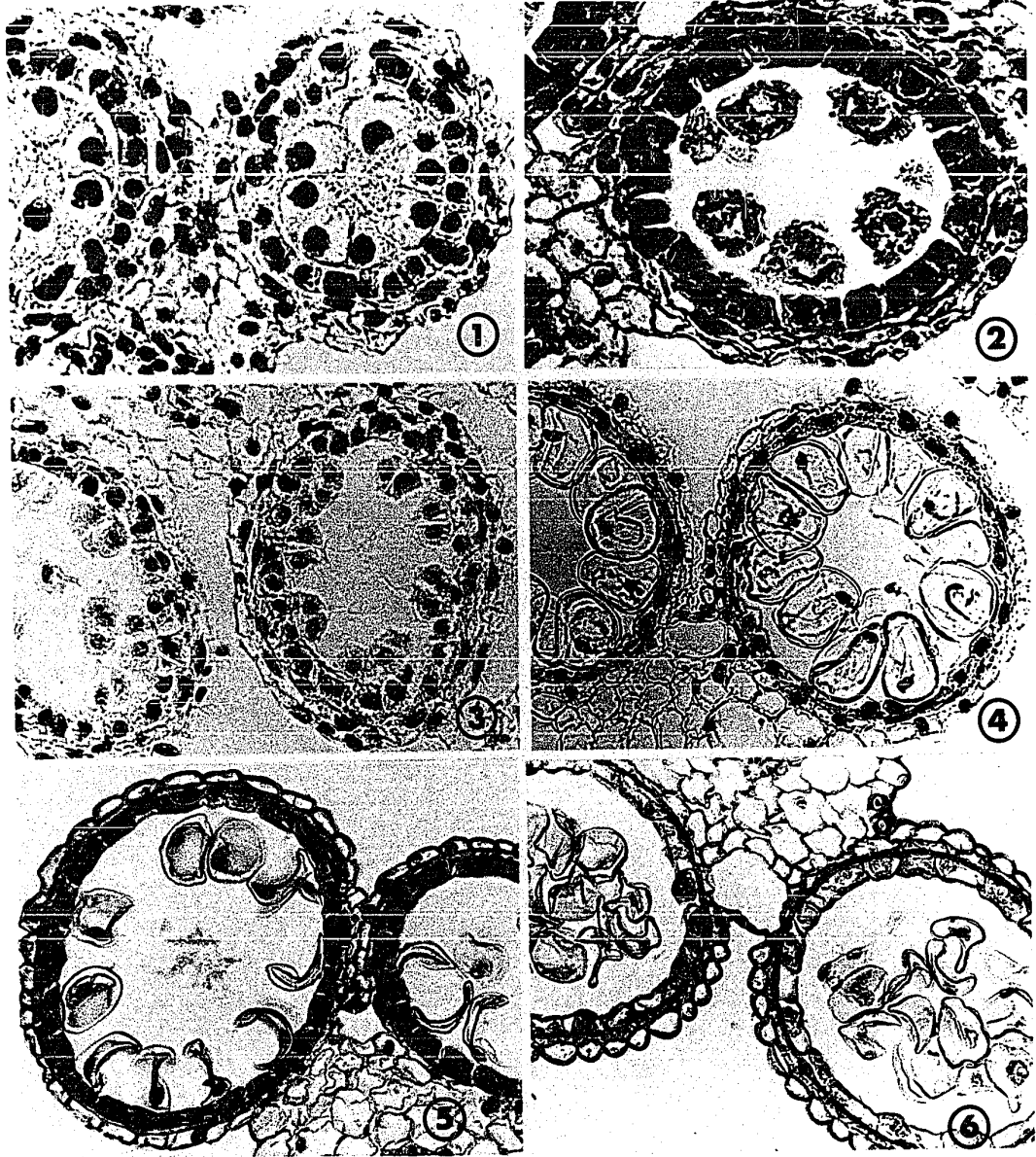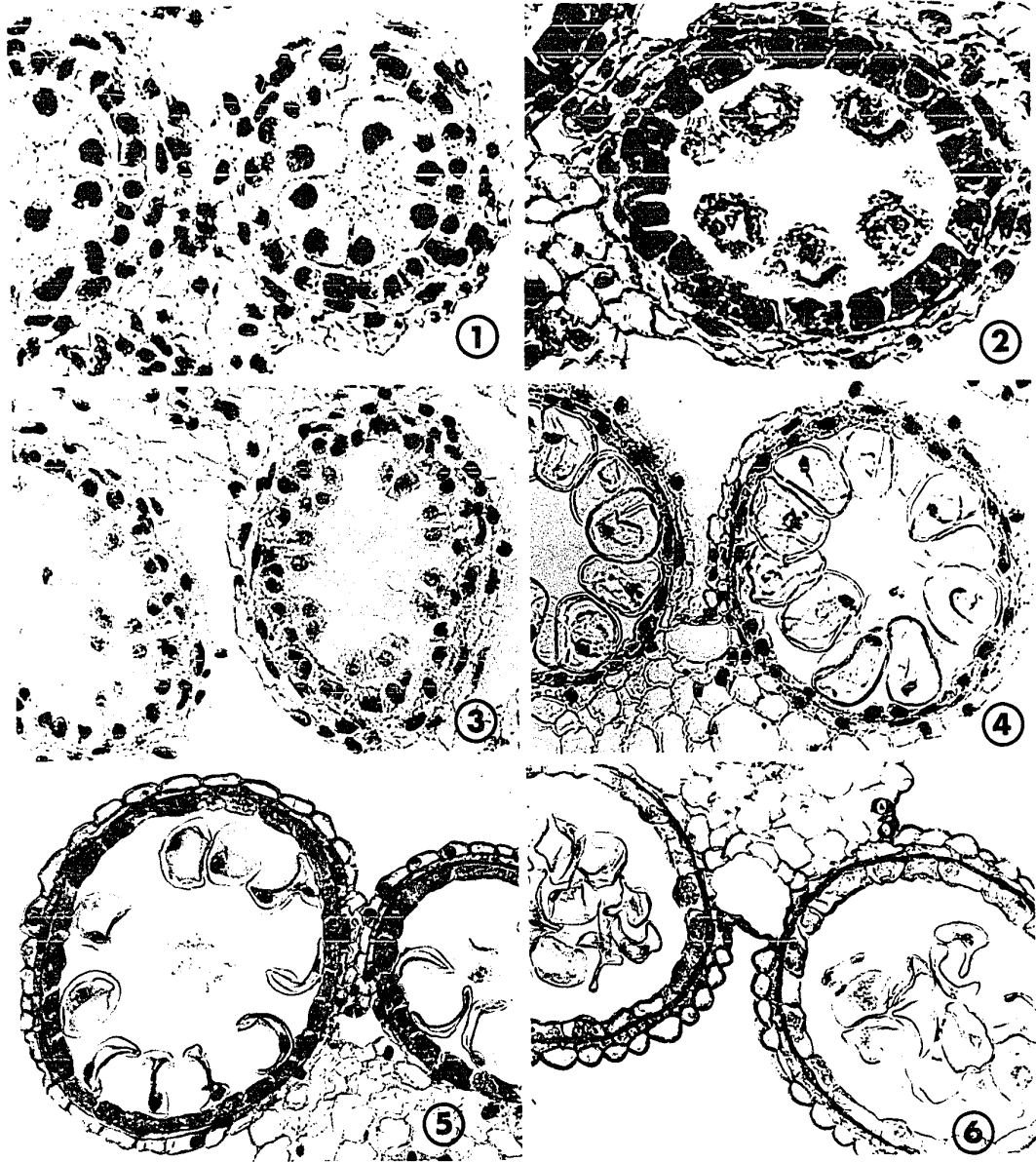
normal anthers until the beginning of MN stage (Fig. 7·4). At this time

the tapetum manifests a state of further expansion (Fig. 7·5) in which

the cells develop thick walls and become rich in darkly staining, amorph-

ous cytoplasmic material so that the nuclei are scarcely traceable. Sub-

sequent degradative processes deplete the cytoplasmic content and the

cells become irregularly vacuolated (Fig. 7·6) with frail and weakly

stainable nuclei.

Beginning at M the endothecium and middle layer dramatically

shrink back, especially the latter, which forms a thick band probably

consisting only of cell walls. At the beginning of the mononucleate stage

the diameters of sporangial lumens are greatly variable between anthers,

but not within the four lobes of the same anther. The average lumen

diameter of male-sterile anthers at the late mononucleate stage remains

about 2/3 that of the normal.

ms 14

Sporogenesis is normal until PM (Figs. 8·1, 8·2), but the free

microspores demonstrate striking abnormalities. It appears as if they are

released from tetrads in a premature condition. They have inconsistent

and poorly developed walls; thus after emerging from tetrads they usually

assume amoeboid shapes with randomly located nuclei (Figs. 8·3, 8·4),

whereas in the normal at this stage the nuclei are centrally located.

There is little evidence of further development in these cells.

They appear to collapse by an inward folding of their walls, giving a

crescent-like shape to the cells (Fig. 8·5). The typical growth pattern

of microspores from the free microspore to the mononucleate stage is never

observed. Ultimately the cytoplasm is nearly completely degraded and what

Fig. 8. Cross-sections of sterile anthers of *ms 14*: 1, premeiotic stage, cellular morphology of different antheridial tissues normal. X1300. 2, meiotic stage (metaphase I); few tapetal cells are binucleate, others have only one nucleus. X970. 3, free microspore stage; microspores with irregularly located nuclei and poorly developed walls, tapetal cells have thick inner tangential walls; most tapetal cells in one anther lobe (top left of photomicrograph) are mitotically active, few in the other lobe are also in active mitosis; tapetal cells which are not dividing have spherical, more compact nuclei of different sizes (arrows). X1400. 4, two anther lobes showing variable karyokinetic behaviour of tapetal nuclei. X1600. 5, mononucleate stage with collapsing microspores and hypertrophied tapetal cells filled with darkly staining material. X1100. 6, complete deformation of different sporangial tissues. X1200.
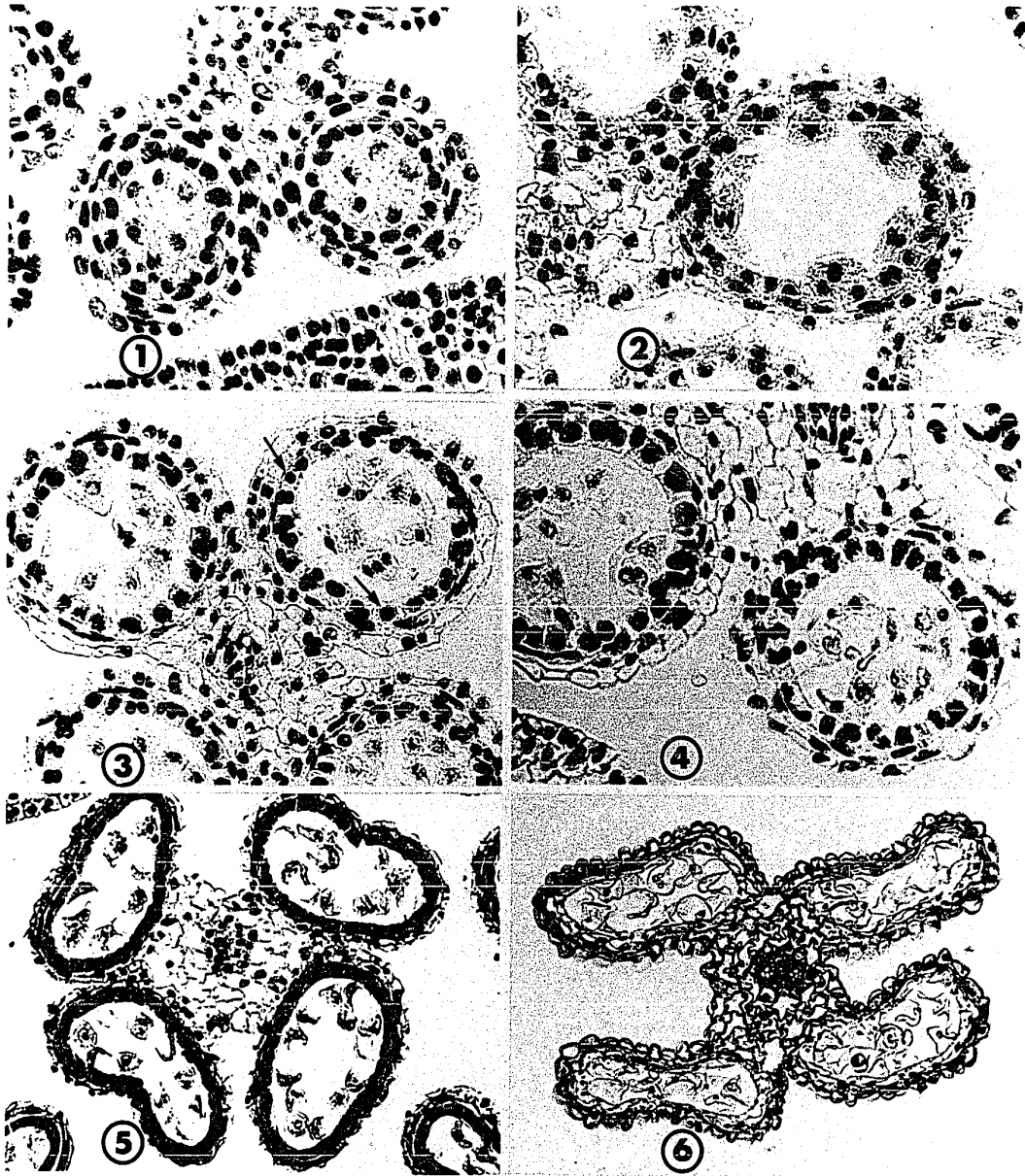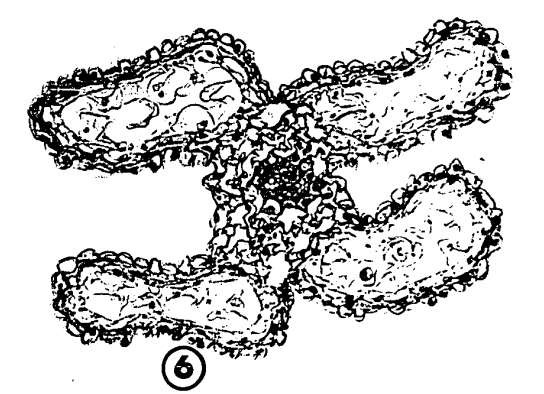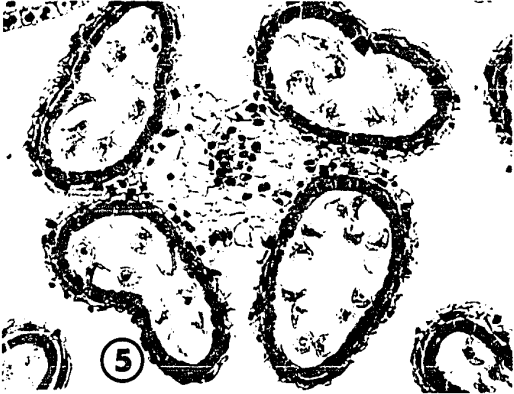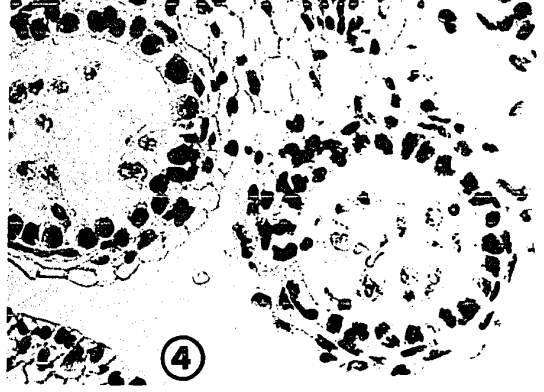
is left is a mass of hollow twisted cell capsules (Fig. 8·6). In a
small proportion of such cells, however, remnants of nuclear material may
still be visible.

The tapetal tissue shows very deviant behaviour. Karyokinesis is
irregularly postponed; a few of the cells begin to divide at pachytene,
others as late as the FM stage and still others (≃ 2%) may not divide at
all (see Figs. 8·2 - 8·4). The nuclei which do not divide at all vary
considerably in diameter (Fig. 8·3 arrows). This lack of synchrony
within the single anther locule extends to the four lobes of the anther
as shown in Fig. 8·4. As the anther matures (near the FM stage) the
proportion of binucleate tapetal cells is increased. They are filled with
densely staining cytoplasm and become hypertrophic. The inner tangential
wall of tapetal cells becomes thicker from the early PM stage. In the
course of time, however, like the sporogenous tissue, they lose their
content, become flaccid and completely deformed (Fig. 8·6).

ms 18

The main histological difference between anthers of this line and
normal ones is a general delay in development. Meiotic stages corre-
sponded with a 2nd-4th intermodal length of 10-1/2 to 11-1/2 inches,
compared with 10 inches for normal (Fig. 1). This length (10-1/2 -
11-1/2 inches) corresponds with the postmeiotic stage in normal. In spite
of this delay, morphologically the differentiation of sporogenous tissue
seems normal until the completion of meiosis (Figs. 9·1, 9·2). The PM
stage is characterised by normal tetrads.

At the onset of the FM stage the cell walls of newly formed spores
start to invaginate and to show retarded growth (Fig. 9·3). The growth

Fig. 9. Cross- and longitudinal sections of sterile anthers of
ms 18: 1, early premeiotic stage; morphology of sporangial tissues
normal. X2400. 2, meiotic stage (telophase I) showing no apparent
deformities. X1700. 3, longitudinal section of free m crospore
stage; microspores with wall invaginations; binucleate (solid
arrow) and mononucleate (hollow arrow) tapetal cells. X1300.
4, longitudinal section of mononucleate stage; deformed microspores;
abnormally degenerating tapetum. X600. 5, as in 4, in transverse
section. X670. 6, as in 4, at higher magnification; note accumu-
lation of granular structures (arrows) in endothecial cells. X1300.
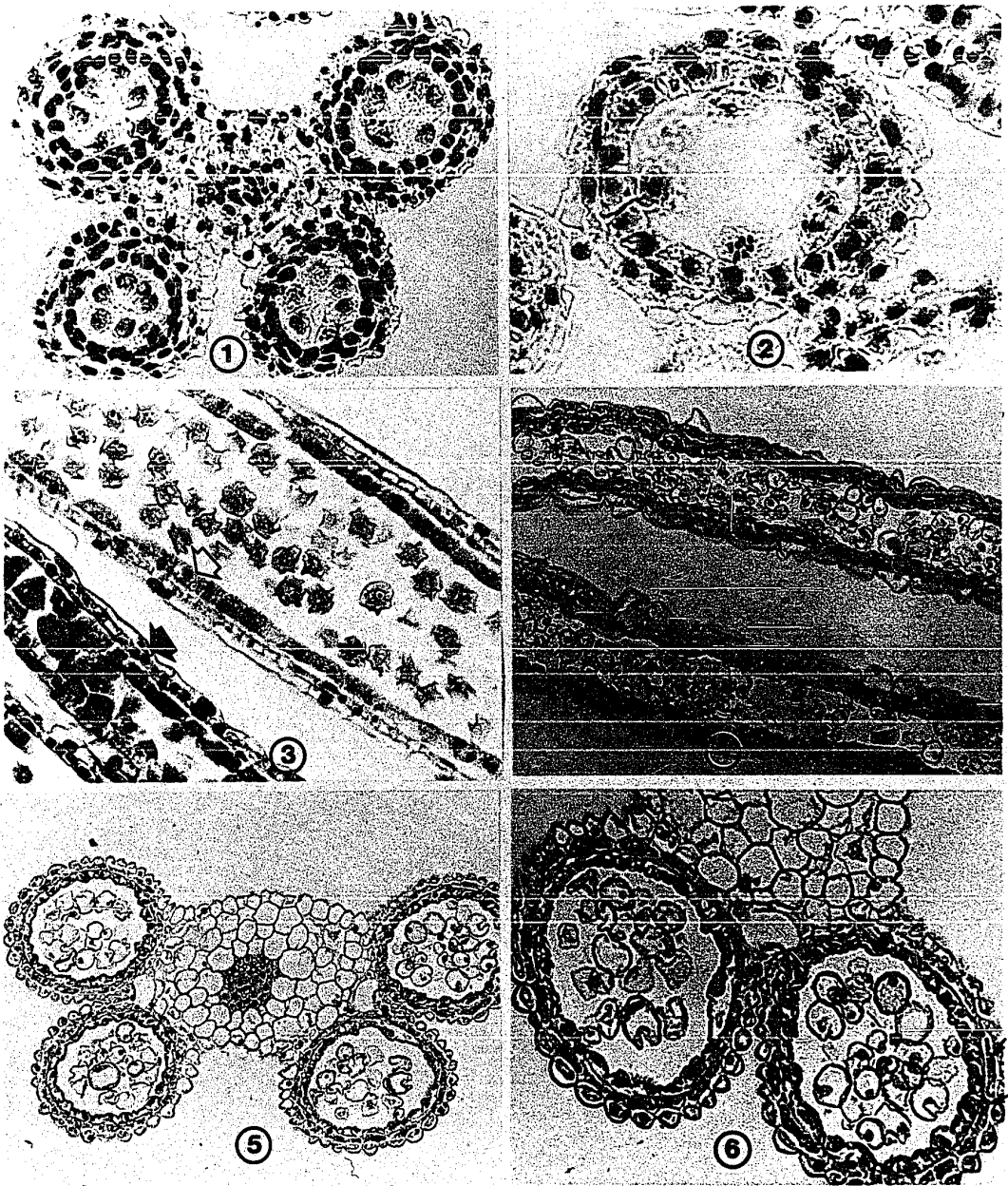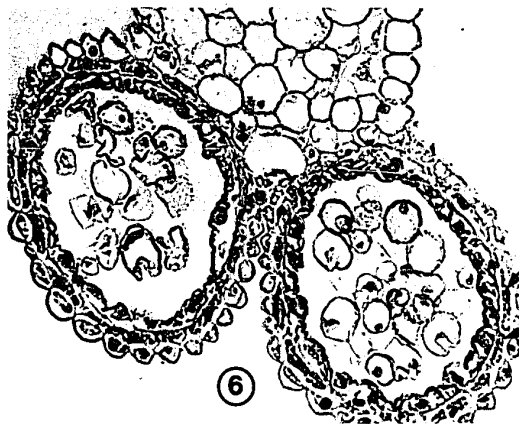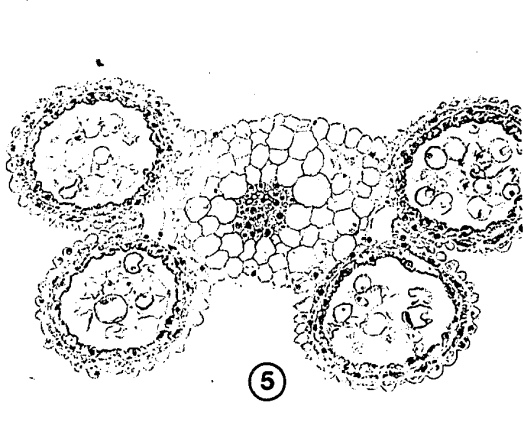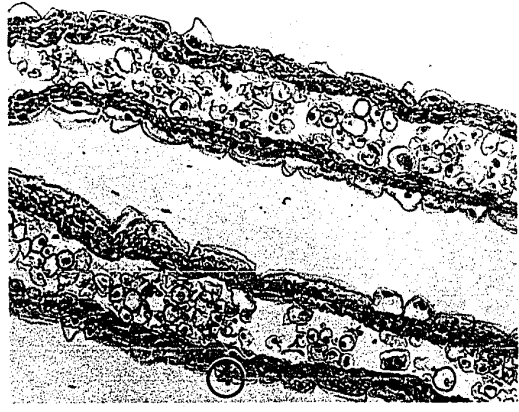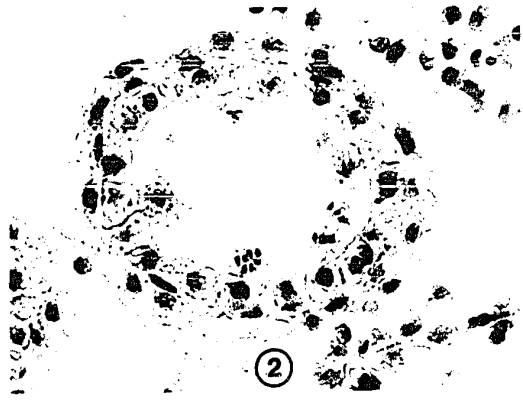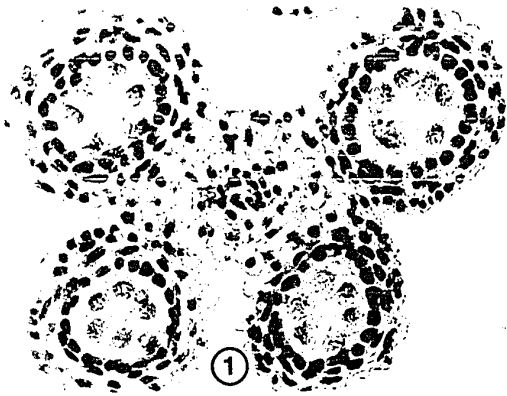
patterns and rates vary greatly from spore to spore within a single locule, so that at MN, cells of different sizes can be seen randomly scattered in the sporangial cavity. The cells are highly vacuolated and poor in cytoplasm and nuclear material, with nuclei invariably displaced to one side (Figs. 9·4, 9·6).

The development of tapetal tissue is dimensionally similar to that in normal anthers up to PM but a large percentage of cells remain uninucleate throughout their life (Fig. 9·3, hollow arrow) and only about 10% (based on a sample of 360 cells) become binucleate (solid arrows). The nuclear diameter in both the uninucleate and binucleate cells is on the average smaller than in the binucleate tapetum of normal anthers (compare Figs. 9·3 and 4·9). Tapetal degeneration is also delayed and different in nature from that of normal anthers. During PM-MN the tapetal layer develops an inner wall having a structured appearance and accumulates clumps of cytoplasm within the cells (Fig. 9·6).

The middle layer is completely absorbed during meiosis whereas the endothecium persists, showing a distinct cellular structure through-out the life of the anther. During the later stages the cells of the endothecium and the epidermis accumulate deeply staining cytoplasmic granules (Fig. 9·6 arrows) which have not been seen in normal anthers. The anther lobes remain stunted in growth and the mature lumen diameter is not more than 1/2 that of the normal.

Cytochemical Studies

The DNA and Histone of Nuclei of Fertile Anthers

DNA: The data on DNA analysis given in Tables II, IV, VI, VII,

and X show that there is an initial phase of DNA synthesis which occurs in both sporogenous and tapetal tissues during P-P_1. The value at P_1 should in all probability mark the 4C quantity. At some time during P_1 to PM the microsporocytes complete meiosis, and thus at PM the DNA values are reduced due to chromosomal segregation. DNA synthesis proceeds almost linearly through the PM-MN period, while the microspores are differentiating in preparation for mitosis. The nuclei of sporogenous tissue, therefore, demonstrate two conclusive periods of DNA synthesis, viz. a premeiotic (P to P_1) and a postmeiotic (PM to MN). At a time when the microspore nucleus is completing its mitosis the spore is rapidly filled with starch granules. This heavy accumulation of starch renders cytophotometric estimation of nuclear material rather difficult and unreliable. Therefore, for the present study, measurements were made up to the mononucleate stage when the nuclei had a fair amount of clear area around them and accurate measurements were ensured.

Like the nuclei of sporogenous tissue the tapetal nuclei also show two periods of DNA synthesis, the first during P to P_1, where there is nearly a twofold increase over the initial value, the second from M to PM, where the gradient of nuclear DNA increase is less marked and the peak value is substantially less than that at P_1. Each of these two periods of synthesis is followed by a decline in DNA amount. From P_1 to M the value falls to about the same level as at P, probably due to the distribution of DNA to daughter nuclei during karyokinesis. During the PM-FM the rate of decline is closely identical to the rate of synthesis during the preceding period (i.e. M-FM), and subsequent to FM it is slightly slowed down.

It may be seen that the second DNA synthesis periods in sporogen-
ous and tapetal nuclei do not exactly coincide as do the first ones.
This in the former is indicated probably at the early PM stage and in the
latter sometimes when the meiocytes are at meta-anaphase I.

Histone: The trends of histone turnover correspond fairly closely
to that observed for DNA. This is true for both the sporogenous and
tapetal tissue. Ostensibly, however, the histone amounts are compara-
tively less than the DNA amounts; eventually the DNA/histone ratios are
always seen to be above one, and mostly in a range of 1.1 to 1.6.

The DNA and Histone of Nuclei of Sterile Anthers

ms 5:

DNA. The DNA-measurement data from the nuclei of sporogenous and
tapetal tissues of male-fertile and male-sterile anthers of *ms 5* are
given in Table II and plotted in Figure 10. The DNA values of sporogenous
tissue of fertile and sterile types are not significantly different up to
PM. The free microspore (FM) stage exhibits marked differences in DNA
values. The microspores of normal anthers have DNA amounts greater than
those of the preceding stage whereas the microspores of sterile anthers
show a drop in DNA. This disparity further increases at MN when the
difference becomes approximately twofold (1.66 vs. 0.80 for fertile and
sterile sporogenous tissues, respectively). The increase in difference,
as is clear from Fig. 10, is due to a simultaneous increase of DNA in the
fertile and a further decrease in the sterile tissue.

The tapetal nuclear DNA values of fertile and mutant anthers are
almost identical throughout the different developmental stages. From the

primordial (P) to the premeiotic (P_1) stage the trend of DNA increase is ostensibly similar to that in sporogenous tissue (Fig. 10). In subsequent stages (PM-MN) the slopes of the tapetal curves parallel those of the sporogenous tissue curve for sterile anthers, whereas the curve for sporogenous tissue of fertile anthers shows a positive gradient during this period.

Histone. Variations in histone amounts through different developmental stages of male-fertile and male-sterile anthers follow trends closely similar to those of the DNA. There is a parallel increase of histone from P to P_1 in sporogenous and tapetal tissues of fertile and sterile anthers (Table III, Fig. 11). The P_1 stage marks the peak amounts of histone due to extensive synthesis. Following this, the M and PM stages indicate a marked decrease, probably due to the segregation of chromatin to the meiotic products. The tapetal tissue shows a minor peak at the PM stage in both fertile and mutant anthers.

DNA/histone ratio. A plot of DNA/histone ratios is given in Fig. 12. It can be seen that the ratios at different developmental stages of male-fertile and male-sterile anthers remain confined to a narrow range of 1 to 1.5, except for tapetal tissue at the FM stage and sporogenous tissue at the MN stage.

Up to the FM the DNA/histone curves for both sterile and fertile sporogenous tissue are in close agreement; the same is true of the tapetum. In both cases, the pairs of curves show an almost parallel form, and are inflectionally identical except at the MN stage, where they clearly differ. Similarly, slight differences become apparent between the tapetal tissues of normal and mutant anthers at the FM stage.

Table II. DNA - Feulgen amounts (arbitrary units) per nucleus of sporogenous and tapetal tissues of male-fertile and male-sterile barley anthers of *ms 5* at six sequential stages of development. (Each value is the mean of a sample of 20 nuclei.)

Developmental stage of anther	SPOROGENOUS TISSUE			TAPETAL TISSUE		
	DNA - Feulgen values ± standard error		t-value	DNA - Feulgen values ± standard error		t-value
	Male-fertile	Male-sterile		Male-fertile	Male-sterile	
P	2.01 ± 0.05	2.22 ± 0.19	0.90	1.86 ± 0.04	1.79 ± 0.04	0.79
P_1	4.22 ± 0.18	4.29 ± 0.19	0.16	4.11 ± 0.03	3.98 ± 0.09	1.18
M	-	-	-	1.76 ± 0.04	1.69 ± 0.03	0.96
PM	1.21 ± 0.04	1.18 ± 0.04	0.38	1.98 ± 0.04	2.00 ± 0.03	0.28
FM	1.53 ± 0.03	1.02 ± 0.01	12.61*	1.65 ± 0.04	1.71 ± 0.03	0.60
MN	1.66 ± 0.10	0.80 ± 0.01	14.9*	1.50 ± 0.09	1.52 ± 0.04	0.12

*Significant at 5% level.

Table III. Histone - Fast green amounts (arbitrary units) per nucleus of sporogenous and tapetal tissues of male-fertile and male-sterile barley anthers of *ms 5* at six sequential stages of development. (Each value is the mean of a sample of 20 nuclei.)

Developmental stage of anther	SPOROGENOUS TISSUE			TAPETAL TISSUE		
	Histone - Fast green values ± standard error		t-value	Histone - Fast green values ± standard error		t-value
	Male-fertile	Male-sterile		Male-fertile	Male-sterile	
P	1.81 ±0.01	1.88 ± 0.03	0.55	1.32 ± 0.04	1.17 ± 0.05	1.79
P₁	2.99 ±0.07	2.89 ± 0.07	0.67	2.75 ± 0.14	2.82 ± 0.05	0.36
M	-	-	-	1.39 ± 0.03	1.33 ± 0.03	0.99
PM	1.16 ±0.03	1.22 ± 0.03	1.09	1.53 ± 0.08	1.65 ± 0.07	0.79
FM	1.42 ±0.03	0.97 ± 0.04	6.47*	1.17 ± 0.04	1.08 ± 0.04	1.06
MN	1.45 ± 0.13	0.92 ± 0.01	3.64*	1.12 ± 0.06	1.16 ± 0.02	0.59

*Significant at 5% level.

Fig. 10. Profile showing amounts (arbitrary units) of DNA -

Feulgen per nucleus at six sequential stages of development in

the sporogenous tissue ●———● and tapetal tissue O··——··O

of male-fertile anthers and the sporogenous tissue ●------● and

tapetal tissue O—— ——O of male-sterile anthers of *ms 5*. Measure-

ments were taken from the interphase nuclei only. Therefore, nuclei

of sporogenous tissues at M were not analysed and arrows with thin

broken lines are given to show the continuity of curve for sporogenous

tissues. (P) Primordial stage; (P_1) Premeiotic stage; (M) Meiotic

stage; (PM) Post-meiotic stage; (FM) Free microspore stage; (MN)

Mononucleate stage.
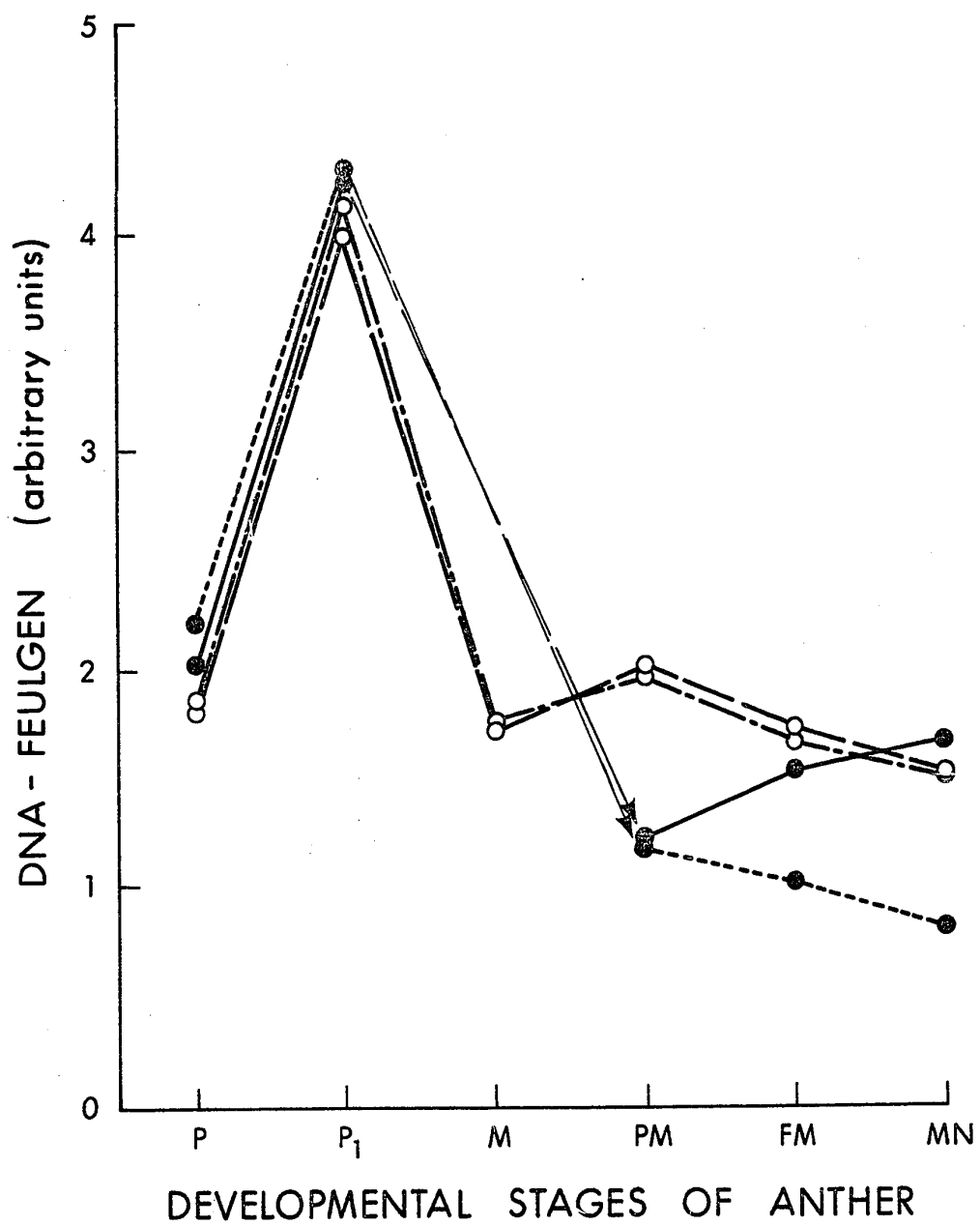
Fig. 11. Profile showing amounts (arbitrary units) of histone - fast green per nucleus at six sequential stages of development in the sporogenous tissue ●————● and tapetal tissue ○—·——·—○ of male-fertile anthers and sporogenous tissue ●————● and tapetal tissue ○—— —○ of male-sterile anthers of *ms 5*. Measurements were taken from the interphase nuclei only; therefore, the nuclei of sporogenous tissue at M were not analysed and arrows with thin broken lines are given to show the continuity of curves. (P) Primordial stage; (P_1) Premeiotic stage; (M) Meiotic stage; (PM) Post-meiotic stage; (FM) Free microspore stage; (MN) Mononucleate stage.
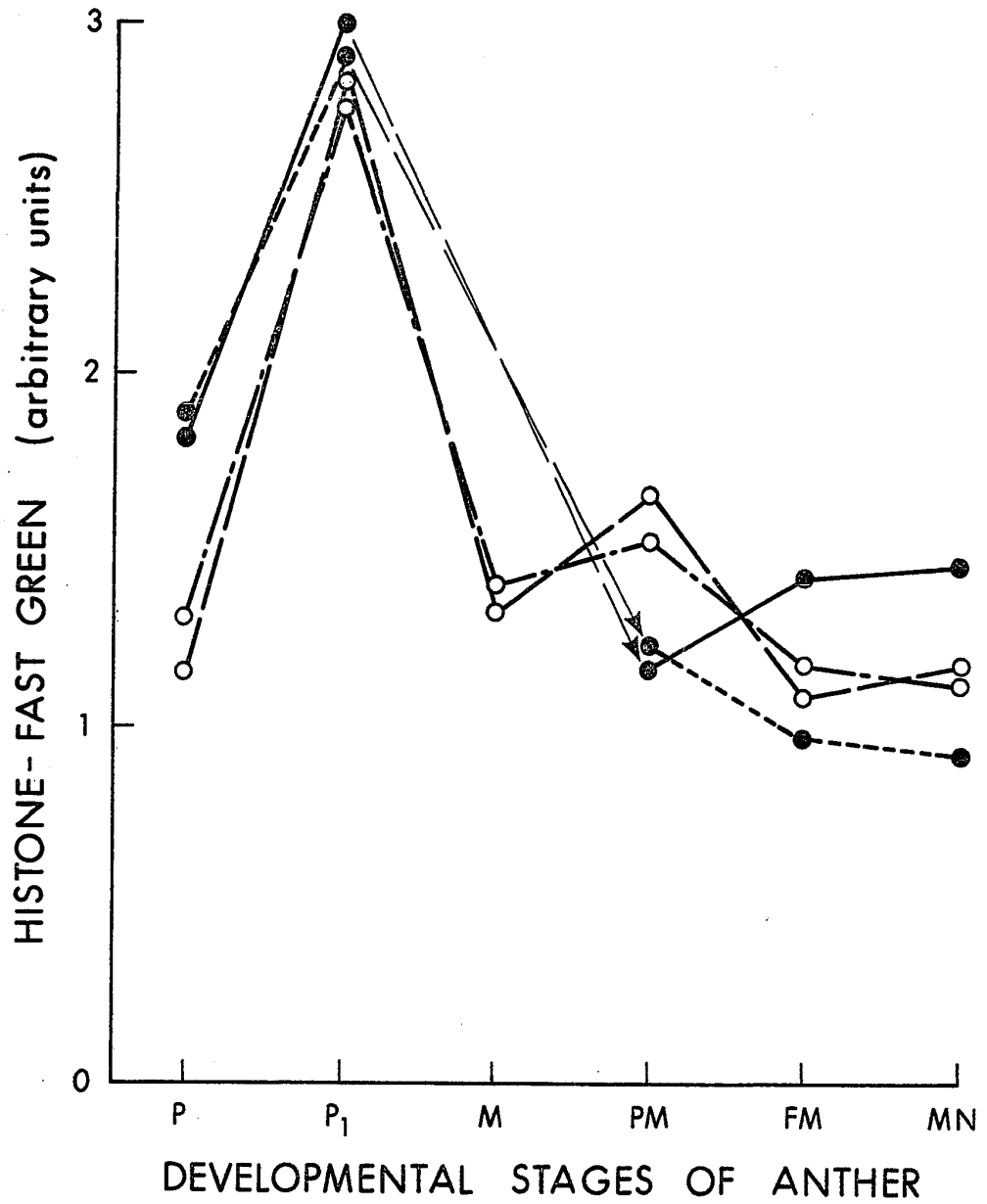
Fig. 12. Graph showing the DNA : histone ratio at the six sequential

stages of development in the sporogenous ●————● and tapetal tissue

○–·—·—○ of male-fertile anthers and sporogenous tissue ●——————●

and tapetal tissue ○—— —— —○ of male-sterile anthers of *ms 5*.

Measurements were taken from the interphase nuclei only; therefore,

the nuclei of sporogenous tissue at M were not analysed and arrows with

thin broken lines are given to show the continuity of curves.
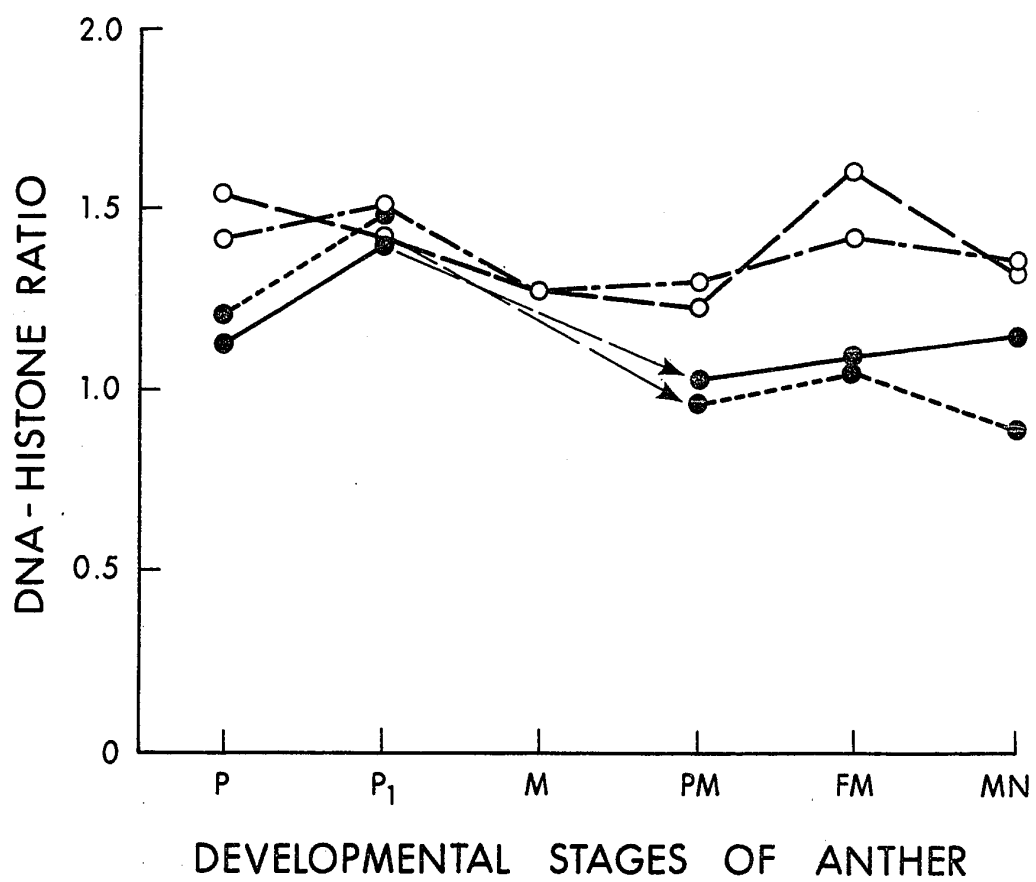
ms 9:

DNA. Table IV and Fig. 13 show the variations in DNA in the nuclei of sporogenous and tapetal tissues of *ms 9* and its fertile counterpart. The pattern of quantitative changes in the sporogenous tissue of fertile anthers is similar to that observed in *ms 5* (see Fig. 11), and the same is true for that of sterile anthers up to and including the P_1 stage. At PM a marked difference is observed between fertile and sterile anthers. The fertile anthers show a gradual increase in DNA amount from PM (1.49 ± 0.05) to the FM stage (1.99 ± 0.15), and a further increase to 2.50 ± 0.09 at the MN stage. The sterile anthers on the other hand show a negative gradient from the PM to the MN stages (Fig. 13) such that the DNA value (0.16) is drastically low compared with the normal for this period.

The curves for tapetal tissue of both normal and sterile anthers follow similar profiles up to the FM stage, but subsequently deviate markedly due to an augmented decline of DNA amount in sterile anthers. Normal anthers invariably exhibit a characteristic decline in tapetal nuclei from PM to MN (Fig. 13). During the FM-MN period only a gradual reduction in nuclear DNA is seen but in sterile tapetum it drops at a rapid rate to a significantly low level at MN.

It may be noted that a crucial quantitative difference between the tapetal nuclei of normal and mutant anthers is first observed after the FM stage. Oddly, however, in the sporogenous tissues the difference becomes obvious only after the completion of meiosis, i.e. at the PM.

Histone. The trend of variations in nuclear histone in sporogenous tissues of fertile and male-sterile anthers of *ms 9* (Table V; Fig. 14) corresponds closely to those of DNA. Thus the first indication of a

quantitative difference between the two phenotypes appears at PM, at which time fertile sporogenous tissue shows a higher value than the sterile (i.e. 1.35 and 0.95, respectively). This difference is enhanced in the ensuing stages, the fertile tissue showing a gradual increase and the sterile a sharp decline. At MN a complete loss of nuclear alkaline-fast green staining capacity is found in the sterile tissue, probably due to augmented degradation of histone.

The DNA and histone variations among tapetal nuclei of normal and mutant anthers are inflectionally similar throughout the six developmental stages of the anther (Fig. 14).

The observations above, together with those made earlier concerning DNA, suggest that the first manifestation of the mutant phenotype appears in the sporogenous tissue at the PM stage and that no evidence of differences is seen in the tapetum at this and subsequent stages, although differences do show up in DNA from the FM stage.

Histone/DNA ratio. In the sporogenous tissue the histone/DNA ratio remains much the same from P to P_1 and during the period P_1 to PM in both the fertile and sterile anthers (Fig. 15). In the PM-MN period a wide difference occurs between the ratios of fertile and sterile sporogenous tissues, the former remaining approximately between 0.7 and 0.9 and the latter declining steadily from PM to FM, and falling to zero at MN.

The extensive divergence of the curves (Fig. 15) of fertile and sterile tapetal tissues becomes apparent from the FM stage on. It is seen that there is a stability of histone/DNA ratio in the fertile tapetum at PM, FM, and MN as shown by a constant ratio level. This is also true for sterile tapetal tissue, but only from PM to FM, after which the ratio increases several-fold due to the sharp decrease in DNA quantity.

Table IV. DNA - Feulgen amounts (arbitrary units) per nucleus of sporogenous and tapetal tissues of male-fertile and male-sterile barley anthers of ms 9 at six sequential stages of development. (Each value is the mean of a sample of 20 nuclei.)

Developmental stage of anther	SPOROGENOUS TISSUE			TAPETAL TISSUE		
	DNA - Feulgen values ± standard error		t-value	DNA - Feulgen values ± standard error		t-value
	Male-fertile	Male-sterile		Male-fertile	Male-sterile	
P	3.09 ±0.15	3.00 ± 0.16	0.284	3.07 ± 0.09	2.85 ± 0.06	1.499
P_1	5.55 ±0.25	5.24 ± 0.32	0.554	5.13 ± 0.23	5.05 ± 0.15	0.216
M	-	-	-	2.22 ± 0.06	2.19 ± 0.09	0.206
PM	1.49 ±0.05	1.05 ± 0.02	6.437*	3.31 ± 0.10	3.46 ± 0.10	0.769
FM	1.99 ±0.15	0.82 ± 0.03	6.843*	2.53 ± 0.05	2.84 ± 0.09	2.314*
MN	2.50 ±0.09	0.16 ± 0.02	22.684*	2.17 ± 0.08	1.11 ± 0.04	8.761*

*Significant at 5% level.

Table V. Histone - Fast green amounts (arbitrary units) per nucleus of sporogenous and tapetal tissues of male-fertile and male-sterile barley anthers of *ms 9* at six sequential stages of development. (Each value is the mean of a sample of 20 nuclei.)

Developmental stage of anther	SPOROGENOUS TISSUE			TAPETAL TISSUE		
	Histone - Fast green values ± standard error		t-value	Histone - Fast green values ± standard error		t-value
	Male-fertile	Male-sterile		Male-fertile	Male-sterile	
P	2.24 ± 0.29	2.15 ± 0.08	0.24	1.86 ± 0.08	1.88 ± 0.07	0.15
P_1	4.13 ± 0.12	3.95 ± 0.09	0.89	3.34 ± 0.04	3.44 ± 0.06	0.95
M	-	-	-	1.47 ± 0.06	1.28 ± 0.05	1.63
PM	1.38 ± 0.04	0.95 ± 0.08	3.56*	1.59 ± 0.05	1.41 ± 0.04	1.99
FM	1.85 ± 0.05	0.48 ± 0.02	20.20*	1.22 ± 0.04	1.24 ± 0.02	0.36
MN	2.06 ± 0.13	0.00 ± -	16.33*	1.01 ± 0.03	1.08 ± 0.03	1.17

*Significant at 5% level.

Fig. 13.   Profile showing amounts (arbitrary units) of DNA -

Feulgen per nucleus at six sequential stages of development in

the sporogenous tissue ●———● and tapetal tissue ○—·—··○

of male-fertile anthers and the sporogenous tissue ●——————● and

tapetal tissue ○— ——○ of male-sterile anthers of *ms 9*.   Measure-

ments were taken from the interphase nuclei only.   Therefore, nuclei

of sporogenous tissues at M were not analysed and arrows with thin

broken lines are given to show the continuity of curve for sporogenous

tissues.   (P) Primordial stage; (P$_1$) Premeitoic stage; (M) Meiotic

stage; (PM) Post-meiotic stage; (FM) Free microspore stage; (MN)

Mononucleate stage.
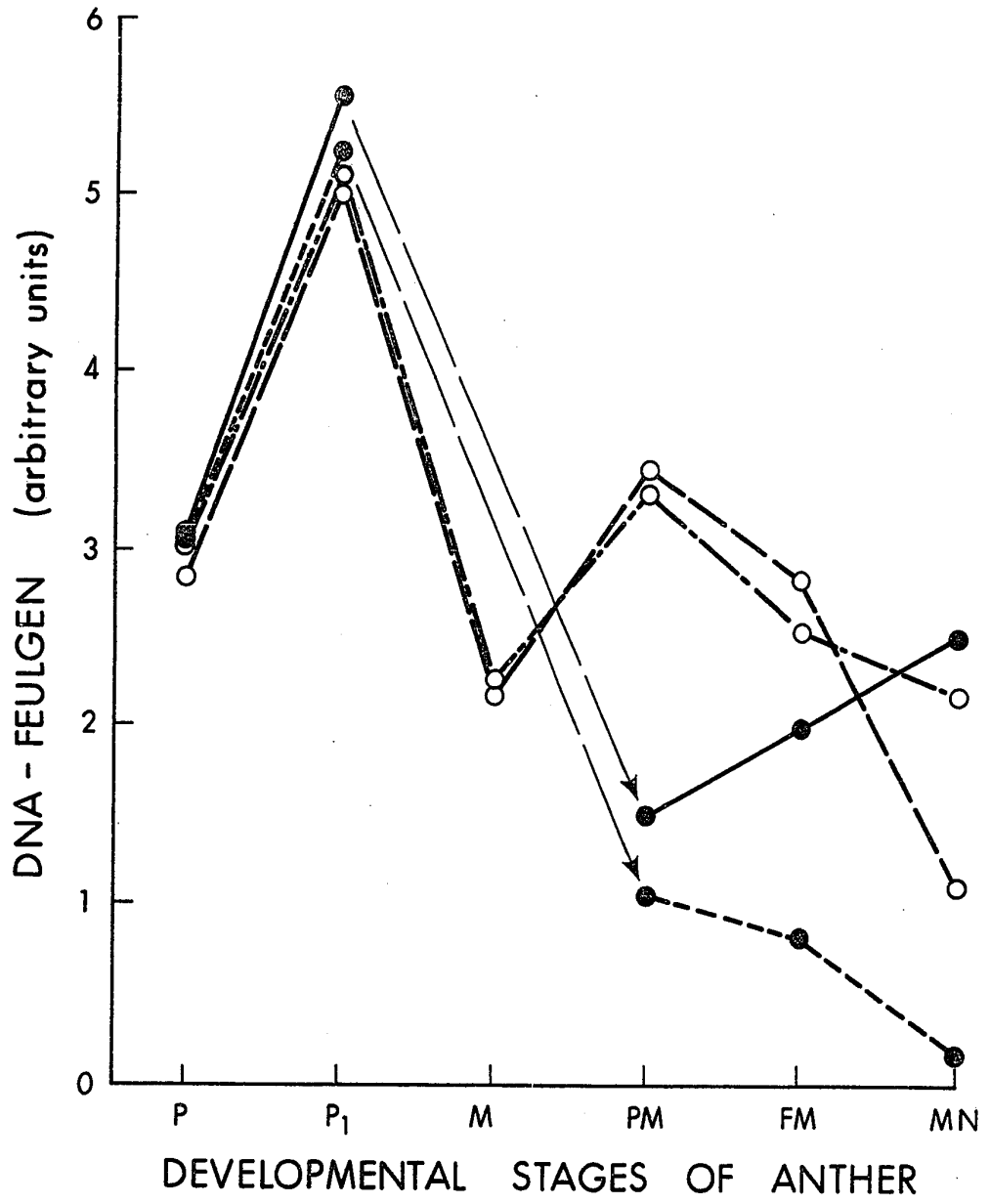
Fig. 14. Profile showing amounts (arbitrary units) of histone - fast

green per nucleus at six sequential stages of development in the

sporogenous tissue ●————● and tapetal tissue ○—·—·—○ of male-

fertile anthers and sporogenous tissue ●——————● and tapetal tissue

○————○ of male-sterile anthers of *ms 9*. Measurements were taken

from the interphase nuclei only; therefore, the nuclei of sporogenous

tissue at M were not analysed and arrows with thin broken lines are

given to show the continuity of curves. (P) Primordial stage;

(P₁) Premeiotic stage; (M) Meiotic stage; (PM) Post-meiotic stage;

(FM) Free microspore stage; (MN) Mononucleate stage.
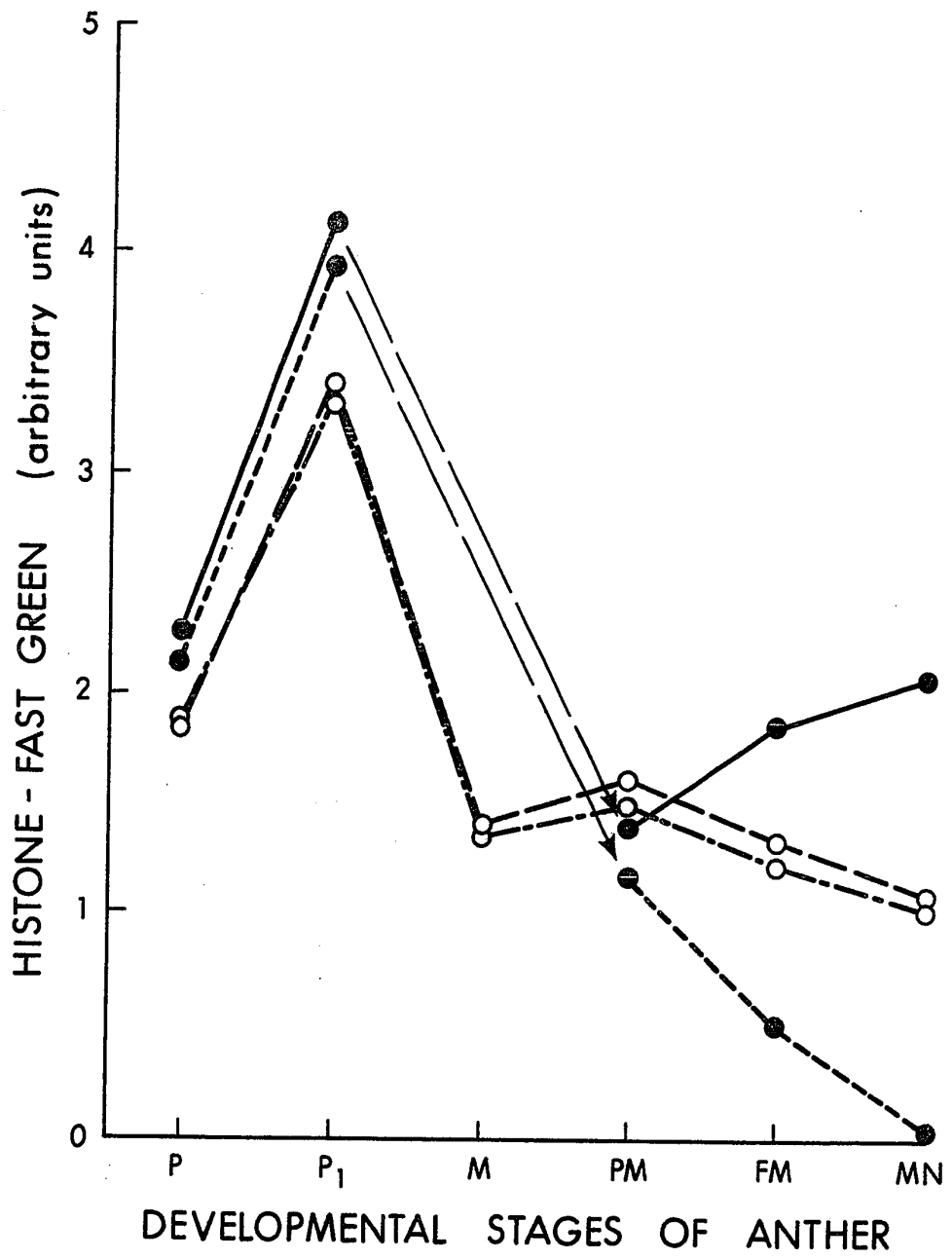
Fig. 15. Graph showing the DNA : histone ratio at the six sequential

stages of development in the sporogenous ●━━━━━● and tapetal tissue

○━·━·━○ of male-fertile anthers and sporogenous tissue ●━━━━●

and tapetal tissue ○━━ ━━ ○ of male-sterile anthers of *ms 9*.

Measurements were taken from the interphase nuclei only; therefore,

the nuclei of sporogenous tissue at M were not analysed and arrows with

thin broken lines are given to show the continuity of curves.
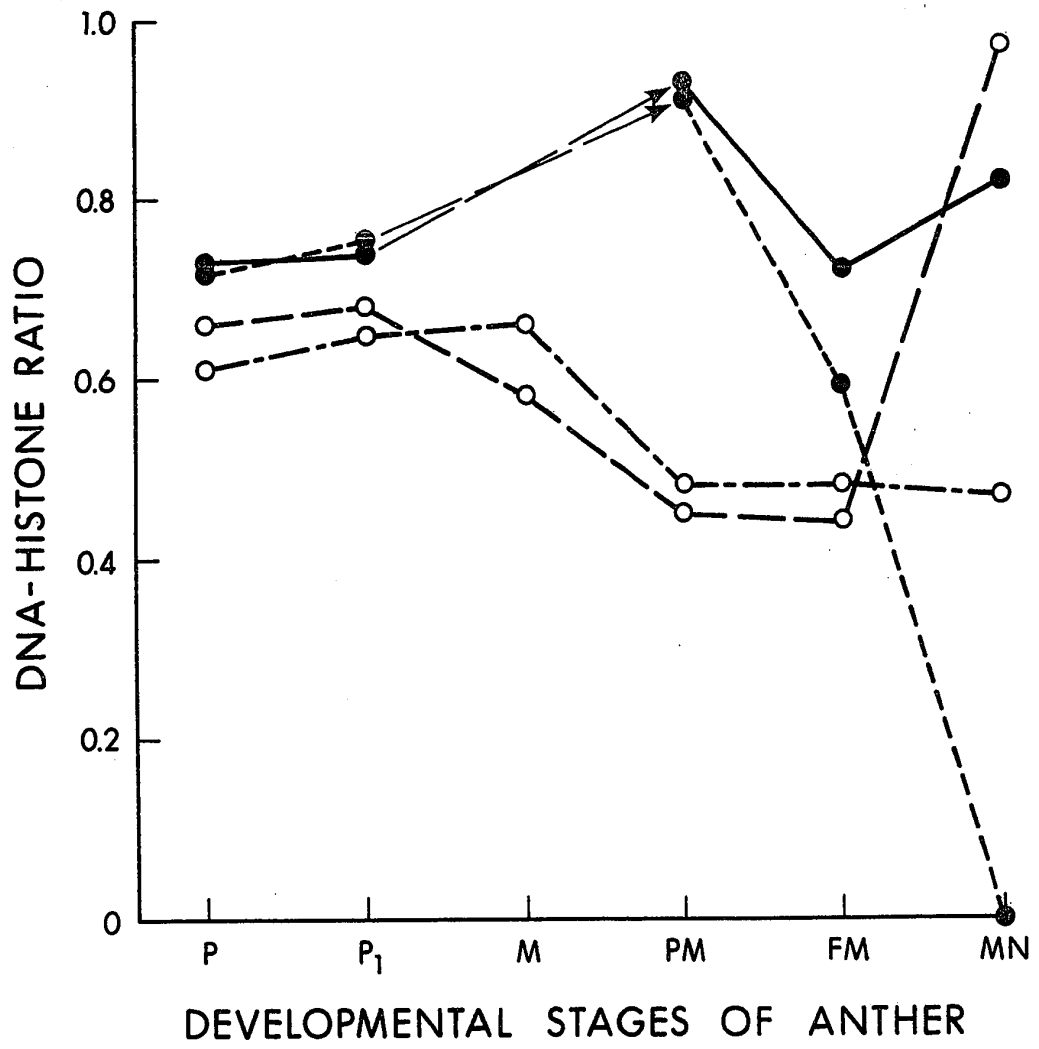
ms 10:

  DNA. It may be seen from the data presented in Table VI and Figure 16 that the amounts of DNA in sporogenous tissues of fertile and sterile anthers are in close agreement until after the completion of meiosis. At PM the meiotic products in fertile anthers have significantly higher DNA amounts than those of sterile anthers. From PM to FM a parallel increase is observed in both tissues (Fig. 16) after which the two curves diverge. That for normal anthers continues to increase while the one for sterile anthers shows a steep decline.

  In the tapetal tissues, on the other hand, a difference in the DNA between the fertile and sterile anthers is seen as early as P, the former containing a significantly higher amount than the latter. The two tissues subsequently represent a concomitant drop in DNA values from P_1 to M (Fig. 16) and again diverge from the M stage on. During the last three stages (PM, FM and MN), however, the nuclear DNA values of sterile tapetum are seen to be consistently at a higher level than those of the fertile tapetum.

  Histone. The changes in histone amounts are given in Table VII and illustrated in Figure 17. The trend of variations in sporogenous and tapetal tissues of both fertile and sterile anthers is quite similar to that seen in the DNA analysis throughout the development. The significant difference between histone values of tapetal nuclei of normal and sterile anthers also appear at the same time as that of DNA, i.e. at FM stage.

  DNA/histone ratio. In both the sporogenous and tapetal tissues of fertile as well as sterile anthers, the DNA/histone ratios remain within a narrow range throughout the developmental period (Fig. 18). In

Table VI. DNA - Feulgen amounts (arbitrary units) per nucleus of sporogenous and tapetal tissues of male-fertile and male-sterile barley anthers of *ms 10* at six sequential stages of development. (Each value is the mean of a sample of 20 nuclei.)

Developmental stage of anther	SPOROGENOUS TISSUE			TAPETAL TISSUE		
	DNA - Feulgen values ± standard error		*t*-value	DNA - Feulgen values ± standard error		*t*-value
	Male-fertile	Male-sterile		Male-fertile	Male-sterile	
P	2.84 ±0.03	2.83 ± 0.03	0.09	2.36 ± 0.09	3.33 ± 0.12	4.52*
P_1	4.78 ±0.03	4.66 ± 0.08	1.05	4.36 ± 0.06	4.27 ± 0.06	0.76
M	-	-	-	1.55 ± 0.06	1.51 ± 0.07	0.35
PM	1.40 ±0.04	1.10 ± 0.05	3.56*	2.58 ± 0.04	2.97 ± 0.04	4.52*
FM	2.11 ±0.08	1.58 ± 0.06	3.57*	1.75 ± 0.04	2.42 ± 0.09	5.32*
MN	2.35 ±0.09	0.86 ± 0.03	12.11*	1.67 ± 0.02	2.08 ± 0.02	9.78*

*Significant at 5% level.

Table VII. Histone - Fast green amounts (arbitrary units) per nucleus of sporogenous and tapetal tissues of male-fertile and male-sterile barley anthers of *ms 10* at six sequential stages of development. (Each value is the mean of a sample of 20 nuclei.)

Developmental stage of anther	SPOROGENOUS TISSUE			TAPETAL TISSUE		
	Histone - Fast green values ± standard error		t-value	Histone - Fast green values ± standard error		t-value
	Male-fertile	Male-sterile		Male-fertile	Male-sterile	
P	2.06 ±0.03	2.03 ± 0.04	0.46	1.22 ± 0.04	2.23 ± 0.12	6.32*
P_1	3.32 ±0.17	3.27 ± 0.17	0.13	3.04 ± 0.11	2.87 ± 0.06	1.02
M	-	-	-	1.06 ± 0.01	1.12 ± 0.02	2.01
PM	1.27 ±0.08	0.97 ± 0.05	2.33*	1.86 ± 0.03	2.10 ± 0.03	4.17*
FM	1.99 ±0.07	1.29 ± 0.03	7.32*	1.32 ± 0.05	1.52 ± 0.03	2.75*
MN	2.16 ±0.10	0.68 ± 0.02	12.02*	1.18 ± 0.02	1.32 ± 0.03	2.88*

*Significant at 5% level.

Fig. 16.   Profile showing amounts (arbitrary units) of DNA -

Feulgen per nucleus at six sequential stages of development in

the sporogenous tissue ●————● and tapetal tissue ○—·—··○

of male-fertile anthers and the sporogenous tissue ●———————● and

tapetal tissue ○—— ———○ of male-sterile anthers of *ms 10*. Measure-

ments were taken from the interphase nuclei only. Therefore, nuclei

of sporogenous tissues at M were not analysed and arrows with thin

broken lines are given to show the continuity of curve for sporogenous

tissues.   (P) Primordial stage; (P_1) Premeitoic stage; (M) Meiotic

stage; (PM) Post-meiotic stage; (FM) Free microspore stage; (MN)

Mononucleate stage.
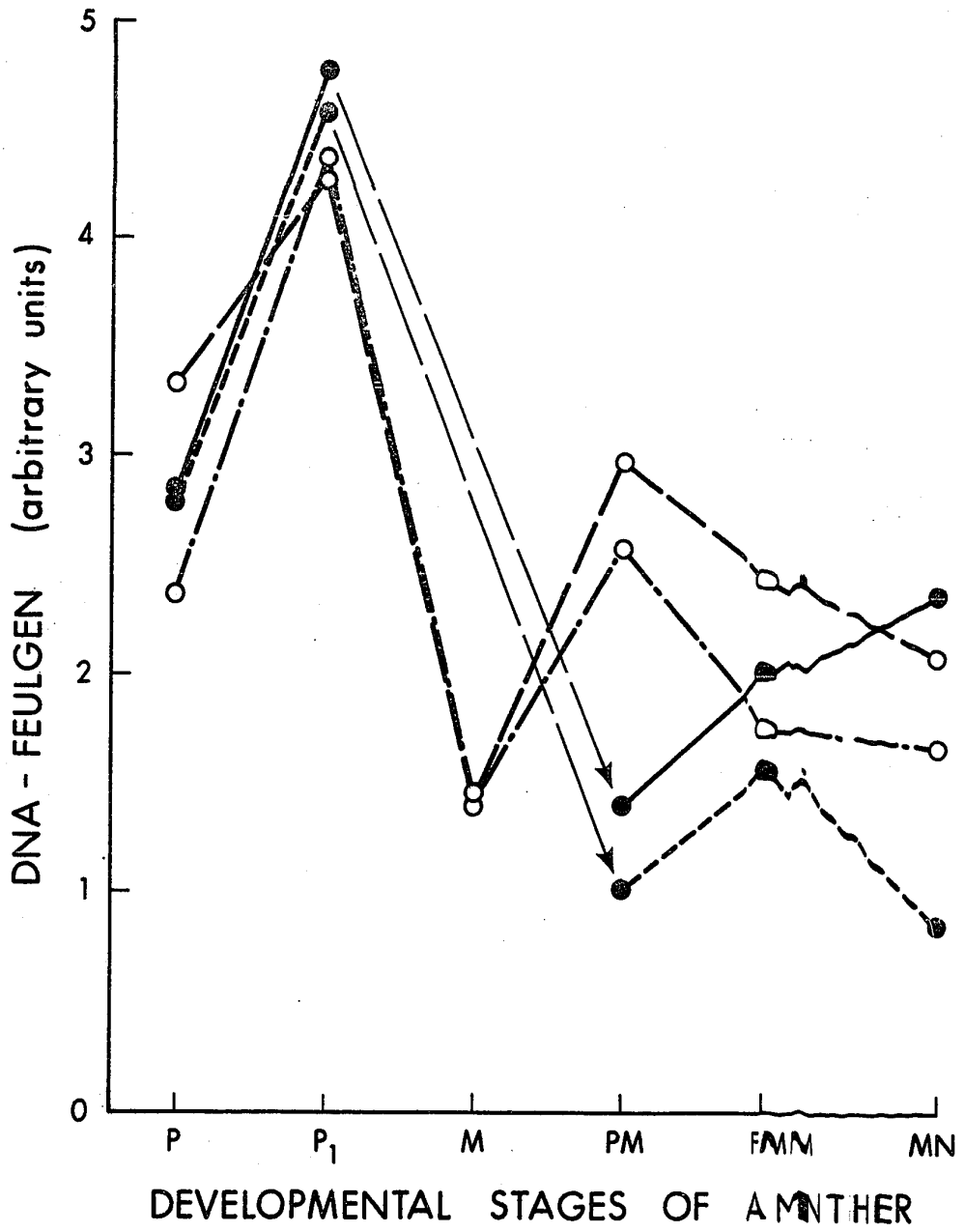
Fig. 17. Profile showing amounts (arbitrary units) of histone - fast green per nucleus at six sequential stages of development in the sporogenous tissue●————●and tapetal tissue O—·—·—Oof male-fertile anthers and sporogenous tissue●——————●and tapetal tissue O————Oof male-sterile anthers of *ms 10*. Measurements were taken from the interphase nuclei only; therefore, the nuclei of sporogenous tissue at M were not analysed and arrows with thin broken lines are given to show the continuity of curves. (P) Primordial stage; (P$_1$) Premeiotic stage; (M) Meiotic stage; (PM) Post-meiotic stage; (FM) Free microspore stage; (MN) Mononucleate stage.
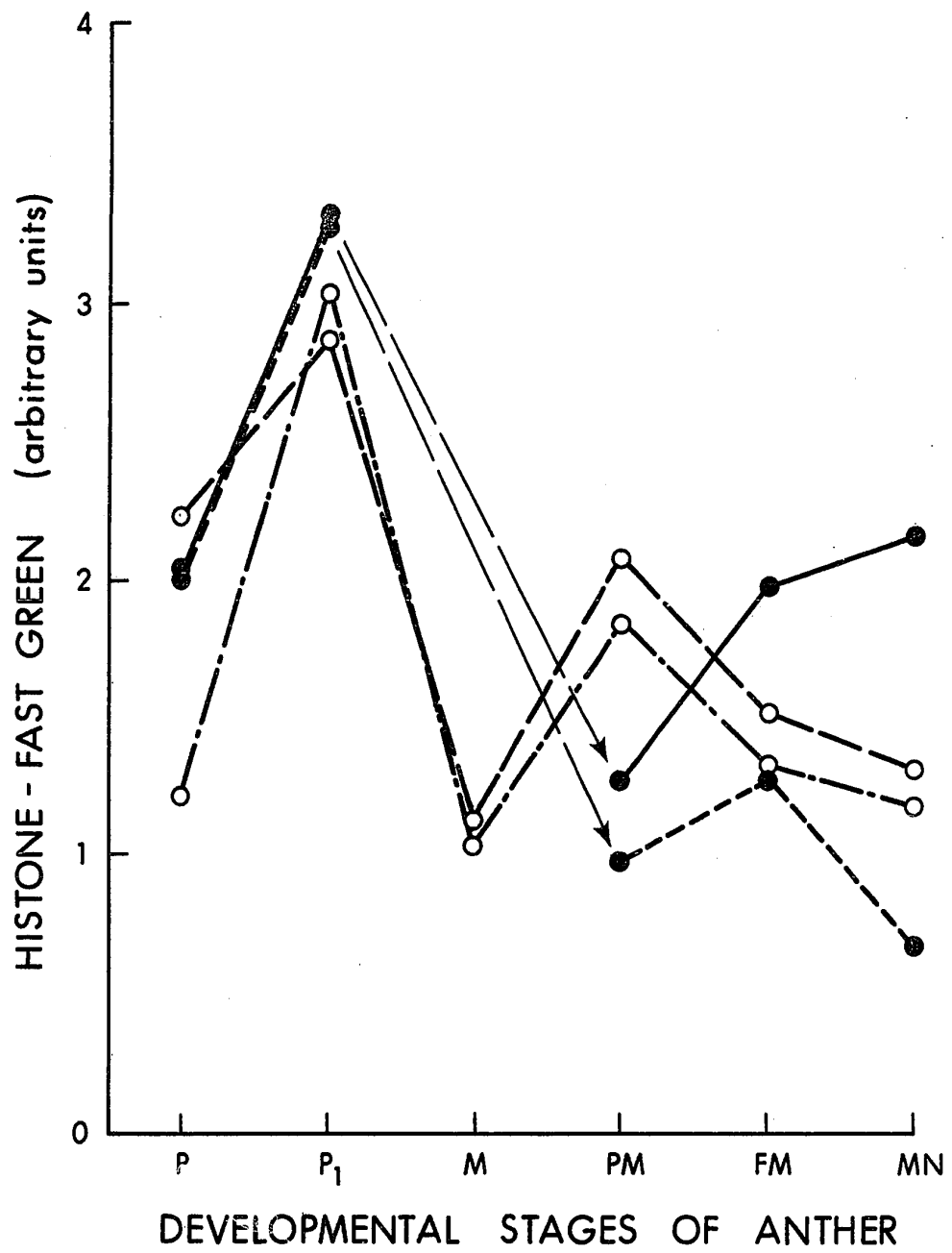
Fig. 18.   Graph showing the DNA : histone ratio at the six sequential

stages of development in the sporogenous ●————● and tapetal tissue

○—.—.—○ of male-fertile anthers and sporogenous tissue ●-----●

and tapetal tissue ○———.—○ of male-sterile anthers of *ms 10*.

Measurements were taken from the interphase nuclei only; therefore,

the nuclei of sporogenous tissue at M were not analysed and arrows with

thin broken lines are given to show the continuity of curves.
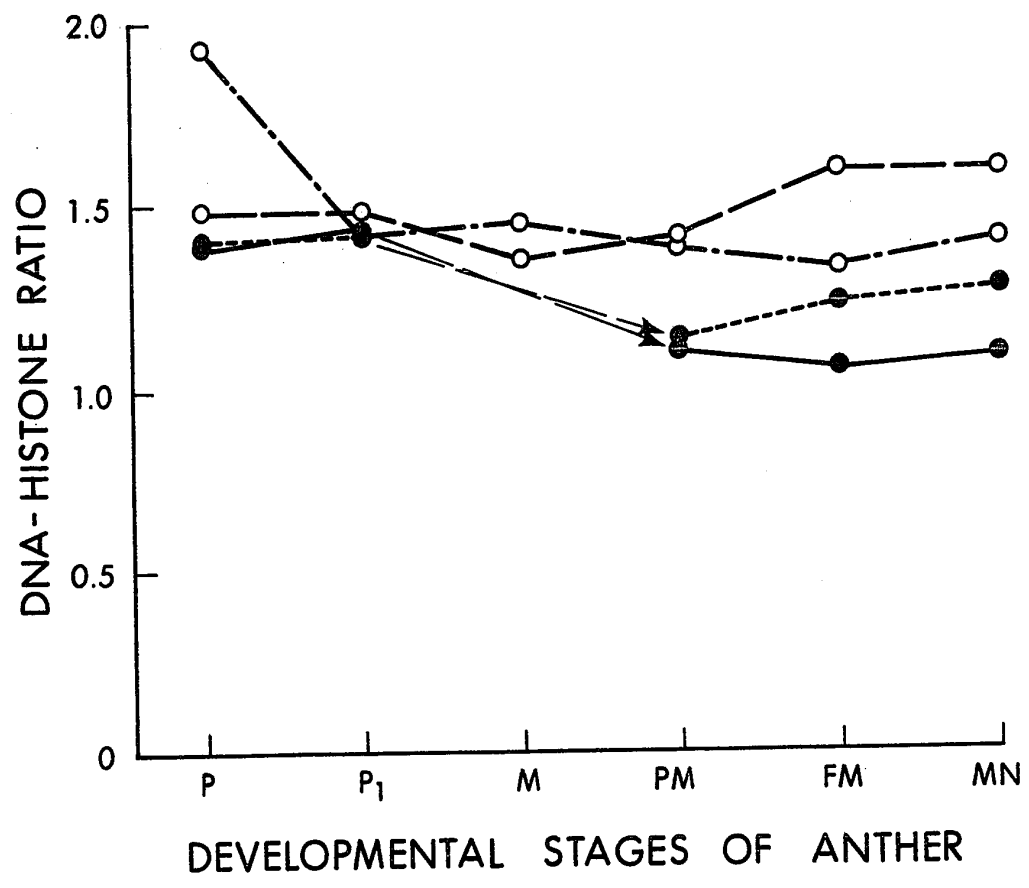
sporogenous tissues the range is 1.1 to 1.4, and in the tapetal tissues it is 1.3 to 1.6. The single exception in the tapetum of fertile anthers at P is not critical since values subsequent to this are more representative.

ms 14:

DNA. The nuclei of sterile sporogenous tissue show a notably high DNA value as compared with the normal at the primordial (P) stage (Table VIII). This difference seems rather transitory since it is abridged by the time the meiocytes are at the P_1 stage. At PM the young microspores of sterile anthers show a significant deficit of DNA content. During the subsequent FM and MN stages the disparity continuously increases, normal sporogenous tissue showing a linearly increasing synthetic activity and the mutant a bimodal decline (Fig. 19; faster from PM to FM and negligible from FM to MN).

In fertile anthers of this line, DNA variations in the nuclei of tapetal cells follow a course similar to that of fertile anthers of the other lines throughout anther development. In male-sterile anthers, however, a quantitatively significant deviation in DNA curves from the normal becomes obvious from the postmeiotic stage onward. Thus in the normal there is an increase in DNA from M to PM followed by a two-step decline during the period PM to MN, whereas in the sterile tapetum there is a concomitant but slow increase during the M-PM period. Furthermore, in sterile tapetum the DNA values consistently remain at about the same level during the FM-MN period (Fig. 19).

Histone. It is evident from a comparison of Figures 18 and 19 that the profiles of histone and DNA curves for sporogenous tissues are almost

Table VIII. DNA - Feulgen amounts (arbitrary units) per nucleus of sporogenous and tapetal tissues of male-fertile and male-sterile barley anthers of *ms 14* at six sequential stages of development. (Each value is the mean of a sample of 20 nuclei.)

Developmental stage of anther	SPOROGENOUS TISSUE			TAPETAL TISSUE		
	DNA - Feulgen values ± standard error		t-value	DNA - Feulgen values ± standard error		t-value
	Male-fertile	Male-sterile		Male-fertile	Male-sterile	
P	3.52 ± 0.03	3.85 ± 0.10	2.44*	3.78 ± 0.07	4.01 ± 0.14	1.11
P_1	5.74 ± 0.03	6.01 ± 0.47	0.56	5.50 ± 0.23	5.34 ± 0.04	0.24
M	-	-	-	2.09 ± 0.05	1.97 ± 0.06	1.12
PM	1.60 ± 0.08	1.36 ± 0.04	2.12*	3.35 ± 0.08	2.81 ± 0.02	5.49*
FM	2.07 ± 0.05	0.63 ± 0.02	21.30*	1.85 ± 0.07	2.97 ± 0.06	8.42*
MN	2.64 ± 0.08	0.57 ± 0.02	19.78*	1.65 ± 0.03	3.02 ± 0.09	10.90*

*Significant at 5% level.

Table IX. Histone - Fast green amounts (arbitrary units) per nucleus of sporogenous and tapetal tissues of male-fertile and male-sterile barley anthers of *ms 14* at six sequential stages of development. (Each value is the mean of a sample of 20 nuclei.)

Developmental stage of anther	SPOROGENOUS TISSUE			TAPETAL TISSUE		
	Histone - Fast green values ± standard error		*t*-value	Histone - Fast green values ± standard error		*t*-value
	Male-fertile	Male-sterile		Male-fertile	Male-sterile	
P	3.00 ± 0.09	2.91 ± 0.10	0.49	2.67 ± 0.06	3.12 ± 0.05	4.02*
P_1	4.35 ± 0.05	4.09 ± 0.05	2.83*	3.50 ± 0.07	3.59 ± 0.18	0.38
M	-	-	-	1.39 ± 0.01	1.26 ± 0.04	2.35*
PM	1.51 ± 0.05	1.26 ± 0.05	2.58*	2.09 ± 0.08	2.21 ± 0.03	1.06
FM	1.94 ± 0.03	0.57 ± 0.03	23.06*	1.16 ± 0.02	2.26 ± 0.08	11.77*
MN	2.46 ± 0.05	0.39 ± 0.03	24.30*	1.25 ± 0.03	2.72 ± 0.04	20.82*

*Significant at 5% level.

Fig. 19.   Profile showing amounts (arbitrary units) of DNA -

Feulgen per nucleus at six sequential stages of development in

the sporogenous tissue ●————● and tapetal tissue ○—·—··○

of male-fertile anthers and the sporogenous tissue ●———————● and

tapetal tissue ○—— ——○ of male-sterile anthers of *ms 14*. Measure-

ments were taken from the interphase nuclei only. Therefore, nuclei

of sporogenous tissues at M were not analysed and arrows with thin

broken lines are given to show the continuity of curve for sporogenous

tissues. (P) Primordial stage; (P$_1$) Premeitoic stage; (M) Meiotic

stage; (PM) Post-meiotic stage; (FM) Free microspore stage; (MN)

Mononucleate stage.

Fig. 20. Profile showing amounts (arbitrary units) of histone - fast green per nucleus at six sequential stages of development in the sporogenous tissue ●————● and tapetal tissue ○—·——·—○ of male-fertile anthers and sporogenous tissue ⊕——————⊕ and tapetal tissue ○—————○ of male-sterile anthers of *ms 14*. Measurements were taken from the interphase nuclei only; therefore, the nuclei of sporogenous tissue at M were not analysed and arrows with thin broken lines are given to show the continuity of curves. (P) Primordial stage; (P₁) Premeiotic stage; (M) Meiotic stage; (PM) Post-meiotic stage; (FM) Free microspore stage; (MN) Mononucleate stage.

DEVELOPMENTAL STAGES OF ANTHER
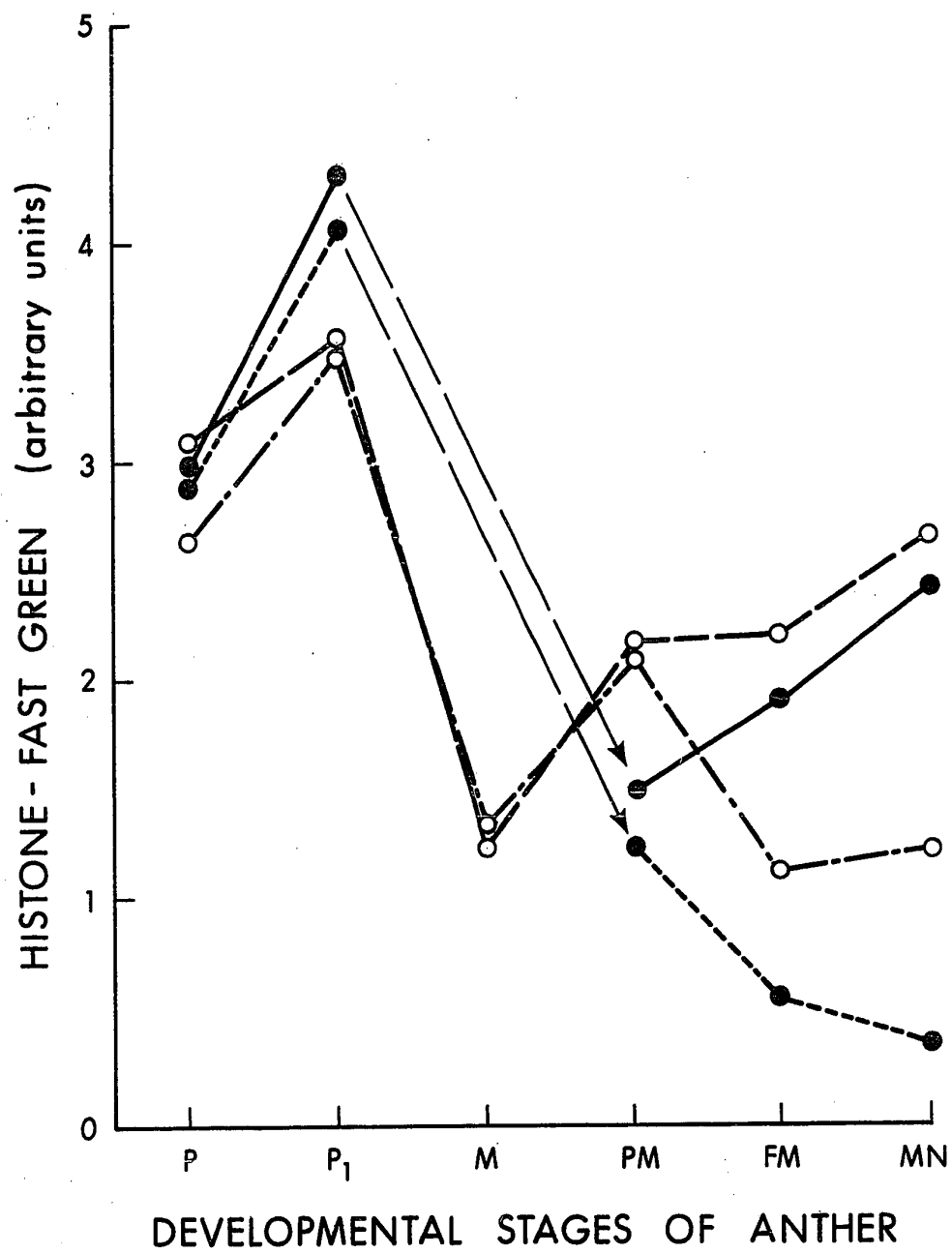
Fig. 21. Graph showing the DNA : histone ratio at the six sequential

stages of development in the sporogenous ●━━━━● and tapetal tissue

○━·━·━○ of male-fertile anthers and sporogenous tissue ●━ ━ ━ ●

and tapetal tissue ○━ ━ ━ ○ of male-sterile anthers of *ms 14*.

Measurements were taken from the interphase nuclei only; therefore,

the nuclei of sporogenous tissue at M were not analysed and arrows with

thin broken lines are given to show the continuity of curves.

identical. Quantitatively significant differences in histone between the normal and male-sterile anthers are first observed at P_1 (Table IX; Fig. 20) and persist throughout the rest of anther development.

Male-sterile anthers exhibit a significantly higher tapetal nuclear histone content than normal during the primordial (P) stage (Table IX). This accords with the observation of a relatively high DNA value for sterile sporogenous tissue at this time. It appears probable, however, that this difference at P may be due to a change in the sample source of male-sterile anthers used for these estimations and hence is somewhat doubtful. During the PM-MN period the sterile tapetum indicates that, rather than the normal decline in histone, there is a continued synthetic activity, especially pronounced from FM to MN.

DNA/histone ratio. The DNA/histone ratio (Fig. 21) shows a very narrow range of variation throughout anther development. The nuclei of fertile tapetum vary between 1.3 and 1.6 at different developmental stages of the anther, compared to those of the sterile tapetum, which have a slightly greater range. The fertile sporogenous tissue during PM-MN exhibits approximately a ratio of one, whereas during this period the nuclei of sterile microspores have values fairly close to the fertile one for PM and FM but at MN a decisive drop in histone amount increases the ratio to about 1.5.

ms 18:

DNA. The earliest significant difference between the DNA content of normal and sterile sporogenous tissues is observed at P_1, at which time the latter shows a serious deficit in DNA synthesis during the P to P_1 period (Table X; Fig. 22). At some time during meiosis, however, this

difference is compensated for, and at the PM stage the DNA values of both the phenotypes are identical.

The period following PM again shows an acute divergence. The curve for fertile sporogenous tissue shows the usual marked rise (from a value of 1.86 ± 0.04 at PM to 2.99 ± 0.10 at MN), whereas that for sterile sporogenous tissue shows a marked decline during PM-FM and then levels off during the FM-MN period.

As described in the histological studies of *ms 18*, the nuclei in tapetal tissue of male-sterile anthers may or may not undergo karyokinesis. Therefore, the DNA and histone analyses were carried out separately for the two types of cells, viz. binucleate and uninucleate. The data presented in Tables X and XI pertain to both types. Column A is for nuclei of karyokinetic, and column B for nuclei of non-karyokinetic behaviour. The curves A and B in the graphs (Figs. 22, 23, and 24) respectively pertain to each type of data.

There is close agreement between curve A (tapetum of sterile anthers showing karyokinesis) and that of fertile tapetum up to and including M (Table X; Fig. 22). From this point on the two curves deviate distinctly. That of fertile shows a definite ascent between M and PM and a gradual decline in PM-MN, while that of sterile shows a very slow and continuous rise from M to MN. With the exception of the DNA values at P, the B-type tapetal nuclei (nuclei of sterile tapetum showing no karyokinesis) significantly differ from those of the normal throughout the anther developmental stages. In these nuclei, during the first two stages (P, P_1) a negative DNA gradient is observed which continues up to the PM stage. This is followed by a slow increase in DNA from PM to MN.

Table X. DNA - Feulgen amounts (arbitrary units) per nucleus of sporogenous and tapetal tissues of male-fertile and male-sterile barley anthers of ms 18 at six sequential stages of development. (Each value is the mean of a sample of 20 nuclei.)

Developmental stage of anther	SPOROGENOUS TISSUE			TAPETAL TISSUE				
	DNA - Feulgen values ± standard error		t-value	DNA - Feulgen values ± standard error			t-value	
	Male-fertile	Male-sterile		Male-fertile	Male-sterile		A	B
					A	B		
P	1.96 ± 0.05	2.11± 0.07	1.37	2.37 ± 0.10	2.24 ± 0.03	2.09 ± 0.07	1.08	1.77
P$_1$	4.06 ± 0.10	2.84± 0.07	7.51*	4.09 ± 0.20	3.91 ± 0.08	1.61 ± 0.10	0.64	8.55*
M	-	-	-	1.49 ± 0.05	1.30 ± 0.08	1.08 ± 0.04	1.41	4.54*
PM	1.86 ± 0.04	1.83± 0.07	0.23	2.47 ± 0.17	1.58 ± 0.02	1.06 ± 0.04	4.79*	6.90*
FM	2.83 ± 0.06	1.09±0.01	24.32*	1.78 ± 0.07	1.65 ± 0.03	1.42 ± 0.05	1.26	2.89*
MN	2.99 ± 0.10	1.10± 0.02	16.29*	1.47 ± 0.02	1.68 ± 0.06	1.62 ± 0.02	2.48*	3.24*

*Significant at 5% level.
A - Tapetal nuclei showing karyokinesis.
B - Tapetal nuclei showing no karyokinesis.

Table XI. Histone - Fast green amounts (arbitrary units) per nucleus of sporogenous and tapetal tissues of male-fertile and male-sterile barley anthers of *ms i8* at six sequential stages of development. (Each value is the mean of a sample of 20 nuclei.)

Developmental stage of anther	SPOROGENOUS TISSUE			TAPETAL TISSUE					
	DNA - Feulgen values ± standard error		t-value	DNA - Feulgen values ± standard error				t-value	
	Male-fertile	Male-sterile		Male-fertile	Male-sterile				
					A	B		A	B
P	1.63 ± 0.03	1.70 ± 0.03	0.12	1.95 ± 0.08	1.81 ± 0.02	1.35 ± 0.03		1.50	5.66*
P₁	2.72 ± 0.03	2.69 ± 0.16	0.17	2.81 ± 0.16	2.54 ± 0.03	0.93 ± 0.02		1.43	10.51*
M	-	-	-	1.23 ± 0.03	1.18 ± 0.05	0.90 ± 0.02		0.69	7.32*
PM	1.78 ± 0.02	1.63 ± 0.03	3.21*	1.84 ± 0.04	1.37 ± 0.03	0.89 ± 0.04		6.58*	10.85*
FM	2.12 ± 0.09	1.02 ± 0.03	9.35*	1.42 ± 0.04	1.44 ± 0.03	1.01 ± 0.03		0.32	5.95*
MN	2.38 ± 0.04	0.89 ± 0.04	18.43*	1.09 ± 0.02	1.48 ± 0.04	0.97 ± 0.01		6.73*	3.51*

*Significant at 5% level.
A - Tapetal nuclei showing karyokinesis.
B - Tapetal nuclei showing no karyokinesis.

95

Fig. 22. Profile showing amounts (arbitrary units) of DNA -
Feulgen per nucleus at six sequential stages of development in
the sporogenous tissue ●———● and tapetal tissue O—·——·—O
of male-fertile anthers and the sporogenous tissue ●—————● and
tapetal tissue O———O of male-sterile anthers of *ms 18*. Measure-
ments were taken from the interphase nuclei only. Therefore, nuclei
of sporogenous tissues at M were not analysed and arrows with thin
broken lines are given to show the continuity of curve for sporogenous
tissues. (P) Primordial stage; (P$_1$) Premeiotic stage; (M) Meiotic
stage; (PM) Post-meiotic stage; (FM) Free microspore stage; (MN)
Mononucleate stage.

A. Profile of DNA amount from tapetal nuclei showing karyokinesis.

B. Profile of DNA amount from tapetal nuclei with no karyokinesis.
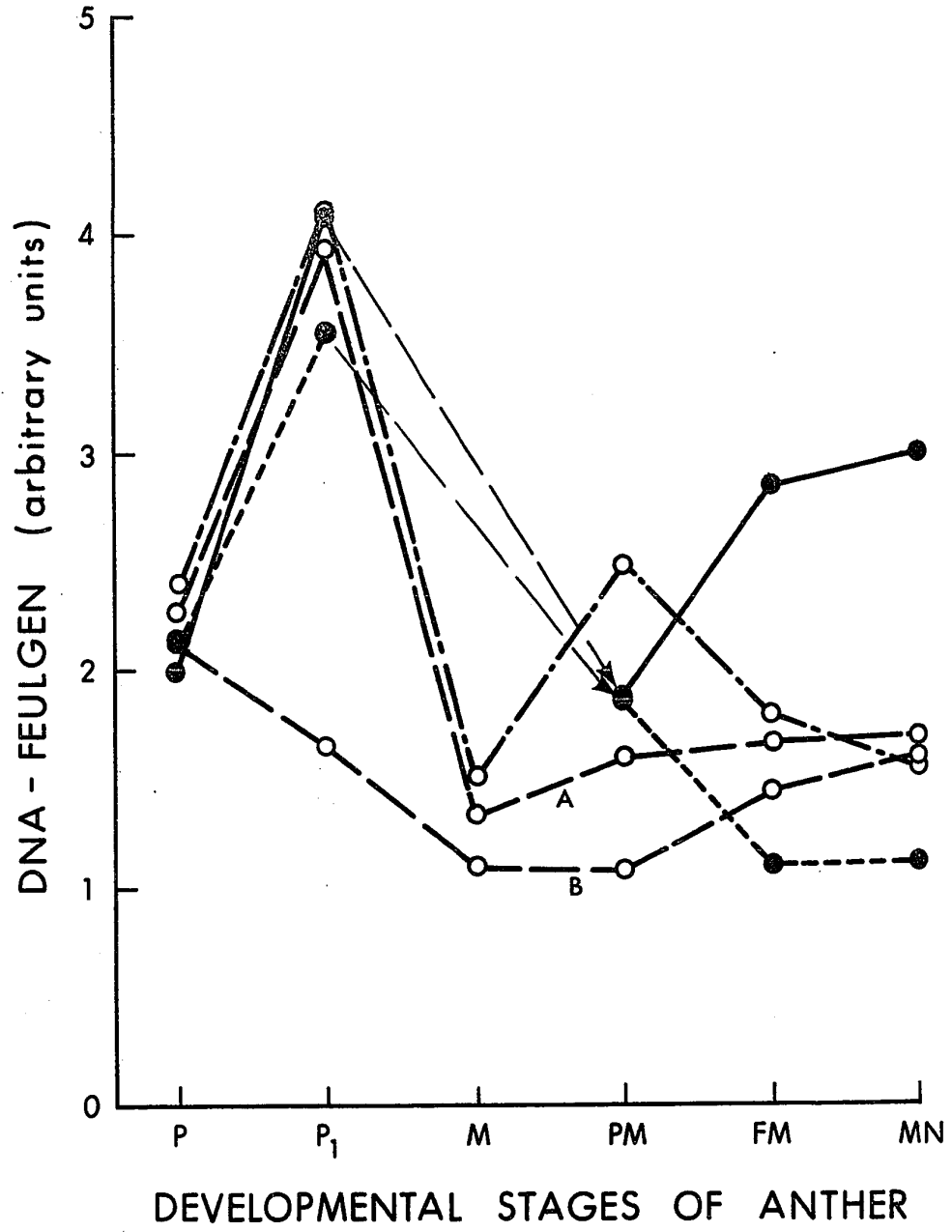
Fig. 23. Profile showing amounts (arbitrary units) of histone - fast green per nucleus at six sequential stages of development in the sporogenous tissue ●————● and tapetal tissue ○——·——·○ of male-fertile anthers and sporogenous tissue ●——————● and tapetal tissue ○——— —○ of male-sterile anthers of *ms 18*. Measurements were taken from the interphase nuclei only; therefore, the nuclei of sporogenous tissue at M were not analysed and arrows with thin broken lines are given to show the continuity of curves.   (P) Primordial stage; (P$_1$) Premeiotic stage; (M) Meiotic stage; (PM) Post-meiotic stage; (FM) Free microspore stage; (MN) Mononucleate stage.

A.   Profile of histone amount from tapetal nuclei showing karyokinesis.

B.   Profile of histone amount from tapetal nuclei with no karyokinesis.

Fig. 24. Graph showing the DNA : histone ratio at the six sequential
stages of development in the sporogenous ⬤————⬤ and tapetal tissue
O—·——·—O of male-fertile anthers and sporogenous tissue ⬤————⬤
and tapetal tissue O————O of male-sterile anthers of *ms 18*.
Measurements were taken from the interphase nuclei only; therefore,
the nuclei of sporogenous tissue at M were not analysed and arrows with
thin broken lines are given to show the continuity of curves.

A. Profile of DNA/histone ratio from tapetal nuclei showing karyokinesis.

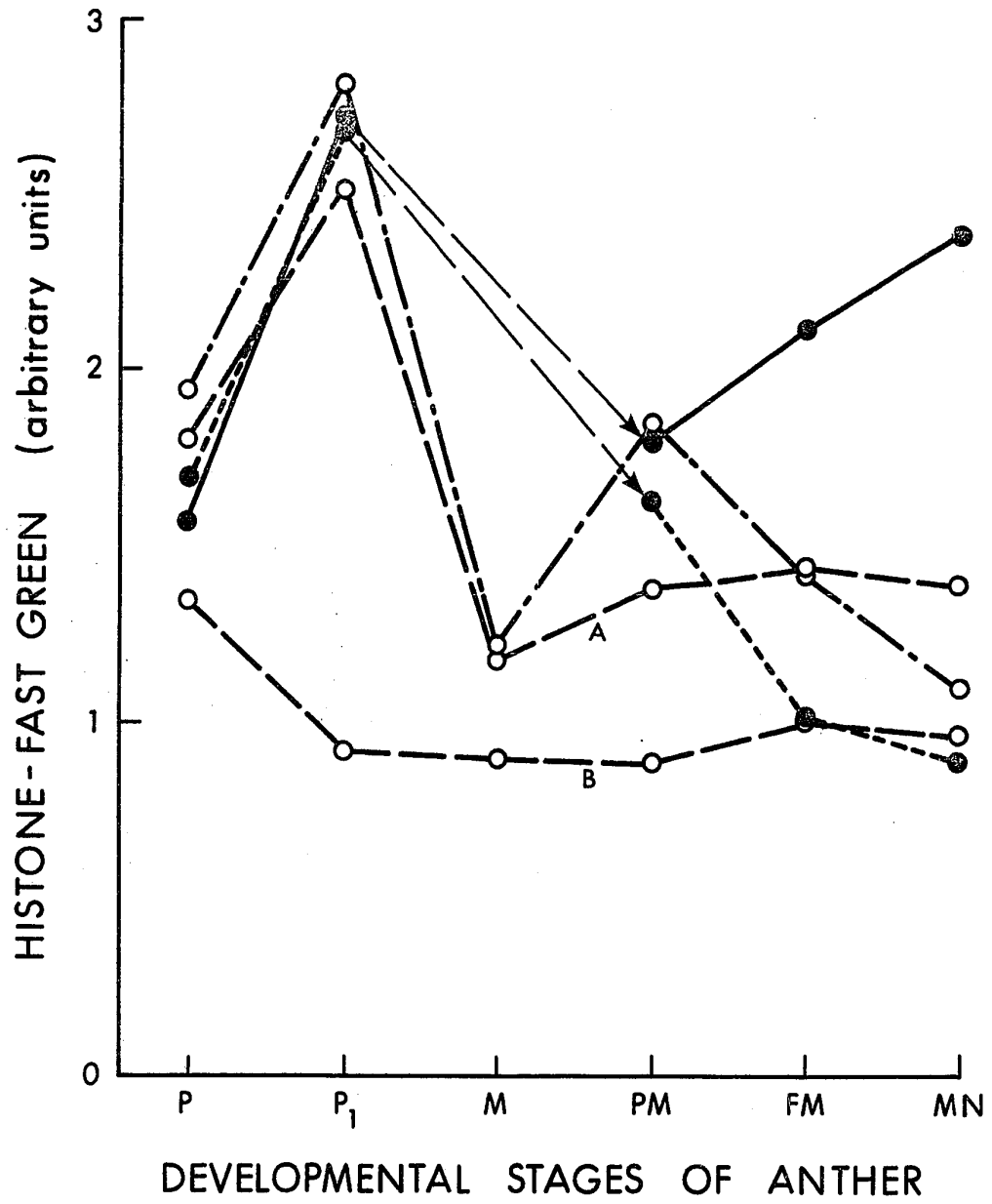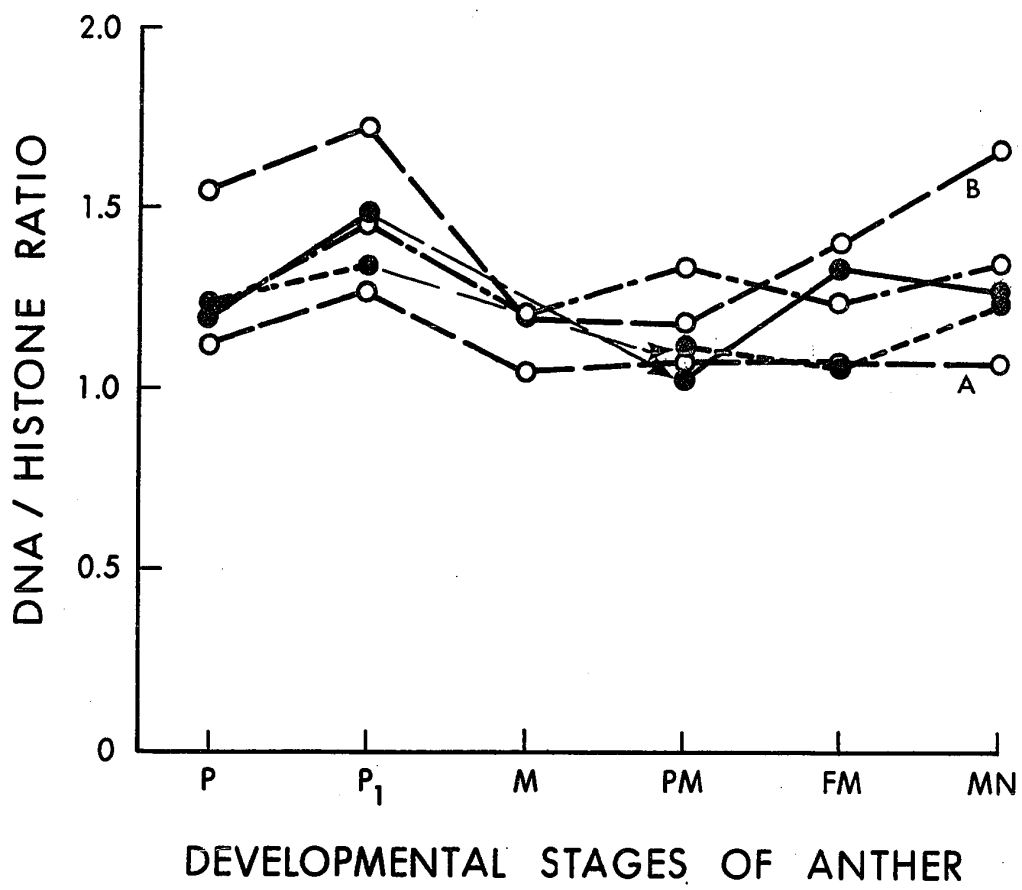B. Profile of DNA/histone ratio from tapetal nuclei with no karyokinesis.

Histone. The histone turnover manifests a profile similar to that observed for DNA. The data from histone measurements (Table XI), however, indicate that the sterile sporogenous nuclei are critically deficient in this macromolecule at PM, rather than FM, as observed for DNA. The trends of histone curves (Fig. 22) during stages subsequent to PM generally correspond to those of the DNA curves (Fig. 22), and this is also true for A- as well as B-type tapetal cells (Fig. 23). Nonetheless, two points need consideration. First, the *t*-test supports a null hypothesis for differences between A-type tapetal cells and normal at FM (Table XI) but the graph clearly indicates that functionally these cells are markedly different from normal. Second, the B-type cells deviate significantly from normal from the earliest to the last developmental phase of the male-sterile anther, and therefore may be considered perpetually deficient in histone concentration.

DNA/histone ratio. The DNA/histone ratios are given in Figure 24. It is evident that the two macromolecules maintain a balance within a narrow range of variation (1.0 to 1.5) throughout, in both sporogenous and tapetal tissue, and in both normal and sterile anthers. The ratios of B-type tapetal cells, however, demonstrate exceptional behaviour at some stages (viz. P, P_1 and MN) where a relatively wider imbalance is evidenced by abnormally high ratios, implying comparatively low concentrations of histone.

Studies on Nucleoli

Sporogenous Tissue

Comparative shape, size, number per nucleus and stainability of

nucleoli were studied in the male-fertile and male-sterile anthers.

Shape. The nucleolar shape, irrespective of the source (i.e., fertile or sterile tissues), was commonly observed to be an oblate spheroid (Figs. 25.1 to 25.3) and rarely spherical. The fully developed or regenerating nucleolus as seen at pachytene and at the PM stage is almost invariably an oblate spheroid, but the shape becomes nearly spherical when it is disappearing as in late diakinesis. The mature nucleolus usually contains two or three lightly staining internal zones, whereas immature nucleoli or those in degradation exhibit uniform staining throughout.

Volume. The data on nucleolar volume are presented in Table XII. During the $P-P_1$ period the nucleolar volumes of both fertile and sterile tissues occupy an intermediate range, and pachytene marks the onset of an increase which reaches maximum at early diakinesis (shown as 'diakinesis' in the table). Thereafter the nucleoli start to diminish in size and in late diakinesis the nucleolar material merges with the nucleoplasm.

At telophase II the chromosomes are probably very rich in high molecular weight ribonucleoproteins since they stain a distinctly bright orange with pyronin Y. It is likely that this material eventually coalesces with the nucleolus. Thus in good preparations at late telophase II one or two tiny droplets—initials of nucleoli—can be seen attached to the nucleolar organising chromosomes. These remain small during the first stages of PM but gradually show a definite growth in volume and at this time the nucleoli of normal and sterile tissues are volumetrically uniform (Fig. 27). Subsequently, however, defective behaviour becomes obvious in all the male-steriles, whereas in the normal tissue the nucleolar size

TABLE XII. Average nucleolar volume (in cubic microns) of the nuclei of sporogenous tissues and tapeta of male-fertile and male-sterile lines at different stages of anther development. (Figures indicated in parentheses are the total number of nucleoli measured.)

Developmental stages of anther	AVERAGE NUCLEOLAR VOLUME IN CUBIC MICRONS					
	Male-fertile*	Male-sterile lines				
		ms 5	ms 9	ms 10	ms 14	ms 18
P	19.30 ± 0.99(17)	16.10 ± 0.78(15)	24.68 ± 0.70(15)	16.39 ± 0.92(17)	22.31 ± 1.03(21)	18.41 ± 0.87(15)
Pachytene	20.43 ± 0.69(21)	20.73 ± 0.99(11)	27.76 ± 0.82(15)	18.97 ± 0.77(19)	22.30 ± 1.03(13)	24.79 ± 0.99(15)
Diakinesis	35.28 ± 1.08(19)	37.60 ± 1.73(17)	36.65 ± 1.02(15)	30.15 ± 1.71(15)	31.86 ± 0.97(15)	24.79 ± 0.94(15)
PM	8.67 ± 0.93(15)	10.00 ± 0.55(20)	9.38 ± 0.49(15)	7.1 ± 0.55(16)	9.90 ± 0.81(18)	6.71 ± 0.88(15)
FM	10.97 ± 0.73(17)	8.00 ± 0.67(15)	3.58 ± 0.57(15)	10.84 ± 0.71(16)	8.90 ± 0.70(15)	10.19 ± 0.48(15)
MN	29.32 ± 0.72(20)	6.55 ± 0.59(19)	0.00 ± 0.53(15)	11.53 ± 0.48(19)	0.00 ± 0.61(21)	4.86 ± 0.52(15)
Tapetal nucleoli (at pachytene)	10.52 ± 0.39(16)	9.92 ± 0.48(15)	8.67 ± 0.50(12)	11.06 ± 0.51(13)	9.58 ± 0.49(13)	8.06 ± 0.62(10)

*This data was obtained from sections of male-fertile anthers irrespective of the source.

increases through the PM-MN period. In *ms 5* and *9*, a progressive diminution of nucleoli is observed throughout the PM-MN period, which is more severe in *ms 9*, since in this mutant the nucleolus is completely resorbed at MN. In *ms 14* there is zero growth during PM-FM followed by a severe loss of the nucleolar material. In *ms 10* and *ms 18* nucleolar volume is almost equal to the normal at FM but not at the ensuing MN stage, since the nucleoli of *ms 10* show at most a very stunted growth during FM-MN (Table XII), while in those of *ms 18* there is a reduction in volume to approximately one-half.

Number. The frequency data for one- and two-nucleolate nuclei are presented in Table XIII. Early prophase microsporocytes (leptotene to pachytene) and the differentiating microspores of fertile anthers show one or rarely two nucleoli per nucleus (Fig. 25·2). At diakinesis, binucleolate nuclei were not seen, probably because of nucleolar fusion, and at FM they are again quite rare.

In the male-sterile anthers, however, the frequencies of binucleolate nuclei are very high at all stages. All five male-sterile lines show increased frequencies, but *ms 10* and *ms 14* have notably higher frequencies at all stages. The data also suggest that some coalescence does occur between the pachytene-diakinesis period, for at diakinesis (with the exception of *ms 5* and *ms 9*) the percentage of binucleolate nuclei is approximately one-third less than at pachytene, although the frequency rises again at FM to about the pachytene level.

In binucleolate nuclei, the nucleolar size is relatively much smaller than that of uninucleolate nuclei, and the paired nucleoli are usually unequal in size (see Fig. 25·2).

TABLE XIII. Percentage of sporogenous cells of normal and male-sterile anthers having two nucleoli at pachyte e, diakinesis, and free microspore stages. (Figures shown in parentheses are the total number of cells examined.)

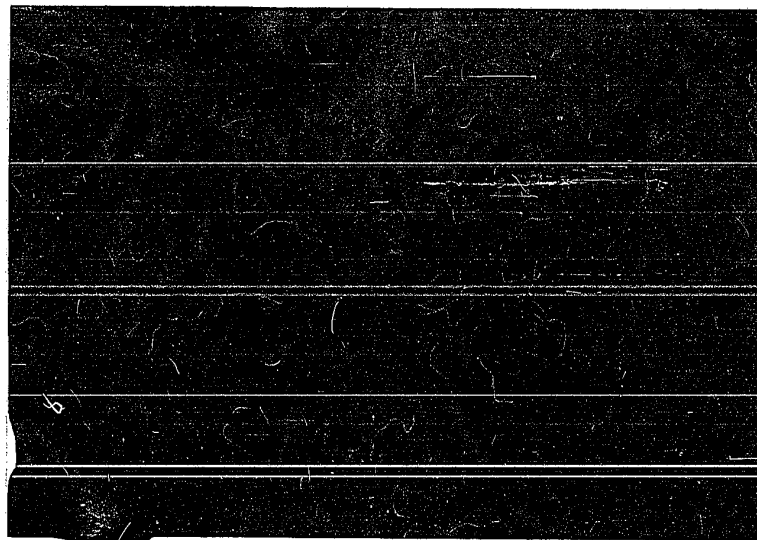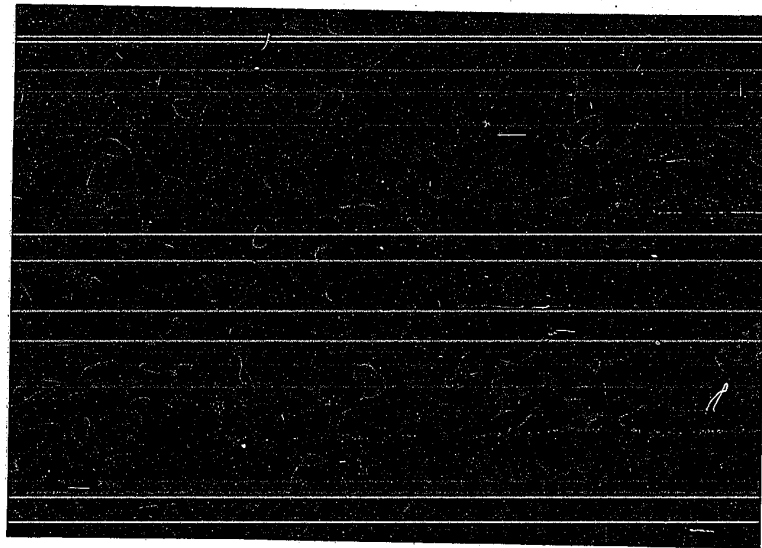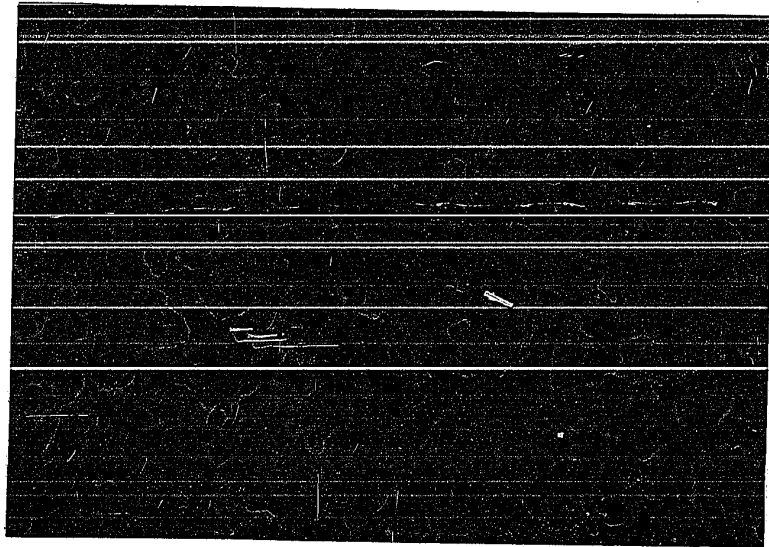| Line	FERTILE ANTHERS			STERILE ANTHERS		
	Pachytene	Diakinesis	Free microspore	Pachytene	Diakinesis	Free microspore
ms 5	0.0(197)	0.0(137)	0.0(148)	18.5(184)	17.6(264)	24.8(214)
ms 9	0.0 (88)	0.0 (97)	1.8(113)	17.1(210)	15.4(130)	20.6(136)
ms 10	5.7(105)	0.0(186)	0.0(211)	31.8(110)	22.9(240)	38.4(219)
ms 14	3.8(238)	0.0(107)	1.3 (77)	33.3 (93)	19.1(178)	35.8(260)
ms 18	0.0 (80)	0.0(123)	0.0(130)	21.6(190)	13.8(268)	26.1(245)

Stainability. No differences in nucleolar stainability between and within the meiocytes and microspores could be detected visually. Similarly, the nucleoli of fertile and sterile anthers did not reveal any cytological difference; rather, they exhibit a uniform staining capacity. Figures 26·1 to 26·6 give a comparison of the nucleoli of sporogenous tissues of male-fertile and male-sterile anthers of different lines at late diplotene-early diakinesis stages.

Tapetal tissue. The tapetal nucleoli are not visible with standard cytological procedures during most of the cell cycle. This is probably because they are surrounded by heavily staining chromatin. DNase-extraction, even for extended periods up to 40 hrs or with elevated enzyme concentrations up to 0.08 mg/ml fail to reveal them clearly. The only period in which they are seen with some degree of clarity is the early M stage (up to and some time before pachytene). This actually is the time when the chromosomes in tapetal nuclei are preparing for karyokinesis and/or are at prophase. The results of volumetric estimations of pachytene stage tapetal nuclei are shown in the bottom line of Table XII. It is seen that the volume, irrespective of source (male-fertile or male-sterile) varies between a range of about 8 to 11 cubic microns.

All cells in which nucleoli could be seen contained only one nucleolus. It is possible that some nuclei may have more than one nucleolus but none could be discerned.

Fig. 25. 1, section of a meiocyte at late diplotene showing one
nucleolus of nearly spherical shape and attached to two different
bivalents. X7800. 2, section through a binucleolate nucleus at
diakinesis; the two nucleoli are oblate spheroid. X5600. 3, section
through two microsporocytes at the free microspore stage; the
nucleoli enlarge rapidly from this stage on and they are oblate
spheroid in shape. X8500.
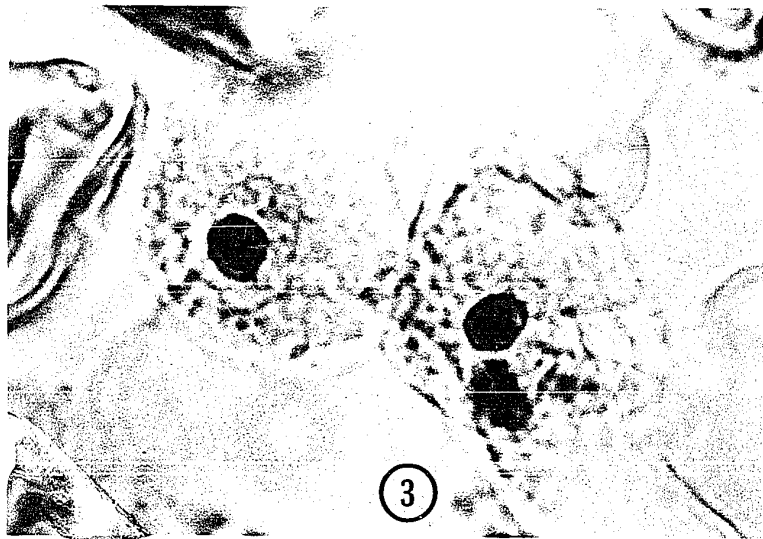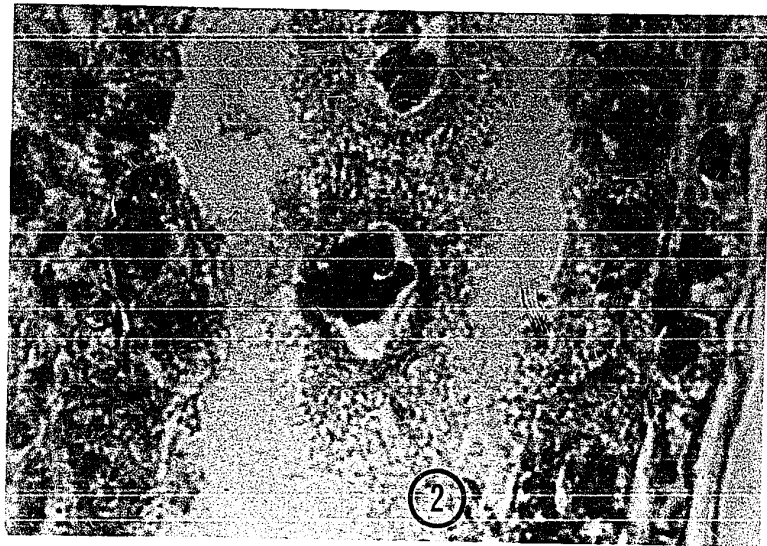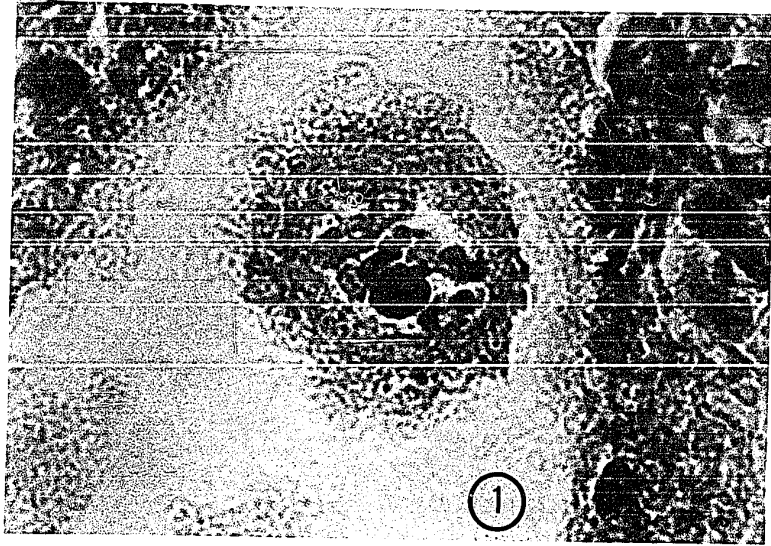
Fig. 26. Colour micrographs 1 through 6 show the density of staining

in the nucleoli of sporogenous tissues of normal and male-sterile

anthers. The preparations were made from DNase treated 5 micron thick

sections and stained with Methyl green-Pyronin. The differences in

colouration between different micrographs is only due to the background

tint.   1. male fertile anther;   2. *ms 5*;   3. *ms 9*;   4. *ms 10*;

5. *ms 14*;   6. *ms 18*.   All micrographs X2400.
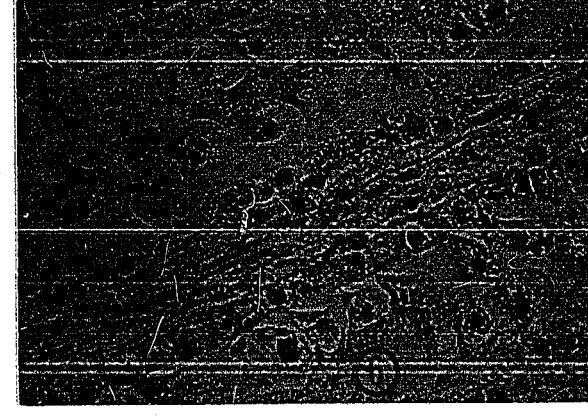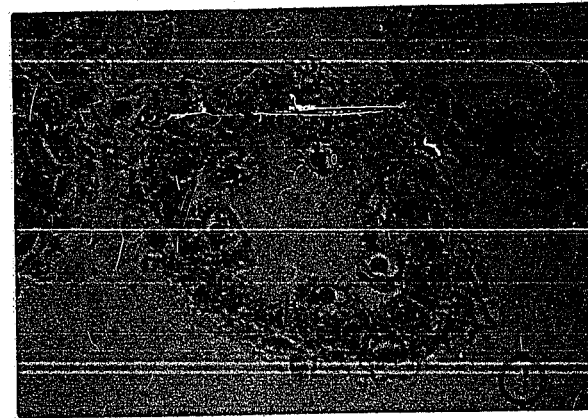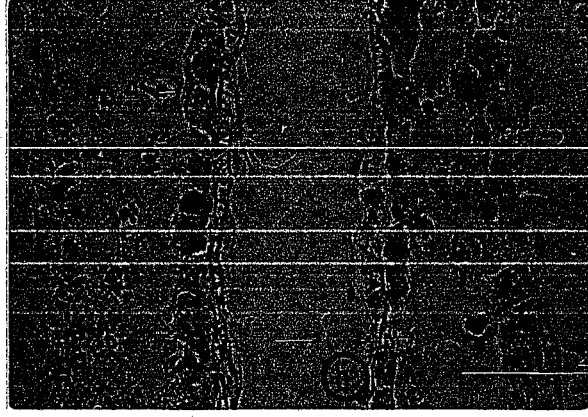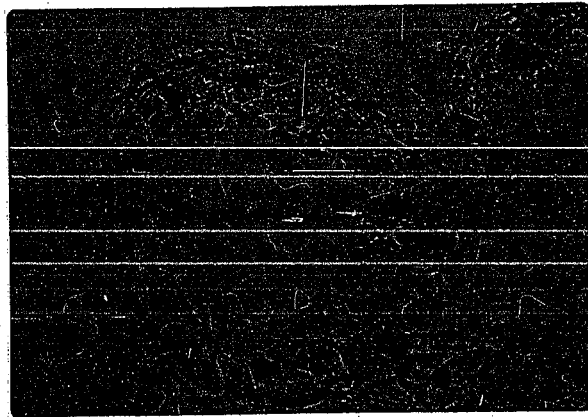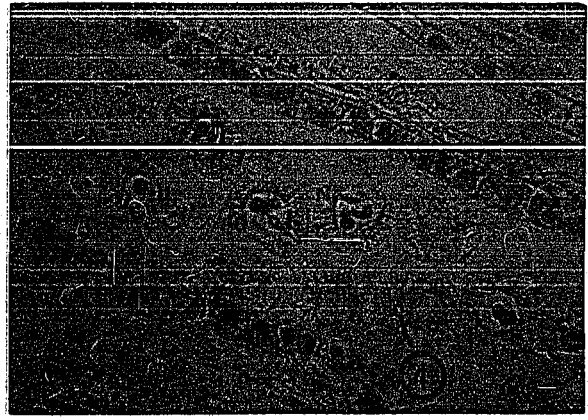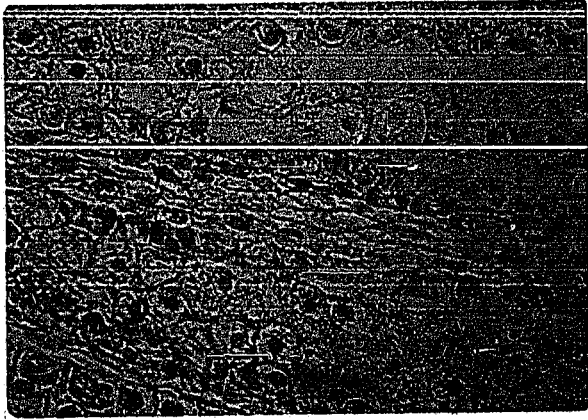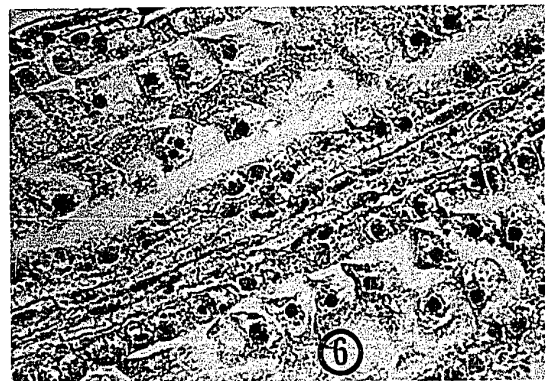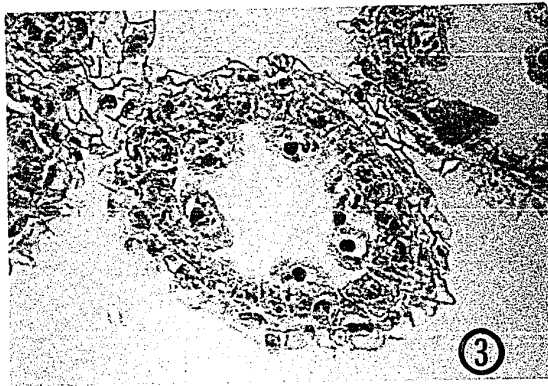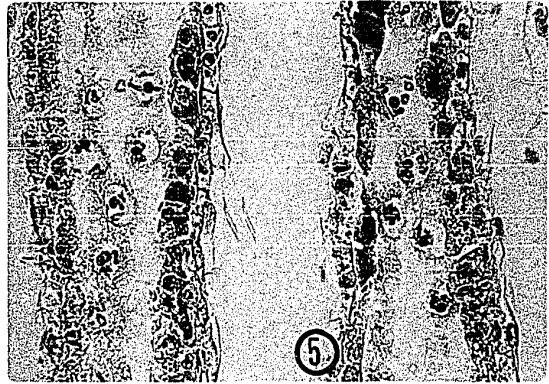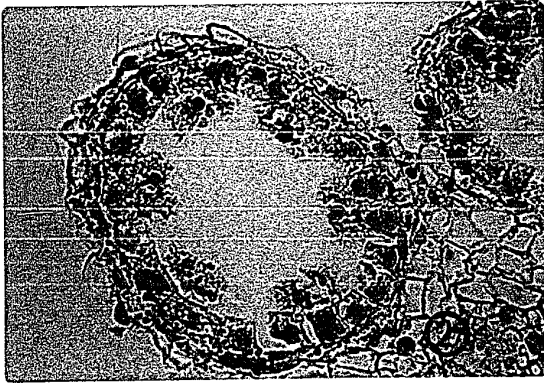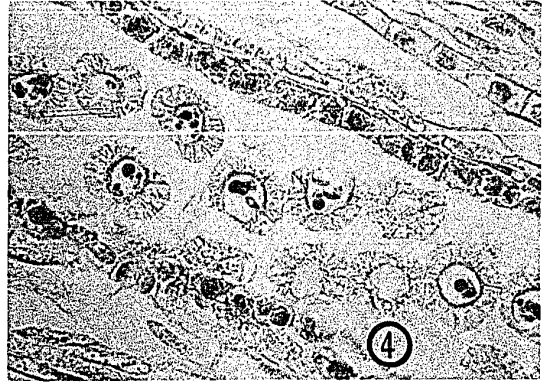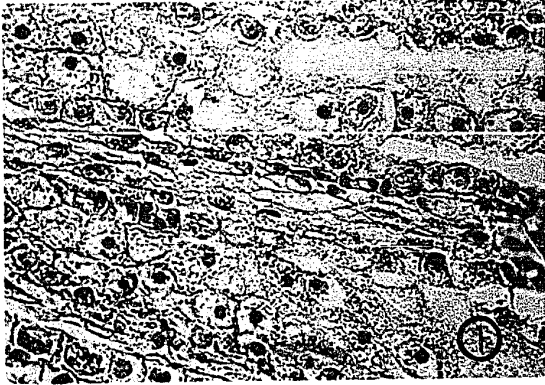
Fig. 27. Nucleoli of sporogenous and tapetal tissues during meiosis
and after meiosis. 1, longitudinal sections with meiocytes at
pachytene; note the nucleoli protruding to cne side of the pachytene
chromatin cluster. X2700. 2, same as 1, shown in cross section with
one meiocyte at diakinesis; two bivalents are attached to one nucleolus.
X3500. 4, cross section of anther at free microspore stage; two cells
have binucleolate nuclei. This section was taken from *ms 9* anther.
X1800. 5, microspores at midway between the free microspore and
mononucleate stages. This section was taken from *ms 10*. X1800. 6,
nucleoli at mononucleate stage. X1600.
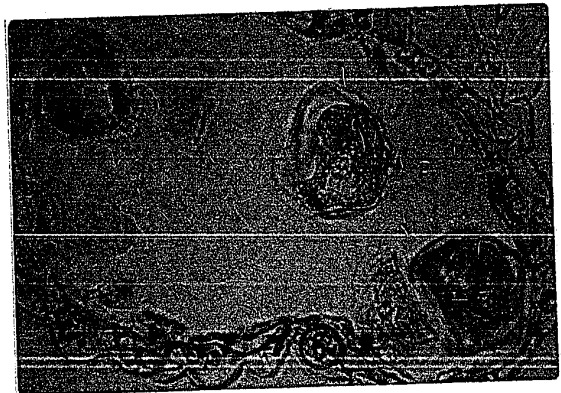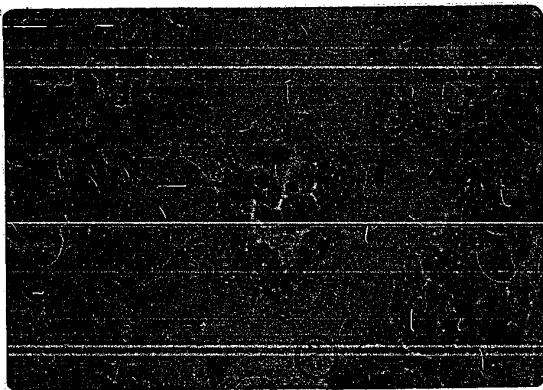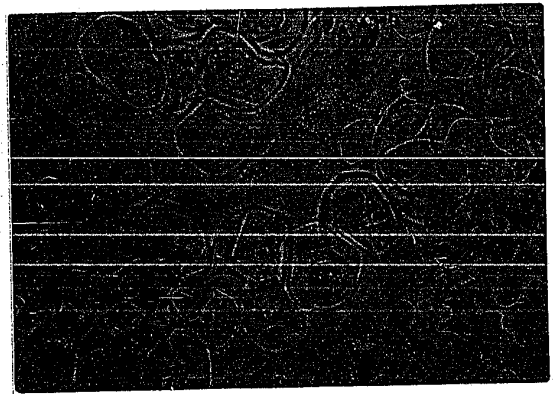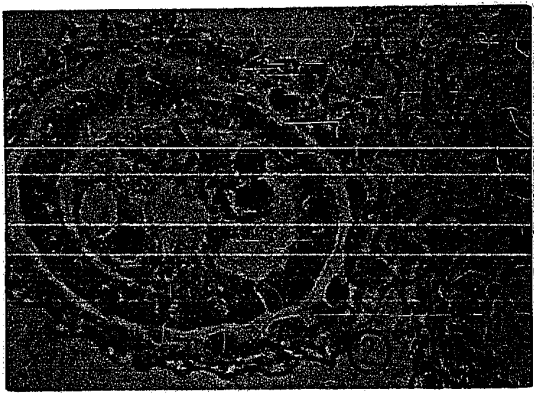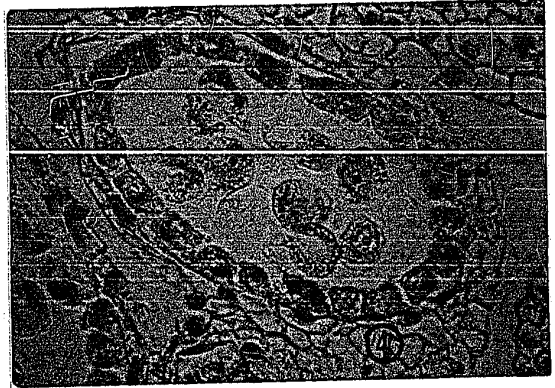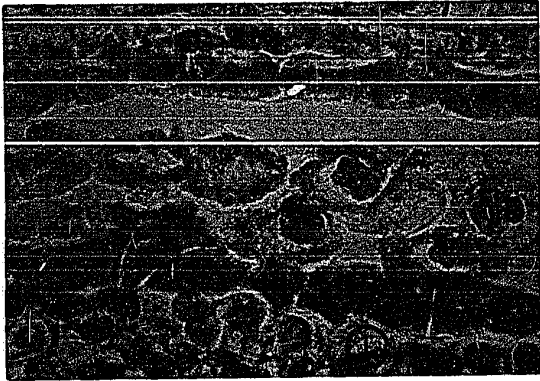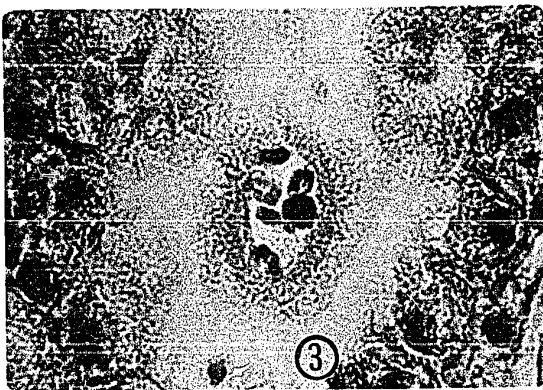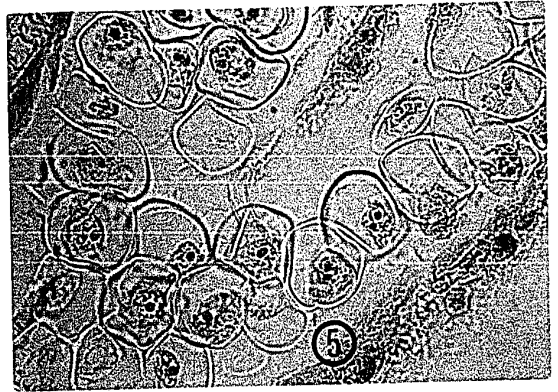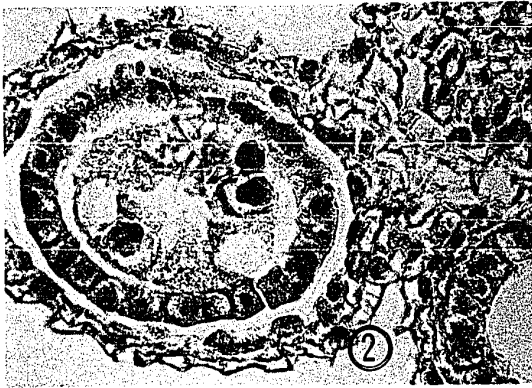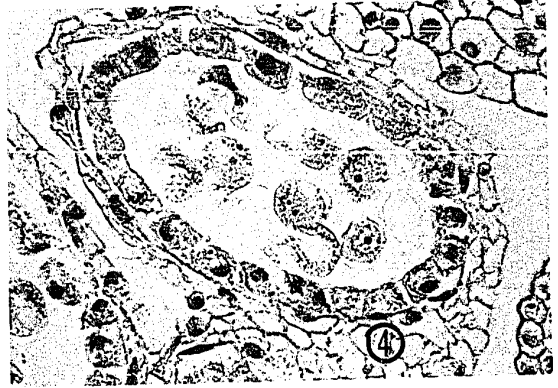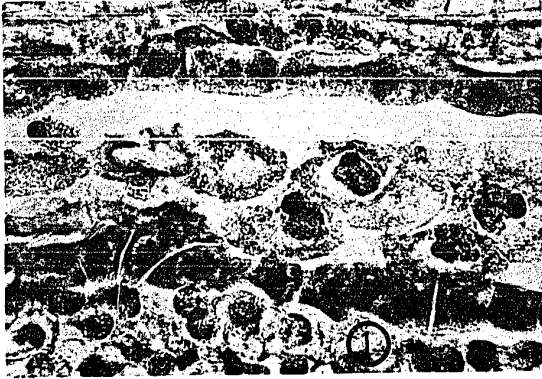
DISCUSSION

A comparative analysis of the course of anther development at six sequential stages reveals that the time of manifestation of male-sterility (*ms*) genes is specific with respect to the particular male-sterile line and is restricted to the anther tissue. The abnormalities are exhibited exclusively in the sporogenous and tapetal tissues. Further, the deviations from the normal occur both at the histological and cytochemical levels. A summary of these observations has been given in Table XIV. Both the histological and histochemical data indicate that the effects of different *ms* genes are unique. It might, therefore, be inferred that the genes differ in their effect with regard to the time and the nature of the developmental process affected. These processes will be discussed separately.

ms 5

The first functional defect observed in *ms 5* is the delay in the release of tetrads from the callose capsule and an inward curving of their septal walls (Fig. 5·3). Later, at FM, the tetrads show arrested growth and loss of DNA and histone from the nuclei (Figs. 10, 11). This is followed, in the FM-MN period, by an overall cytoplasmic degeneration and cellular deformation. In the tapetum a departure from the normal structural development first appears at PM and becomes more obvious during the subsequent stages. This strongly suggests that the sporogenous and tapetal tissues are intimately related in such a way that prior imbalance in the one adversely affects the structure and functioning of the other.

114

TABLE XIV. Different stages of anther development at which first indications and reappearances of abnormality is observed in the sporogenous and tapetal tissues of male-sterile anthers.

| Male sterile line | HISTOLOGICAL ABNORMALITIES | | CYTOCHEMICAL ABNORMALITIES | | | |
| | | | DNA | | Histone | |
	Sporogenous tissue	Tapetal tissue	Sporogenous tissue	Tapetal tissue	Sporogenous tissue	Tapetal tissue
ms 5	PM Tetrad dissociation delayed	PM Nondegeneration MN enlargement of cells	FM	N·D*	FM	N·D*
ms 9	PM Dark staining of nuclei and cytoplasm FM Decline of cytoplasm	PM Increase in radial thickness FM Rapid degeneration Loss of cytoplasm	PM	FM	PM	N·D*
ms 10	MN Clumping of cytoplasm and loss of stainability	Delay in karyokinesis	PM	P# + FM	PM	P# + PM
ms 14	FM Poorly developed walls and arrested growth	Delay in karyokinesis	P† + PM	PM	P_1	P† + FM
ms 18	Delay in various histological events FM Invaginating cell walls and retarded growth	90% nuclei do not show karyokinesis	P_1 +FM (A) (B)	PM# +MN P_1	PM (A) (B)	PM# +MN P

*N·D = no difference from the normal; # = the difference appears first + no difference at inbetween stages;
† = the difference at P is probably due to a change in sample.

The absence of any deviation from the normal nuclear DNA and histone patterns of tapetum, however, indicates that this correlation does not extend to these two macromolecules. In other words, the enlargement of tapetal cells beginning at PM appears to be primarily due to an increase in cytoplasmic mass. This may be the result of a blockage in the passage of components of the tapetal cytoplasm through the tapetal plasmalemma or cell wall and into the thecal lumen. A blockage by the plasmalemma itself, or alternatively an excessive build-up of such components in the sporangial lumen, on account of a failure of young microspores to absorb and utilize them, could give this effect. The latter possibility seems more plausible since, according to Heslop-Harrison (1964), the 'callose special mother cell wall' which surrounds the tetrads forms an effective barrier to the passage of molecules between the maternal tissue and the tetrads. Thus in *ms 5* a more prolonged blockage due to delayed microspore emergence from the callose capsule could result in the increased tapetal growth.

It could also cause a deprivation of microspores for nutrients crucial to their early development, and hence could eventually cause the observed microspore degeneration. These evidences tend to suggest that the *ms 5* gene is involved at some level in the regulation of the mechanism of release of tetrads from the callose envelope.

ms 9

The unusually denser staining of the cellular contents of microspores before their separation from tetrads (Fig. 6·4), closely resembles the normal tapetum in its degeneration during the terminal stages.

Although the free microspores appear normal in shape, size, and nuclear morphology during the initial period of FM, significant quantitative differences exist in their nuclear DNA and histone content as indicated by the significantly lower amounts of both macromolecular species at the PM stage. As a consequence, the appearance of histological abnormalities succeed the cytochemical changes in this tissue.

The expression of structural abnormalities of sporogenous tissue and tapetum coincide in time from the PM stage onward. However, this is not true for DNA and histone variations in these two tissues. The nuclei of young microspores become deficient in DNA and histone sometime during the early PM stage and this deficiency becomes progressively more acute as the tissue proceeds from FM into the MN stage (Figs. 13, 14). In tapetal nuclei, on the other hand, DNA deficiency relative to the normal occurs only during the later developmental period, i.e., past FM stage (Table IV), whereas the histone levels remain unaltered throughout anther development (Table V). From this it follows that the more direct effect of the *ms 9* gene occurs in sporogenous nuclei in the form of DNA and histone decline, which probably initiates the eventual structural deformation and developmental failure of these cells. The abnormal behaviour of the tapetum may thus be a direct response to this. Since the morphological aberrations in tapetal tissue precede the rapid DNA loss during FM-MN, it is possible that the aberrant development actually begins in the cytoplasm of these cells and subsequently extends to the nucleus where only DNA degradation occurs and histone level remains constant.

The behaviour of DNA and histone metabolism in the tapetal nuclei throws some light on their temporal relationship with respect to the

expression of *ms 9* in this tissue. First, the synthesis of these two macromolecules occurs simultaneously, as is seen during the P to P_1 and M to PM periods, but their catabolic fates appear not to be correlated. Thus the degradation of DNA observed during FM-PM does not have any quantitative effect on the histone content of these nuclei. Second, since histone turnover in the tapetum appears insensitive to the *ms 9* gene, and structural abnormalities in this tissue are still observed, it can be inferred that histones as such play no role in the expression of these tapetal abnormalities.

The inference made above, that the direct effect of *ms 9* is on the microspores derives some support from evidence for a relatively high auto-trophy of sporogenous tissue during M to PM (from pachytene until the release of tetrads from callose wall) since in this period the tetrads are enclosed in callose capsules and isolated from maternal molecules (Taylor, 1959; Heslop-Harrison, 1967). In this line (*ms 9*) the micro-spores newly emerged from callose, i.e. at FM, are deficient for a sub-stantial amount of DNA.

The observation that a loss of DNA without histone loss occurs in the tapetum during FM-MN is difficult to explain. It seems possible, however, that a histone independent DNA degrading enzyme system may diffuse from the sporogenous tissue to the tapetal cells and initiate DNA breakdown. Stern (1961) has demonstrated the presence of phosphodi-esterase in anthers of lily (*Lilium regale*), but no precise evidence as to its origin and action was given. Alternatively, a general increase in nuclease and histone-specific protease in the sporangial lumen could bring about a simultaneous degradation of DNA and histone in the nuclei of microspores.

ms 10

In *ms 10* there appears to be good evidence of a close functional relationship between sporogenous tissue and the tapetum. Both tissues show significant quantitative differences from normal DNA and histone simultaneously at PM (Tables VI, VII). In addition, within a particular phenotype, i.e. male-sterile or male-fertile, the trends of both macromolecular species are inflectionally similar during the different anther developmental stages (Figs. 16, 17). The effects of *ms 10* appear quite suddenly on sporogenous tissue at FM and in both DNA and histone, whereas there is an increase in both substances in sterile anthers closely parallel with that in normal anthers to this stage. Subsequently there is a dramatic decline in DNA to a very low level (0.86 ± 0.03 vs. 2.35 ± 0.09 of the normal) paralleled by a similar decrease in histone. Significant differences also appear in the tapetum at PM, but in this case the amounts of DNA and histone are increased, and this increased level persists during the subsequent stages.

The DNA deficiency in the nuclei of young microspores at PM signifies that DNA loss from these nuclei begins soon after the completion of meiosis. DNA increase during PM-FM proceeds at the same rate as in the normal anther, indicating that the mechanism for DNA synthesis is normal in these cells. The quantitative deficit of these nuclei in DNA is therefore probably due to causes other than deficient synthesis. One possibility is an excess in activity of DNA-degradative enzymes over DNA-synthetic during the period occurring when the PMC's are invested by the callose special mother cell wall. The resumption of normal DNA synthesis during the PM-FM period would in this case be explained by a

shutdown of degradation with release from callose. This, however, does
not explain the high nuclear DNA and histone content of the tapetal cells
during the PM-MN period. The DNA and histone variations of sporogenous
and tapetal nuclei seem normally to be strongly related during anther
development after meiosis. This relationship is an inverse one; the
DNA increase in normal microspore nuclei is seen to be accompanied by an
abatement of DNA in the tapetal nuclei. It is thus very likely that this
characteristic feature of the tapetum is a response to a specific stimulus
from the sporogenous cells. It appears necessary, therefore, to invoke
two systems for the correlation of functions in the tapetum and the
sporogenous tissue. First, this stimulus derepresses the DNA synthesis
in the tapetal nuclei in the M-PM period and a gradual loss of this
macromolecule during PM-MN. Second, it provides for a mobilization of
DNA breakdown products and the pollen wall precursors from the tapetum to
the young microspores. According to this hypothesis the abnormal behav-
iour of the sporogenous and tapetal tissues in male-sterile anthers would
be due to a barrier between the two tissues, preventing a normal flow of
substances from the tapetal nuclei to the sporogenous tissue. Conse-
quently DNA and associated histones would accumulate and remain localized
within the nuclei of tapetal cells, and their inward movement to the
developing pollen would be stopped, as observed, resulting in the starva-
tion of young microsporocytes. As a consequence the developing microspores
would show first a DNA and histone deficiency beginning at PM and then a
sudden breakdown from FM onward.

Transport of Feulgen positive bodies, originating in the tapetum,
passing into the anther lumen and associating with the microspores was

reported by Cooper (1952) in *Lilium regale* anthers. Foster and Stern

(1959) have also demonstrated a quantitative increase in 'soluble

deoxyribosidic material' in the anthers of *Lilium longiflorum* at periods

corresponding to those of DNA synthesis in meiocytes, microspores, and

pollen grains. The tapetum was presumed to be the probable source of

this material since it degenerated during microspore development. Takats

(1962), using H^3-thymidine autoradiography, observed an accumulation of

the DNA breakdown products on the microspore walls. The actual utiliza-

tion of these DNA products by the developing microspores is, however,

still a matter of conjecture.

ms 14

The differences between anthers of *ms 14* and the normal sporogenous

nuclear DNA at P, histone at P_1, and in tapetal nuclear DNA at P, although

significant, do not seem to be critical for development since at these

stages both tissues of sterile anthers appear histologically normal.

Moreover, their tapetal nuclei later (at M) show normal amounts of DNA

and histone content. In addition, the general delay of karyokinesis in

the male-sterile tapetum seems to be of little developmental significance

since eventually about 98% of the nuclei become binucleate. These devia-

tions, therefore, may not be related to the differences occurring during

the subsequent M stage.

The histone trends in sporogenous and tapetal nuclei of *ms 14*

anthers closely correspond to those of the DNA (Figs. 19, 20) maintaining

the DNA/histone ratio within a narrow range, i.e. between 1 to 1.6 (Fig.

21). The occurrence of a significant deficiency of DNA and histone in

sporogenous tissue at PM indicates an effect immediately before this stage. The DNA in these nuclei drops during PM-FM to a very low level, e.g. 0.63 ± 0.02 arbitrary units as against 2.07 ± 0.05 for the normal (Table VIII). The tapetal nuclei compared with those of normal anthers also show a significantly low DNA amount at M which may indicate a slow DNA replication rate during M to PM period. Subsequent to this and extending up to MN, a still slower rate of DNA increase is noted. With the exception of the M stage, the histone metabolism in these tapetal nuclei also follows a similar profile (Fig. 20). This interrelated cytochemical behaviour of the sporogenous and tapetal tissues associated with the histological abnormalities observed during the PM-MN anther developmental period clearly suggests a defective information flow between the two tissues. The impact of such a defect becomes obvious simultaneously in both tissues during the M-PM period.

The drastic reduction of DNA and histone in *ms 14* sporogenous tissue may be regarded as due either to degradation without synthesis or starvation for precursors from the tapetum. The increase rather than the normal drop in tapetal DNA and histone during PM-MN is coincidental with the microspore S period, strongly suggesting that the microspores are being deprived of a tapetal contribution of DNA precursors. A mechanism that might cause the block has not been described to date, although the tapetal wall bordering the sporangial lumen may be a suspect. The histological observations indicate that in sterile anthers this wall is comparatively thicker and more prominent (Fig. 8·5) than in normal anthers (Fig. 3·7). Moreover the tapetal cells become rich in densely staining cytoplasmic material, which in all probability consists of Ubisch

bodies. These bodies are known to carry pollen exine precursors from the tapetum to the sporogenous cells as reported by Echlin and Godwin (1968) and Ford (1971), and blockage of their migration would, therefore, cause serious defects in pollen wall development, as observed in the microspores during PM-MN (Figs. 8·3, 8·6).

ms 18

In *ms 18* the nuclei of tapetal cells show DNA and histone deficiencies at P_1, which are closely followed by the developmental abnormalities, whereas a similar deficit in the sporogenous nuclei at this stage is not directly followed by apparent cytological abnormalities, which appear only after the PM stage. These become ostensible in the tapetum at M (failure of karyokinesis) and in the sporogenous tissue at FM when microspore walls show drastic shrivelling. Although initially a small proportion of tapetal cells (A type cells) appear to develop normally, this development is not carried beyond the M stage after which both structural and cytochemical defects are observed (Figs. 9, 22, 23). Thus these observations tend to suggest that a critical temporal relation between the sporogenous and tapetal tissues is established after the completion of meiosis and sporogenous tissue can be regarded as dependent on earlier effects on the tapetum. Moreover, the occurrence of deviant behaviour, first in tapetum and then in sporogenous tissue, clearly suggests that the direct action of the *ms 18* gene is on the tapetal rather than the sporogenous tissue. The resultant deficit in tapetal DNA and associated histone synthesis seems serious enough to explain quite adequately the karyokinetic failure in the tapetal nuclei. These observations support the suggestion made earlier that the tapetum may normally supply DNA and histone precursors

along with other material (e.g. sporopollenin) to the microsporocytes

after the PM stage. The observation that 10% of the tapetal cells show

a normal karyokinesis and become binucleate suggests that the tapetal

effect of the mutant gene (ms 18) may be a leaky one up to the M stage.

Afterwards the binucleate cells become abnormal like the others (Figs.

22, 23).

The investigations on the behaviour of nucleoli in sporogenous

tissues of normal and sterile anthers show that the nucleoli of meiocytes

grow considerably from P_1 to diakinesis (Table XII). This nucleolar

increase is indicative of the accumulation of ribosomal RNA since it is

now well established that nucleoli contain large proportions of rRNA.

Gall (1966) observed accumulation of large amounts of rRNA during

diplotene of Amphibian oocytes and a similar finding has been reported

by Stern and Hotta (1963) from their studies on *Trillium erectum*.

These authors, however, indicated that the RNA synthesized during

zygotene and early- and mid-pachytene is of the non-ribosomal type but

during the subsequent stages most of the RNA formed is similar to the rRNA.

The nucleolar volumes in sterile sporogenous tissues of the male-

sterile lines studied here do not depart from the normal until FM. From

this stage on male-steriles of all lines show degradative changes, the

degree of effect being characteristic for each line. The most drastic

effect occurs in *ms 9* where the nucleolar volume decreases somewhat

earlier (from PM) terminated by nucleolar disappearance at MN. In *ms 14*

a similar development begins at FM. In *ms 5* and *ms 18* reduction in

nucleolar volume does not occur until FM-MN and is relatively less drastic,

while in *ms 10* the nucleolar growth ceases almost completely during FM-MN.

These nucleolar defects appear somewhat later than the histological effects and the DNA and histone abnormalities discussed earlier (generally detected from the PM stage). This implies that in the developing microspores of male-steriles the nucleoli function normally for some time after the appearance of nuclear DNA losses. Hence these nucleolar effects are probably of a secondary nature rather than a direct consequence of male-sterile gene action.

The occurrence of binucleolate nuclei in the sporogenous tissue of male-sterile anthers cannot be satisfactorily explained in the light of existing information. Barley is known to have two nucleolar organizing chromosomes (Sarvella, 1958), both of which are understood to participate in the formation of a single nucleolus. Thus it appears likely that the *ms* genes affect this participation. This might be a consequence of the male-sterility gene action or because of certain physiological phenomena arising therefrom, since Swift (1960) found that HeLa cells cultured in nutrient deficient medium show increased number of nucleoli per nucleus. Herich (1965), working with cytoplasmic male-steriles in corn, showed defective formation of nucleoli; the sterile variety showed an increased number of nucleoli per nucleus in the microsporocytes whereas the fertile variety had only one nucleolus. His speculation was that the effect could be due to a defective functioning of the nucleolar organizing regions.

The present investigations have shed some light on the nature of developmental processes in sporogenous and tapetal tissues of normal anthers. In the first place during P to P_1 these two tissues together show a phase of cell proliferation and growth when their patterns of DNA and histone turnover are also observed to be closely parallel. From the

initiation of meiosis in sporogenous cells and karyokinesis in tapetal
nuclei these tissues begin to show divergence with respect to histological
behaviour and DNA-histone turnover. The tapetum gradually passes into a
phase of decline and senescence while the microspores continue growth and
differentiation, which ends in the formation of mature pollen grains.
The fact that DNA in tapetal nuclei drops drastically during PM-MN while
at the same time the DNA in the nuclei of microspores increases continu-
ously indicates that the tapetal DNA and possibly the associated histones
or their breakdown products are utilized for the DNA histone synthesis
of the microspores. It is interesting to note that the pre-breakdown
(i.e. during M to PM) DNA-histone synthesis in tapetal nuclei seldom
reaches more than one-half the level expected for a complete replication
synthesis, suggesting that the onset of DNA-histone losses from these
nuclei occur before the synthesis is complete.

The above conclusion of a nutritive function of tapetum is
supported by the behaviour of the *ms* genes studied here and by evidence
from other workers (Echlin, 1971; Ford, 1971; Cutter, 1971). The claim
for the movement of DNA precursors from tapetum to the sporogenous tissue
(Cooper, 1952; Taylor, 1959; Takats, 1962) has been described earlier.
In addition, the evidence for the uptake of exogenous DNA by plant cells
has recently been demonstrated (Ledoux and Huart, 1969; Stern and Hotta,
1971). It is quite likely that in the tapetal-sporogenous tissue system
the DNA supplied by the tapetum is first modified and then taken up by
the microspores, since from *in vivo* H^3-thymidine labelling of *Lilium
longiflorum* anthers Takats (1962) could not observe intact incorporation
of tapetal DNA by the microspores.

As a result of the manifestation of *ms* genes the deleterious
effects (histological or cytochemical) on the sporogenous tissue invari-
ably occur during or after the PM stage (Table XIV) in which these cells
show cellular deformation in association with the drastic decreases of
DNA and histone amounts in their nuclei. In contrast the effect on
tapetal tissue is variable with the *ms* gene involved. Generally these
cells do not show normal degeneration; rather they begin to enlarge and
accumulate increased amounts of cell contents.

Each of the mutant (*ms*) genes investigated here shows a specific
mode and locale of action. On this basis a classification of the dif-
ferent mutants into groups has been made. The effects in *ms 5* are best
explained from the inference that the gene products disrupt a mechanism
which is crucial for the prompt release of young microspores from the
callose capsule, the control of which on *a priori* reasoning lies within
the young microspores.

From cytological inferences alone it appears that the manifestation
of the *ms 9* gene also begins in the cells of sporogenous tissue and in
this case the effect is related with the DNA and histone turnover in the
nuclei of these cells. Considering these evidences *ms 5* and *ms 9* should
be classed as 'sporogenous tissue' mutants.

In contrast, in *ms 14* a communication blockage between sporogenous
tissue and the tapetum appears to exist during PM, as a consequence of
which the newly emerging microspores show arrested growth. Similar if
somewhat modified effects are found for the *ms 10* gene. These two mutants
thus influence the structure or permeability of tapetal or sporogenous
tissue cell walls, or some other barrier-producing mechanism between the

two tissues. These functional and morphogenic similarities of *ms 10* and *ms 14*, when viewed in the light of a recent finding by Hockett (unpublished data) that these two genes are very closely linked (showing less than 1% crossing over), tend to suggest that they are duplicate loci, and it will be worthwhile to further investigate this point. In view of this uncertainty about the tissue directly affected, these mutants, however, should be tentatively classed as 'micro-sporangial' mutants.

Finally, *ms 18* demonstrates a genetic effect in which tapetal involvement is more obvious. The nuclei of this tissue depict drastic abnormalities both functionally and metabolically from the very early stages of anther development. The breakdown of PMC's in contrast is not initiated until FM. This observation unambiguously supports the inference that a sporogenous tissue dependence on tapetum begins after PM. In this particular case the tapetum may be regarded as solely responsible for failure of pollen grains. Hence this gene (*ms 18*) should be called a 'tapetal' mutant.

BIBLIOGRAPHY

AKINRIMISKI, E.O., BONNER, J., TS'O, PAUL O.P. Binding of basic proteins
    to DNA. J. Mol. Biol. 11: 128-136, 1965.

ALAM, S., SANDAL, P.C. Cytohistological investigations of pollen
    abortion in male-sterile sudan-grass. Crop Sci. 7: 587-589,
    1967.

ALFERT, M. Quantitative cytochemical studies on patterns of nuclear
    growth. In: *Symposium on Fine Structure of Cells Leiden 1954.*
    Groningen: P. Noordhoff Ltd., 1955. pp. 157-163.

ALFERT, M. Chemical differentiation of nuclear proteins during
    spermatogenesis in the salmon. J. Biophys. Biochem. Cytol. 2:
    109-114, 1956.

ALFERT, M., GESCHWIND, I. A selective staining method for the basic proteins
    of cell nuclei. Proc. Nat. Acad. Sci. 39: 991-999, 1953.

ALLFREY, V., MIRSKY, A. On the role of histones in regulating RNA
    synthesis in the cell nucleus. Proc. Nat. Acad. Sci. 49: 414-
    421, 1963.

ANSLEY, H.R. Histones of mitosis and meiosis in *Loxa flavicolis*
    (Hemipteran). J. Biophys. Biochem. Cytol. 4: 59-62, 1958.

ANTROPOVA, E.N., BOGDANOV, YU F. Cytophotometry of DNA and histone in
    meiosis of *Pyrrhocoris apterus.* Exp. Cell Res. 60: 40-44,
    1970.

BARR, G.C., BUTLER, J.A.V. Histone and gene function. Nature 198: 1170-
    1177, 1963.

BERLOWITZ, L. Analysis of histone *in situ* in developmentally inactivated
    chromatin. Proc. Nat. Acad. Sci. 54: 476-480, 1965.

BERLOWITZ, L., PALLOTA, D., PAWLOWSKI, PH. Isolated histone fractions
    and the alkaline fast-green reaction. J. Histochem. Cytochem.
    18: 334-339, 1970.

BOGDANOV, YU F., ANTROPOVA, E.N. Delayed termination of nuclear histone
    doubling after premeiotic DNA synthesis in *Triturus vulgaris*
    male meiosis. Chromosoma 35: 353-373, 1971.

BONNER, J., TS'O, P. (Eds.) *The Nucleohistones.* San Francisco, London,
    Amsterdam: Holden-Day, Inc., 1964. p. 376.

BRACHET, J. La détection histochimique des acids pentosenucléiques.
    Compt. Rend. Soc. Biol. (Paris) 133: 88-90, 1940.

BROOKS, M., BROOKS, J.S., CHIEN, L. The anther tapetum in cytoplasmic-
    genetic male sterile sorghum. Amer. J. Bot. 53: 902-908, 1966.

BUTLER, J.A.V. Role of histones and other proteins in gene control.
Nature 207(5001): 1041-1042, 1965.

CASPERSSON, T.O. *Cell Growth and Cell Function — A Cytochemical Study*.
New York: W.W. Norton & Co. Inc., 1950.

CHOOI, W.Y. Variation in nuclear DNA content in the genus *Vicia*.
Genetics 68: 195-211, 1971.

CLEVER, U. Regulation of chromosome function. Ann. Rev. Genet. 2:
11-30, 1968.

COLE, A. A molecular model for biological contractility: Implications
in chromosome structure and function. Nature 196: 211-214,
1962.

COLLINS, G.B., LEGG, P.D., ANDERSON, M.K. Cytophotometric determination
of DNA content in *Nicotiana* megachromosomes. Can. J. Gen. Cytol.
12: 769-778, 1970.

COMING, D.E. Histones of genetically active and inactive chromatin.
J. Cell Biol. 35: 699-708, 1967.

COOPER, D.C. The transfer of DNA from the tapetum to the microsporocytes
at the onset of meiosis. Amer. Nat. 86: 219-229, 1952.

COX, P.G., SYMPSON, S.B. A microphotometric study of myogenic lizard
cells grown *in vitro*. Dev. Biol. 23: 433-443, 1970.

CUTTER, E.G. *Plant Anatomy: Experiment and Interpretation. Part 2:
organs*. London, England: Edward Arnold, 1971. pp. 227-238.

DAHMUS, M.E., BONNER, J. Nucleoproteins in regulation of gene function.
Fed. Proc. 29: 1255-1260, 1970.

DULBECCO, R. The histones as candidates for a role in genetic repression.
In: *The Nucleohistones*. Edited by J. Bonner and P. Ts'o.
San Francisco, London, Amsterdam: Holden-Day Inc., 1964.
pp. 362-366.

ECHLIN, P. Production of sporopollenin by tapetum. In: *Sporopollenin*.
Edited by J. Brooks, P.R. Grant, M. Muir, P. van Gijzel, and
G. Shaw. London, New York: Academic Press, 1971. pp. 220-247.

ECHLIN, P., GODWIN, H. The ultrastructure and ontogeny of pollen in
Helleborns foctidus L. I. The development of the tapetum and
Ubisch bodies. J. Cell Sci. 3: 175-186, 1968.

ELY, J.O., ROSS, M.H. Deoxyribonucleic acid contents of rat liver nuclei
influenced by diet. Science 114: 70-73, 1951.

ESAU, K. *Plant Anatomy*. New York: John Wiley & Sons Inc., 1953.
pp. 550-551.

FAUTREZ-FIRLEFYN, N. Expulsion d'acide thymonucleique hors du noyau de
        certaines cellules de l'ovaire d'*Artemia salina* L. C.R. Soc.
        Biol. Paris 144: 1127-1128, 1950.

FEDER, N., O'BRIEN, T.P. Plant microtechnique: some principles and new
        methods. Amer. J. Bot. 55(1): 123-142, 1968.

FILION, W.G., CHRISTIE, B.R. The mechanism of male sterility in a clone
        of orchid grass (*Dactylis glomerata* L.) Crop Sci. 6: 345-347,
        1966.

FLAMM, W.G., BIRNSTIEL, M.L. Studies on the metabolism of nuclear basic
        proteins. In: *The Nucleohistones*. Edited by J. Bonner and
        P. Ts'o. San Francisco, London, Amsterdam: Holden-Day Inc.,
        1964. pp. 230-241.

FLAX, M., HIMES, M. Microphotometric analysis of metachromatic staining
        of nucleic acids. Physiol. Zool. 25: 297-311, 1952.

FORD, J.H. Ultrastructural and chemical studies of pollen wall develop-
        ment in the Epacaridaceae. In: *Sporopollenin*. Edited by
        J. Brooks, P.R. Grant, M. Muir, P. van Gijzel, and G. Shaw.
        London, New York: Academic Press, 1971. pp. 130-173.

FOSTER, T.S., STERN, H. The accumulation of soluble deoxyribosidic
        compounds in relation to nuclear division in anthers of *Lilium
        longiflorum*. J. Biophys. Biochem. Cytol. 5: 187-192, 1959.

FUKUHARA, H. Transcriptional origin of RNA in mitochondrial fraction of
        yeast and its bearing on the problem of sequence homology between
        mitochondrial and nuclear DNA. Molec. Gen. Genetics 107: 58-70,
        1970.

GABELMAN, W.H. Male sterility in vegetable breeding. In: *Genetics in
        Plant Breeding*. Brookhaven Symp. Biol. No. 9, 1956.

GALL, J. Macronucleolar duplication in the ciliated protozoan *Euplotes*.
        J. Biophys. Biochem. Cytol. 5: 295- 08, 1959.

GALL, J.G. Nuclear RNA of the salamander oocyte. Natl. Cancer Inst.
        Monograph 23: 475-488, 1966.

GOMORI, G. Preparation of buffers for use in enzyme studies. In: *Methods
        in Enzymology*. *Vol. I*. Edited by Sidney P. Colowick and Nathan
        O. Kaplan. New York: Academic Press, 1955. pp. 138-146.

GRANT, W.E. Decreased SNA content of Birch (*Betula*) chromosomes at high
        ploidy as determined by cytophotometry. Chromosoma 26: 326-336,
        1969.

HARDONK, M.J., van DUIJN, P. Studies on the Feulgen reaction with
        histochemical model systems. J. Histochem. Cytochem.

HARNEY, P.M., KUNG, H.C.C. Development of nondehiscent anthers in partially male sterile plants of *Plargonium* x *Hortorum* Bailey C.V. "Jacqueline." Can. J. Genet. Cytol. 9: 359-366, 1967.

HERICH, R. Nucleoli and cytoplasmic male sterility. Z. Vererbungsl. 96(1): 22-27, 1965.

HESLOP-HARRISON, J. Origin of exine. Nature 195: 1069-1071, 1962.

HESLOP-HARRISON, J. Ultrastructural aspects of differentiation in sporogenous tissue. S.E.B. Symposia No. 17: 315-336, 1963.

HESLOP-HARRISON, J. Cell walls, cell membranes and protoplasmic connections during meiosis and pollen development. In: *Pollen Physiology and Fertilization*. Edited by H.F. Linskens. Amsterdam: North Holland Publishing Co., 1964. pp. 39-47.

HESLOP-HARRISON, J. Sporopollenin in the biological context. In: *Sporopollenin*. Edited by J. Brooks, P.R. Grant, M. Muir, P. van Gijzel, and G. Shaw. London, New York: Academic Press, 1971.

HESLOP-HARRISON, J., MacKENZIE, A. Autoradiography of soluble [2-^{14}C] thymidine derivatives during meiosis and microsporogenesis in *Lilium* anthers. In: *Sporopollenin*. Edited by J. Brooks, P.R. Grant, M. Muir, P. van Gijzel, and G. Shaw. New York: Academic Press, 1971. pp. 1-30.

HOCKETT, E.A., ESLICK, R.F. Genetic male-sterility in barley. I. Non-allelic genes. Crop Sci. 8: 218-220, 1968a.

HOCKETT, E.A., ESLIK, R.F., REID, D.A., WIEBE, G.A. Genetic male sterility in barley. II. Available spring and winter stock. Crop Sci. 8: 754-755, 1968b.

HOTTA, Y., STERN H. Uptake and distribution of heterologous DNA in living cells. In: *Informative Molecules in Biological Systems*. Edited by L. Ledoux. Amsterdam, London: North-Holland Publishing Co., 1971. pp. 176-186.

HUANG, R.C., BONNER, J. Histone a suppressor of chromosomal RNA synthesis. Proc. Nat. Acad. Sci. 48: 1216-1222, 1962.

JAIN, S.K. Male sterility in flowering plants. Bibliogr. Genet. 18: 101-166, 1959.

JONSSON, M., LAGERSTEDT, S. Loss of nucleic acid derivatives from fixed tissues during flattening of paraffin sections on water. Experientia 14(4): 157-159, 1958.

JOPPA,LL.R., McNEAL, F.H., WELSH, J.R. Pollen and anther·development in cytoplasmic male sterile wheat. Crop Sci. 6: 296-297, 1966.

KASHA, K.J., WALKER, G.W.R. Several recent barley mutants and their linkages. Can. J. Gen. Cytol. 2: 397-415, 1960.

KASTEN, F.H. The Feulgen-DNA absorption curve *in situ*. Histochemie
6: 123-150, 1958.

KURNICK, N.B. Methyl green-pyronin. I. Basis of selective staining of
nucleic acids. J. Gen. Physiol. 33: 243-264, 1950.

KURNICK, N.B. Pyronin Y in the methyl-green-pyronin histological stain.
Stain Technol. 30: 213-230, 1955.

KURNICK, N.B., MIRSKY, A.E. Methyl green-pyronin. II. Stoichiometry of
reaction with nucleic acids. J. Gen. Physiol. 33: 265-274,
1950.

KURNICK, N.B., HERSKOWITZ, I. The estimation of polyteny in Drosophila
salivary gland nuclei based on determination of DNA content.
J. Cell. Comp. Physiol. 39: 281-299, 1952.

LACOMTE, C., de SMUL, A. Effect du régime hypoproteique sur la teneur en
acide déoxyribonucleique desnoyaux hepatiques chez la rat jeune.
C.R. Acad. Sci. (Paris), 234: 1400-1402, 1952.

LaCOUR, L.F., DEELEY, E.M., CHOYEN, J. Variation in amount of Feulgen-
stain in nuclei of plants grown at different temperatures.
Nature 177: 272-273, 1956.

LEDOUX, L., HUART, R. Fate of bacterial deoxyribonucleic acids in
barley seedlings. J. Mol. Biol. 43: 243-262, 1969.

LESSLER, M.A. The nature and specificity of the Feulgen-nucleal reaction.
Intern. Rev. Cytol. 2: 231-247, 1953.

LINDNER, A., KUTKAM, T., SAMKARANARAYANAN, K., RUCKER, R., ARRANDONDO, J.
Inhibition of Ehrilich ascites tumor with 5-fluorouracil and
other agents. Expt. Cell Res. Suppl. 9: 485-508, 1963.

LOVE, R. Improved staining of the nucleoproteins of the nucleolus. J.
Histochem. Cytochem. 10: 227, 1962.

McLEISH, J., SUNDERLAND, N. Measurement of DNA in higher plants by
Feulgen photometry and chemical methods. Expt. Cell Res.
24: 527-540, 1961.

MEEK, E.S. A quantitative cytochemical study of chromosomal basic
proteins in static and proliferative cell populations. Expt.
Cell Res. 33: 355-359, 1964.

MIKSCHE, J.P. Variation in DNA content of several Gymnosperms. Can. J.
Genet. Cytol. 9: 717-722, 1967.

MOORE, B.C. DNA in embryonic diploid and haploid tissues. Chromosoma
4: 563-576, 1952.

MOSS, G.I., HESLOP-HARRISON, J. A cytochemical study of DNA, RNA, and
protein in the developing maize anther. Annals of Botany
31: 555-572, 1967.

NALEPA, S. Studia cytologiezne I genetyczne nad meska sterylnoseia u jeczmienia cz. I. Hodowla Roslin Aklim. I Nasie Tom 15: 17-34, 1971.

NOESKE, K. Stochiometrische Probleme der quantitativen Fastgreen-Zytophotometrie bei der Histonbestimmung. Histochemie 27: 243-252, 1971.

PASTEELS, J., LISON, L. Teneur des noyaux au repos enacide desoxyribo-nucléique dans differents tissus chez le rat. Compt. Rend. Acad. Sci. Paris 230: 780-782, 1950.

PATAU, K., SWIFT, H. The DNA content of nuclei during mitosis in a root tip of onion. Chromosoma 6: 149-169, 1953.

POLISTER, A.W., SWIFT, H., RASCH, E. Microphotometry with visible light. In: *Physical Techniques in Biological Research*. Vol. 3, Part C. Edited by A.W. Polister. New York: Academic Press, 1969. pp. 201-251.

PY, G. Recherches cytologiques sur l'assise nourriciére des microspores et les microspores des plantes vasculaires. Rev. Gen. Bot. (Paris) 44: 316-413; 450-462; 489-512, 1932.

RAMAGE, R.T. Balanced tertiary trisomics for use in hybrid seed production. Crop Sci. 5: 177-178, 1965.

RASCH, E., WOODARD, J.W. Basic proteins of plant nuclei during normal and pathological cell growth. J. Biophys. Biochem. Cytol. 6(2): 263-276, 1959.

RASCH, E.M., SWIFT, H., KLEIN, R.M. Nucleoprotein changes in plant tumor growth. J. Biophys. Biochem. Cytol. 6: 11-34, 1959.

RICK, C.M. Genetics and development of nine male-sterile tomato mutants. Hilgardia 18: 599-633, 1948.

RIS, H., MIRSKY, A.E. Quantitative cytochemical determination of DNA with Feulgen nucleal reaction. J. Gen. Physiol. 33: 125-146, 1949.

RITTER, C., Di STEFANO, H.S. A method for the cytophotometric estima-tion of RNA. J. Histochem. Cytochem. 9: 97-102, 1961.

ROATH, W.W. Some characteristics and behaviour of anthers and pollen of genetic male sterile barley, *Hordeum sp.* Ph.D. Thesis, Montana State Univ., 1969. 94 pp.

ROATH, W.W., HOCKETT, E.A. Pollen development in genetic male-sterile barley. In: *Barley Genetics II*. Edited by R.A. Nilan. Pullman, Wash.: Washington State Univ. Press, 1971. pp. 308-315.

RUDKIN, G.T. Nonreplicating DNA in *Drosophila*. Genetics 52: 665-681, 1965.

SARVELLA, P., HOLMGREN, J.B., NILAN, R.A. Analysis of barley pachytene chromosomes. Nucleus 1: 183-204, 1958.

SAUTER, J.J. Autoradiographische Untersuchungen zur RNS- und Proteinsynthese in Pollenmutterzellen, jungen Pollen und Tapetumzellen während der Mikrosporogenese von *Paeonia tenuifolia* L. Z. Pfl. Physiol. 61: 1-19, 1969.

SAUTER, J.J., MARQUARDT, H. Die Rolle des Nukleohistons bei der RNS- und Proteinsynthese während der Mikrosporogenese von *Paeonia tenuifolia* L. Z. Pfl. Physiol. 58: 126-137, 1967.

SCHOOLER, A.B. A form of male-sterility in barley hybrids. J. Hered. 58: 206-211, 1967.

SRINIVASACHAR, D., PATAU, K. Proportionality between DNA-content and Feulgen dye-content. Expt. Cell Res. 17: 286-298, 1959.

STEDMAN, E., STEDMAN, E. Cell specificity of histones. Nature 116: 780, 1950.

STERN, H. Periodic induction of deoxyribonuclease activity in relation to the meiotic cycle. J. Biophys. Biochem. Cytol. 9: 271-277, 1961.

STERN, H., HOTTA, Y. Related synthesis of RNA and protein in the control of cell division. Brookhaven Symposium in Biology 16: 59-72, 1963.

STUTZ, E., NOLL, H. Characterization of cytoplasmic and chloroplast polysomes in plants: Evidence for three classes of ribosomal RNA in nature. Proc. Nat. Acad. Sci. 57: 774-781, 1967.

SUNESON, C.A. A male sterile character in barley. J. Hered. 31: 213-214, 1940.

SWIFT, H. The constancy of DNA in plant nuclei. Proc. Nat. Acad. Sci. 36: 643-654, 1950.

SWIFT, H. Studies on nucleolar function. Symp. Mol. Biol. 266-293, 1960.

SWIFT, H. The quantitative cytochemistry of RNA. In: *Introduction to Quantitative Cytochemistry*. Edited by G.L. Wied. New York, London: Academic Press, 1966. pp. 355-386.

TAKATS, S.T. An attempt to detect utilization of DNA breakdown products from the tapetum for DNA synthesis in the microspores of *Lilium longiflorum*. Amer. J. Bot. 49: 748-758, 1962.

TAYLOR, J.H. Autoradiographic studies of nucleic acids and proteins during meiosis in *Lilium longiflorum*. Amer. J. Bot. 46: 477-484, 1959.

WHITED, D.A. Biochemical and histological properties associated with
      genetic male sterility at the *ms* locus in barley, *Hordium
      vulgare* L. Ph.D. Thesis. North Dakota State Univ., 1967.
      88 pp.

WIEBE, G.A. A proposal for hybrid barley. Agron. J. **52**: 181-182,
      1960.

WILKINS, M.H.F., ZUBAY, G., WILSON, H.R. X-ray diffraction studies of
      the molecular structure of nucleohistones and chromosomes.
      J. Mol. Biol. **1**: 179-185, 1959.

WOODARD, J.W., RASCH, E.M., SWIFT, H. Nucleic acid and protein
      metabolism during the mitotic cycle in *Vicia faba*.
      J. Biophys. Biochem. Cytol. **9**: 445-462, 1961.

ZENKTELER, M. Microsporogenesis and tapetal development in normal and
      male-sterile carrots (*Daucus carota*). Amer. J. Bot. **49**: 341-
      348, 1962.